Small-Scale Appropriate Energy Technology Grants Program

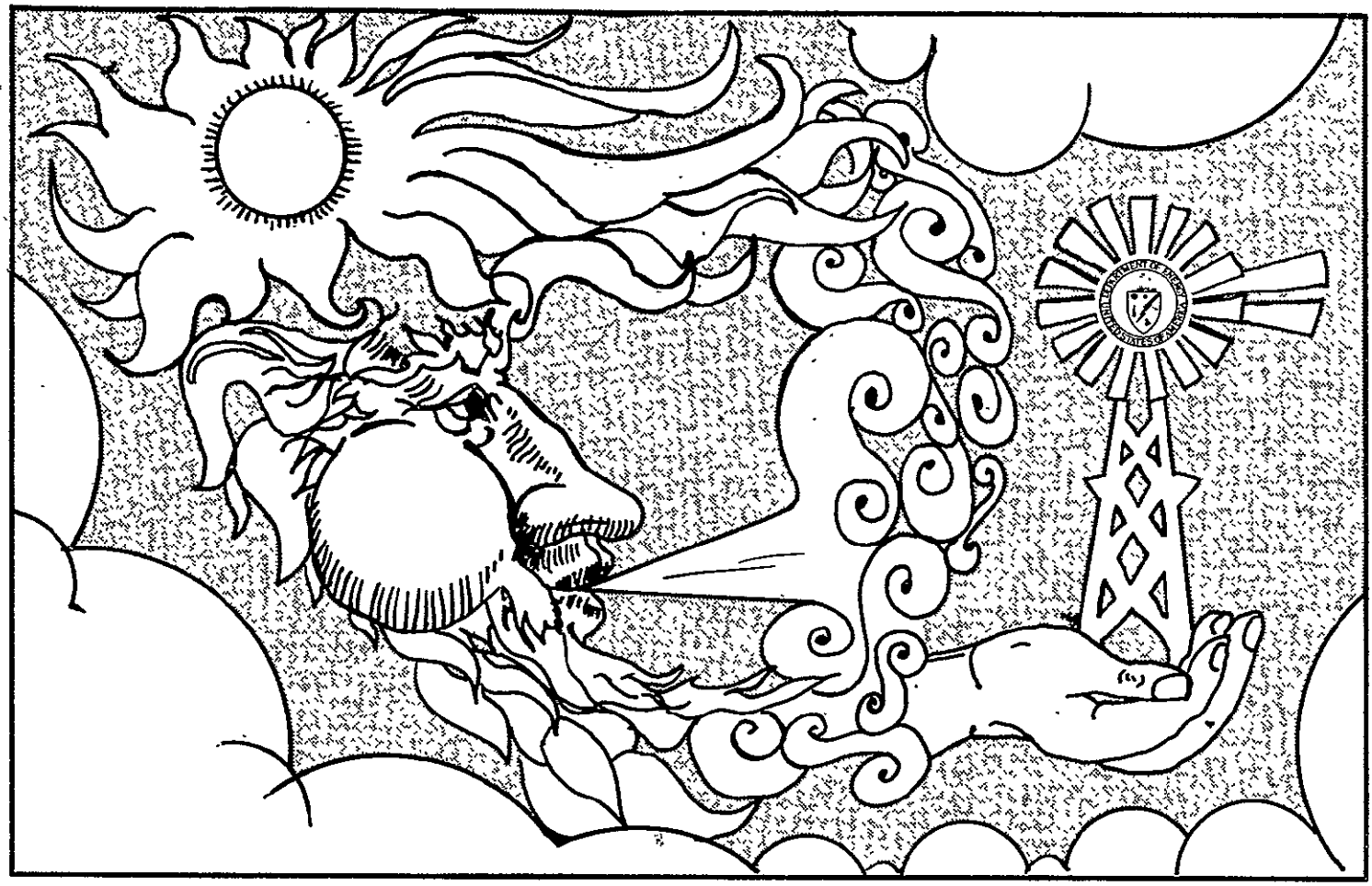

PACIFIC SOUTHWEST REGION
UNITED STATES DEPARTMENT of ENERGY

Low-Cost Solar Concentrating Collector Systems

Printed on 100% recycled paper

FINAL REPORT
LOW-COST SOLAR CONCENTRATING COLLECTOR SYSTEMS

A. Non-Tracking Concentrating Solar Collector Using Evacuated Tubes
Grant No. DE-FG03-78SF01971

B. Non-Tracking Concentrating Solar Collector Using Acylindrical Mirrors
Grant No. DE-FG03-78SF02009

C. Nitinol Tracking Devices for Concentrating Solar Collectors
Grant No. DE-FG03-78SF01970

D. Free-Formed Insulated Concentrating Solar Collector
Grant No. DE-FG03-79SF10552

Prepared For: Small-Scale Appropriate Energy
Technology Grants Program --
Region IX
U.S. Department of Energy
333 Market St., 7th Floor
San Francisco, CA 94105

Prepared By:

A. James V. Harwood
1928 McKinley Street
Honolulu, HI 96822

B. Raymond T. Hebert
P.O. Box 134
Saratoga, CA 95070

C. Charles Raymond
Box 588
Kapaau, HI 96755

D. Glen Goodwin
11151 W. Cumberland
Sun City, AZ 85351

July 1981

U.S. DEPARTMENT OF ENERGY

SMALL SCALE
APPROPRIATE ENERGY TECHNOLOGY GRANTS PROGRAM

REGION IX

BACKGROUND: In 1977, Congress authorized the Energy Research and Development Administration (now the Department of Energy, DOE) to undertake a grants program in small-scale, energy-related technologies referred to as appropriate technologies because they are "appropriate" to local needs and skills. This small grants program has come to be known as the Appropriate Energy Technology (AET) Program.

WHAT: A regional pilot program in appropriate energy technology was implemented to provide monetary grants for small-scale, energy related projects for:

- o Idea development, for concepts demonstrating potential;
- o Concepts testing, for projects that have gone beyond the idea-development phase and are ready for testing;
- o Demonstration, to develop projects which, having been tested, now must be proven through actual use.

In terms of resources, Appropriate Energy Technology ...

- o makes best use of available renewable energy sources
- o conserves nonrenewable resources
- o depends largely on human labor
- o emphasizes use of local materials and labor skills

In scale and efficiency, Appropriate Energy Technology ...

- o is efficient in its use of energy and other resources
- o is simple to install, operate and maintain
- o is compatible with community regulations
- o may employ scaled-downed industrial technology
- o employs novel application of existing technologies
- o emphasizes decentrialized technologies

In relation to the end-user, Appropriate Energy Technology ...

- o satisfies local needs
- o increases community energy understanding and self-reliance
- o is environmentally sound
- o results in durable recyclable systems and/or products

WHERE: The Region IX program covers the states of Arizona, California, Hawaii, and Nevada, as well as American Samoa, Guam, the Northern Mariana Islands, the Pacific Trust Territories. This program is managed by the Office of the Regional Representative, Region IX, of the U.S. Department of Energy. Similar programs are being managed through the other nine regional offices around the country.

WHO: Eligible projects can come from

- o individuals
- o local nonprofit organizations and instiutions
- o state and local agencies
- o American Indian tribes
- o Small businesses

WHEN: Contact the regional DOE office for the annual awards cycle.

RESULTS: Over one hundred and eighty applicants in Region IX have been granted funds with which to start or continue their projects during the first three years of the Appropriate Energy Technology Program.

For additional information on this program, please contact:

Small Scale Appropriate Energy Technology
U.S. Department of Energy
333 Market Street, 7th Floor
San Francisco, California 94105

Nationally, the Small-Scale Appropriate Energy Technology Grants Program is directed by the Office of Small-Scale Technology, U.S. Department of Energy, Washington, D.C.

SMALL-SCALE APPROPRIATE ENERGY TECHNOLOGY
GRANTS PROGRAM - REGION IX
U.S. DEPARTMENT OF ENERGY

PROJECT FACT SHEET

PROJECT #	:	HI-78-25
GRANT #	:	DE-FG03-78SF01971
PROJECT TITLE	:	NON-TRACKING CONCENTRATING SOLAR COLLECTOR USING EVACUATED TUBES
GRANTEE	:	James V. Harwood 1928 McKinley Street Honolulu, Hawaii 96822
AWARD AMOUNT	:	$4,000
DESCRIPTION and RESULTS	:	A non-tracking solar concentrating system that utilizes evacuated tube absorbing elements was constructed and tested. Although the efficiency level was not as high as originally expected, the results indicate that this system is more efficient than unevacuated solar flat-plate collector systems for domestic hot water applications. Preliminary cost analysis indicates that this system could be manufactured at relatively low cost. Mr. Harwood will continue to develop this system on his own in order to address some of the design difficulties identified in his final report.
DATE REPORT SUBMITTED	:	March, 1981

SMALL-SCALE APPROPRIATE ENERGY TECHNOLOGY
GRANTS PROGRAM - REGION IX
U.S. DEPARTMENT OF ENERGY

PROJECT FACT SHEET

PROJECT #	:	CA-78-235
GRANT #	:	DE-FG03-78SF02009
PROJECT TITLE	:	NON-TRACKING CONCENTRATING SOLAR COLLECTOR USING ACYLINDRICAL MIRRORS (Published In: Low-Cost Solar Concentrating Collector Systems)
GRANTEE	:	Raymond T. Hebert P.O. Box 134 Saratoga, CA 95070
AWARD AMOUNT	:	$19,680
DESCRIPTION and RESULTS	:	A unique non-tracking solar concentrator design for residential and commercial applications was designed and tested. The design utilizes acylindrical concentrating mirrors which form high-quality foci on each side of channelled flat-plate collectors. It also incorporates thermally sensitive values at the end of each channel to allow the panel to integrate energy control flows for both direct and diffuse radiation. Difficulties with design, material characteristics and fabrication methods significantly altered the scope, schedule, cost and performance results of this project. The report presents a thorough and very useful documentation of these difficulties, with recommendations for improvements for ongoing research in concentrating collector systems.
DATE REPORT SUBMITTED	:	June, 1980

SMALL-SCALE APPROPRIATE ENERGY TECHNOLOGY
GRANTS PROGRAM - REGION IX
U.S. DEPARTMENT OF ENERGY

PROJECT FACT SHEET

PROJECT #	:	HI-78-9
GRANT #	:	DE-FG03-78SF01970
PROJECT TITLE	:	NITINOL TRACKING DEVICE FOR CONCENTRATING SOLAR COLLECTORS (Published In: Low-Cost Solar Concentrating Collector Systems)
GRANTEE	:	Charles Raymond Box 588 Kapaau, Hawaii 96755
AWARD AMOUNT	:	$10,000
DESCRIPTION and RESULTS	:	A nitinol engine was designed and constructed to serve as a tracking mechanism for solar concentrating (and flat-plate) collectors. Because of the unique properties of the nitinol alloy (which allows it to significantly expand and contract when exposed to certain temperature changes), a nitinol tracking device would provide an inexpensive way of increasing the efficiency of a "stationary" solar collector. The results of Mr. Raymond's research in this area indicate that the nitinol engine design has a great deal of potential for this type of solar application. Mr. Raymond also identifies other possible applications for the nitinol engine, such as water pumping and passive solar design.
DATE REPORT SUBMITTED	:	February, 1980

SMALL-SCALE APPROPRIATE ENERGY TECHNOLOGY
GRANTS PROGRAM - REGION IX
U.S. DEPARTMENT OF ENERGY

PROJECT FACT SHEET

PROJECT #	:	AZ-79-109
GRANT #	:	DE-FG03-79SF10552
PROJECT TITLE	:	FREE-FORMED INSULATED CONCENTRATING SOLAR COLLECTOR (Published In: Low-Cost Solar Concentrating Collector Systems)
GRANTEE	:	Glen Goodwin 11151 W. Cumberland Drive Sun City, Arizona 85351
AWARD AMOUNT	:	$15,484
DESCRIPTION and RESULTS	:	A free-formed insulated solar concentrating-collector was designed, built and tested. The design utilizes a reflector, which is free-formed by hand from a thin steel sheet, requiring minimal skills or equipment. The use of a transparent cover and insulation creates a "greenhouse" environment which reduces heat loss and surface damage. The cover design also includes a highly reflective (but inexpensive) aluminum film which can be readily replaced. This combination achieves simplicity, low-cost, high efficiency and long service life. Tests of the prototype indicate that its efficiency is higher than the commercial unit at temperatures below 160°F -- and comparable with the commercial unit at the boiling point of water. Mr. Goodwin estimates that, on a do-it-yourself basis, a 100 square foot unit would cost only $875.
DATE REPORT SUBMITTED	:	February 1981

TABLE OF CONTENTS

I. Introduction

The need for a durable, highly efficient, low-cost solar panel persists for heat applications that require temperatures at or above the boiling point of water. It is generally recognized that temperatures high enough to efficiently produce mechanical power, refrigeration and most industrial heat applications are beyond the capability of simple flat-plate solar collectors. Although concentrating collector systems can produce these temperatures, the systems currently available are high-cost and, in many cases, of questionable reliability and durability.

Under the Small-Scale Appropriate Energy Technology Grants Program, four different projects addressing these cost and reliability problems were funded during the first two years of the program. Each of these projects identified and developed alternative approaches to improving the cost-effectiveness of concentrating collector systems. Mr. James V. Harwood of Honolulu, Hawaii constructed and tested a non-tracking solar concentrating system that utilizes evacuated tube absorbing elements. The results indicate that this system is more efficient than unevacuated solar flat-plate collector systems for domestic hot water applications, although the efficiency level is not as high as originally expected. Preliminary cost analysis indicates that this system could be manufactured at relatively low cost. Mr. Harwood will continue to develop this system on his own in order to address some of the design difficulties he identified in his report.

A second award was made to Mr. Raymond T. Hebert of Saratoga, California to develop, test and demonstrate a unique non-tracking solar concentrator design for residential and commercial applications. The design utilizes acylindrical concentrating mirrors which form high quality foci on each side of channelled flat-plate collectors. It also incorporates thermally sensitive valves at the end of each channel to allow the panel to integrate energy control flows for both direct and diffuse radiation. However, the prototype panel fabricated and tested under this grant did not perform as expected. Difficulties with design, material characteristics and fabrication methods significantly altered the scope, schedule, cost and performance results of this project. The report presents a thorough and very useful documentation of these difficulties, with recommendations for improvements for ongoing research in concentrating collector systems.

Mr. Charles Raymond of Kapaau, Hawaii, was awarded a grant to design and construct a nitinol engine to serve as a tracking mechanism for solar concentrating (and flat-plate) collectors. Because of the unique properties of the nitinol alloy (which allows it to significantly expand and contract when exposed to certain temperature changes), a nitinol tracking device would provide an inexpensive way of increasing the efficiency of a "stationary" solar collector. The results of Mr. Raymond's research in this area indicate that the nitinol engine design has a great deal of potential for this type of solar application. Mr. Raymond also identifies other possible applications for the nitinol engine, such as water pumping and passive solar design.

The fourth award was made to Mr. Glen Goodwin of Sun City, Arizona to design, build and test a free-formed, insulated solar concentrating-collector. The design utilizes a reflector which is free-formed by hand from a thin steel sheet, requiring minimum skills or equipment. The use of a transparent cover and insulation creates a hot, still air environment which reduces heat loss and surface damage. Mr. Goodwin also fastens a highly-reflective (but inexpensive) aluminum film which can be readily replaced. This combination achieves simplicity, low cost, high efficiency and long service life. Tests of the prototype indicate that its efficiency is higher than the commercial unit at temperatures below 160°F -- and comparable with the commercial unit at the boiling point of water. Mr. Goodwin estimates that, on a do-it-yourself basis, a 100 square foot unit would cost only $875.

II. Non-Tracking Concentrating Solar Collector Using Evacuated Tubes

Final Report: Grant No. DE-FG03-78SF01971
Principal Investigator: James V. Harwood

1.0 Description of Concept

Evacuated tube solar collectors, such as produced by General Electric and Owens-Illinois, have come into widespread use especially for industrial and process heat applications. Though very expensive per square meter of aperture, they are unequalled for efficiency of heat collection especially at high temperatures. However, because of their high cost, evacuated absorbing tubes have not replaced flat plate collectors for domestic hot water. The concept developed under this grant reduces the cost of the evacuated tubes by providing a relatively inexpensive reflecting surface to take the place of much of the area of the aperture, thus reducing the number of evacuated tubes in the installation. The reflecting surface, a trough with elliptical rather than parabolic cross-section, has a field of view large enough ($\pm 35^{\circ}$) so that tracking of the sun, as is necessary with parabolic concentrators, is not required. The combination of non-tracking reflective concentration with evacuated tube absorbing elements should result in a highly efficient solar receiver of moderate cost per BTU collected for domestic hot water applications.

1.1 The Concentrator

The reflective properties of different conic sections were investigated in order to find a curve with a wide field of view that also provided moderate concentrating gain. The parabola, which is the standard shape for concentrating reflectors, is an excellent high-gain concentrator but requires tracking, since its field of view is extremely limited (around one degree). It is not possible with a parabola to trade off gain for field of view beyond a field of view of more that 5°; the reflected rays bounce all over the place and do not concentrate near the focus of the parabola. A trough of circular cross-section, on the other hand, suffers a great deal from spherical aberration when parallel light is incident and can not be made with moderate concentration gain. An ellipse was the answer; a wide range of gain vs. field of view was possible, with concentration gains from 2 - 6 for fields of view of 40° - 10°. At the University of Hawaii Institute for Astronomy, a computer program was developed to trace the rays reflecting from an elliptical concave surface for parallel light of differing angles of incidence, and for ellipses of varying eccentricity. These studies showed that a concentration gain of about 3 could be obtained concurrently with a field of view of $\pm 35^{\circ}$ for an ellipse of a particular eccentricity. This is the cross-sectional shape used for the concentrating troughs for this project. Figure 1 illustrates the cross-section of one of the solar collector assemblies. (All figures are presented at the end of the report.)

Figure 2 shows the ray tracings plotted by the computer for angles of incidence of 0°, 10°, 20°, and 30°. The arrows represent parallel sunshine coming into the concentrator at the various angles of incidence. (For clarity, they were not shown hitting the reflecting surface.) The vertical line in the center of each ellipse represents the collecting surface that the reflected rays hit. It will be noticed that some of the rays

undergo multiple reflections, but all of them eventually hit the vertical absorbing surface, thus proving the wide field-of-view characteristics of an ellipse.

Figure 3 is a plot of the field of view of the concentrator in polar coordinates representing azimuth and elevation, with the zenith at the center. Also on this figure is a plot of the sun's path (dotted lines) for the summer and winter solstices, the limits of the sun's north-south travel, for 20° north latitude. The position of the sun each hour in local apparent time is also marked. The field-of-view plot is for the concentrators oriented 20° south of the zenith in elevation, with their longitudinal axis east-west. It can be seen from this figure that the sun's path will be substantially within the field of view of the concentrators through most of the day for any time of the year, eliminating the necessity for tracking or seasonal adjustments.

Since Hawaii is south of the Tropic of Cancer, the sun's path for the summer solstice actually passes north of the zenith. Twice during the year, in June and July, the sun passes through the zenith at noon, causing shadows to disappear. Because of the sun's path taking such a wide range so high in the sky at the Hawaii latitude, the field-of-view problem is worse here than anywhere on the Mainland, where the sun never gets above an elevation of 83° for a latitude of 30°, and is always in the south.

On Figure 3, the airmass at which the sun leaves the field-of-view of the concentrators in the afternoon (3:30 PM) is noted. The "airmass" represents the length of atmospheric thickness at a particular elevation angle with respect to the thickness at the zenith (airmass = 1.00), and is defined as the reciprocal of the cosine of the zenith distance, or $1/\cos(z)$. The zenith distance is the complement of the elevation, so in terms of elevation above the horizon the airmass is $1/\cos(90\text{-el.})$. In the winter, the airmass of the sun when it is leaving (or entering) the field-of-view is 2.46, or about two and a half times as much air in the sun's path as at the zenith. Much of the sun's energy is attenuated by this long air path. In the summer, the airmass is only one and a half times the zenith path length when the sun is at the edge of the field-of-view; Hawaii might be losing a half hour's useable energy in midsummer. However, the sun is above 50° elevation from just after 9:00 AM to just before 3:00 PM, so ample energy is being collected.

The gain of a concentrator is defined as the ratio of the area of the aperture to the area of the absorbing element. Strictly speaking, both sides of the center absorbing element should be counted in determining the gain. With a clear aperture of 13 7/8" width and an absorbing element height of 4 1/4", the gain would then be 1.63. However, the collected energy is not spread over the entire area of both surfaces of the absorbing element. The ray traces in Figure 2 show that at any time no more than about half of both sides of the absorbing element is being illuminated, and usually a lot less, making the effective concentration from a point source (the sun) within the field of view at least 3.2. The rest of the absorbing element that is not being illuminated by the sun is receiving radiation from other parts of the field of view.

A new type of concentrator curve called the Compound Parabolic Concentrator is coming into use. It utilizes parabolic sides with cusps at the bottom, as shown:

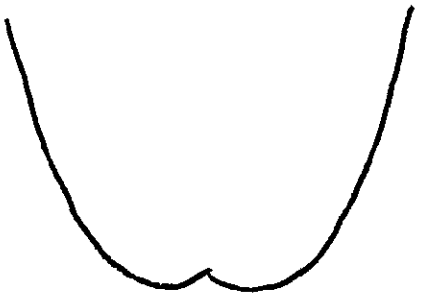

The application of cusps at the bottom in the design, to make a "Compound Elliptical Concentrator", might well permit deleting the lower absorbing tube which would result in higher gain and lower cost. However, they are not included in the collectors that are the subject of this report.

1.2 The Absorbing Tubes

Figure 4 is a longitudinal cross-section of one of the pair of evacuated absorbing tubes in a collector assembly. The tubes themselves are 57mm O.D. Pyrex, four feet long. Brass end flanges are epoxied to the ends of the tubes. The front flange has a hole through which passes the copper tube carrying the water; the rear flange is a solid disk with no perforation.

A serious problem in the design of an evacuated tube through which water must pass is to account for the thermal expansion of the water tube without disturbing the vacuum seals. This was solved in this case by providing a coaxial water flow, so that the water enters and leaves through the same end. The end cap on the coaxial tube assembly rides in a sliding fit in a collar soldered to the inside of the rear end flange; thus, the coaxial tube is free to expand and contract entirely within the vacuum, without distrubing the epoxy seals. (See Fig. 4.) The coaxial arrangement has the additional advantage of high efficiency in heat transfer to the liquid, since the liquid makes two passes within each absorber tube.

Within the evacuated Pyrex tube is the black absorbing sheet metal, "black chrome" from Berry Solar Products, Inc. This material has high absorptivity to visible light, 0.95, yet low thermal emissivity in the infrared (approx. .15). This highly efficient absorbing material is wrapped around the coaxial water tube in a diamond shape, as illustrated in the Figure 1 cross-section. It is bonded to the water tube with a heat-conducting cement called THERMON.

The epoxy seals holding the vacuum caused a great deal of trouble during the course of this project. Numerous leaks were encountered, requiring extensive re-epoxying. It would probably be more cost-effictive to utilize high temperature Teflon O-rings for this application.

To evacuate the absorbing tubes, a vacuum pump system was made available by the Space Astronomy Laboratory of the Institute for Astronomy at no cost. This vacuum system consisted of a mechanical roughing pump, capable of reaching a vacuum of 10^{-3} torr, and an oil diffusion pump that will reach almost 10^{-6} torr. (A "torr" is a millimeter of mercury; atmospheric pressure is about 730mm of mercury.) Sources investigated state that evacuation of 10^{-3} to 10^{-5} torr is required to maintain efficient vacuum insulation.

The gages associated with the vacuum pumps were inoperative and of a primitive electronic technology. A thermocouple gage for the range of pressures from atmospheric to 10^{-3} torr and a used discharge gage for pressures from 10^{-3} torr to 10^{-6} torr were used for this project. Maintaining the vacuum pumps occupied a substantial amount of available time and grant resources since Spring.

2.0 Sources of Inefficiency

The theoretical studies relating to the field-of-view properties of an ellipse, together with the known high efficiency of vacuum insulation, shows a high degree of promise. A special effort was made during the course of this grant to ensure that the design and fabrication of the prototype collector units is as complete and true to the theoretical model as possible. In attempting to achieve this goal, the project was extended way beyond the estimated time of completion, due to unforseen problems. In many instances, it would have been easy to take a short cut or eliminate some aspect of the design, such as evacution of the collector tubes, to save time. At no time was this done, and the time extensions granted by the D.O.E. Appropriate Energy Technology program to verify the excellence of the design are greatly appreciated.

In this section are itemized certain unavoidable energy losses. Some of them are due to the physical properties of the materials and others to the wide tolerances resulting from garage workshop construction with hand tools rather than precise machine tool fabrication.

1. About 6% of the incident sunlight is reflected and absorbed by the Plexiglass covers.

2. The polished sheet metal reflector reflects only about 8% of the incident light. Rays that undergo multiple reflections are attenuated accordingly.

3. The Pyrex tubes absorb and reflect probably around 10% of the light incident on them perpendicularly. Losses increase as the angle of incidence approaches the angle of total internal reflection. Fortunately, many of the rays reflecting at a grazing angle from one tube are directed towards the other tube at a more reasonable angle.

4. The ray traces of Figure 2 show a continuous vertical absorbing element (line) in the center of the trough. In practice, the absorbing element actually consists of two

elements, within the two evacuated tubes. The two absorbing elements are separated by twice the thickness of the Pyrex tubes, or 6mm, plus any space between the end of the element and the inside of the glass tube. This gap in the center of the concentration area represents a leak of radiation across to the other side and back out. This gap could be eliminated by using one large tube 4 1/2" in diameter instead of two smaller tubes one on top of the other, as is done in this design. The difficulties involved in using one large tube are that twice as much air would have to be evacuated, and there would be a lot more glass in the way of incident sunlight. There is a recent Japanese invention of an evacuated glass tube whose cross-section is a narrow oval, rather than a circle, surrounding a flat absorber surface. Replacing the two round absorber tubes in the present design with the Japanese oval of the appropriate size would solve this source of energy loss.

5. For maximum thermal efficiency, the ends of the absorbing sheet metal within the evacuated tubes should be separated from the glass by a paper-thin gap. If they touch the glass, they can conduct heat to the glass resulting in a conduction loss. If the gap is wide, less absorbing area in the concentration region is available. Assembly of the units with this narrow tolerance over the four foot length of the absorbing tubes was not possible. Undoubtedly, the blackened sheet metal is touching the inside of the glass tubes in a number of places, although the total area of contact is very small, minimizing conduction. The oval Japanese tube mentioned in (4) above would help in this problem, since there would be only two edges per concentrator to worry about, rather that four as is the present case.

6. The sheet metal, coated with Black Chrome, within the evacuated tubes absorbs about 90% of the incident energy. A small amount is reradiated. Some of the heat is conducted to the end flanges and the evacuation lines. All these items are of minimum surface area and are insulated with polyurethane foam or foam rubber. Nevertheless, a certain amount of heat will escape.

3.0 Advantages Over Flat-Plate Design

The advantages of the non-tracking concentrating collector design developed under this grant over flat-plate collector systems are summarized below:

1. Greater efficiency of heat transfer takes place, since the water passes twice through each absorber and four times through each concentrator.

2. 40% less hot absorber surface per unit area of aperture is present from which heat can be lost relative to a flat plate collector. (The 40% figure based on a gain of 1.6.)

3. It is possible to evacuate the area around the collector surfaces in this design. With evacuation removing convection losses, the efficiency stays constant with respect to temperature and temperature differential. With unevacuated flat plat collectors, the efficiency drops as these quantities rise.

4. Because of the concentration effect, higher temperatures can be reached than with flat plates, for air conditioning uses.

5. The amount of fluid standing in the collector pipes overnight losing heat and that has to be heated next morning can be a substantial daily heat loss in flat plate collectors. In this design, the standing water is only about a pint per 4 1/2 square feet of aperture.

The disadvantages of this design over a flat plate are the necessity to precisely orient the trough-shaped concentrators, the smaller field of view of the concentrators (180° X 70° vs. 180° X 180°), and the fact that an equivalent area of flat plate is more compact than multiple concentrators.

4.0 Current Status of the Concentrator Assemblies

Twelve of the assemblies, each 4' long by 13 7/8" clear aperture, were built for this project. The total collecting area is 55 1/2 square feet. All of the assemblies are complete with the exception of evacuation of the collector tubes in 5 units, which is waiting the delivery of diffusion pump fluid. Two evacuated units and two unevacuated units have been mounted next to each other and are being tested for performance.

5.0 Test Arrangement

Figure 5 is a diagram of the test arrangement. Two unevacuated and two evacuated concentrators are mounted on the solar collector platform behind a single-family residence. An 82-gallon tank is positioned horizontally on the terrace above the platform, so that thermosyphon operation is possible. The tank is insulated with two inches of polyurethane foam and, in tests, loses only three degrees overnight. A valving arrangement permits the tank to be isolated from the house and from the collectors. The tank is covered with a wooden box to protect it from the elements. Photographs of the system are included in the back of this report.

For the tests, the 82-gallon tank was isolated from the house. Water was pumped through the concentrators from the tank in a closed loop. Since no draw was being made on the tank by the house, the tank water would increase in temperature each day, so testing could be done over a wide range of temperatures. The pump was turned on each day at 8:30 AM and turned off at

4:30 PM. The controller, which normally would cycle the pump on and off depending on the quantity of sunlight, was not used. A constant flow throughout the day was necessary to accurately judge the performance of the collectors, even if they were giving heat up from the water.

Water pumped from the tank was directed through a "Y" to the evacuated bank and unevacuated bank in parallel. (The two concentrators in each bank were connected in series.) Valves and flowmeters in each leg of the "Y" enables accurate adjustment of the water flow through both banks to be the same, about 0.3 gallons per minute. After leaving the banks, the water joined at another "Y" and returned to the tank.

Thermistor temperature sensors were attached to the pipes at the inlet to the input "Y" to measure the temperature of the water going to the concentrators, and at the outlet of the second concentrator in each bank (evacuated and unevacuated). These sensors were attached to a Heliotrop General electronic thermometer. Another thermistor sensor was attached to the halfway point of the tank and interfaced to a Rustrak two-channel recorder. The other channel of the Rustrak records the signal from an Inservco insolometer in watts per square meter located with the concentrators on the platform. Thus, at any time the solar intensity, water flow, and input and output temperatures could be measured from a concentrator bank.

The recorder, insolometer, and pump were all connected to a timer that turned everything on automatically at 8:30 AM and off at 4:30 pm. During holidays and weekends the input and output temperatures of the evacuated and unevacuated banks were recorded every half hour. During the week, the system automatically recorded the solar intensity and tank temperature, however, the input and output concentrator bank temperatures could not be written down. At the end of the series of measurements the temperature sensors were cross-calibrated by disconnecting them from the piping and placing them in a pan of hot water. The individual differences thus obtained were applied to the numbers read from each sensor during the solar testing.

The weather during the testing was for the most part gusty with off-and-on tradewind showers and clouds drifting across. There were a couple of days of full sun.

6.0 Cost Breakdown Per Unit

The cost of each unit was calculated based on the cost, not considering wastage, of the individual components. Retail prices plus 4% state excise tax are incorporated into these costs. No labor costs are included.

Pyrex tubes, 48" X 57mm (2 each)	$ 16.64
Black chrome absorber sheet metal	4.67
Aluminum sheet metal reflector	25.00
Plexiglass cover 3/32"	9.92
Reflective mylar for end pieces	2.43
Copper tubes and fittings	13.85
Brass end flanges for Pyrex tubes (estimated)	3.00
Redwood frame lumber	23.86
Miscellaneous fasteners, calk, and foam	4.20
	$ 102.57

For each unit, the aperture is 4.63 square feet.

The cost per square foot is therefore: $ 22.18
not including labor.

The aluminum reflector, redwood lumber, and Pyrex tubes were the major cost items. Purchasing items in quantity could probably reduce costs by at least 40%. An additional cost savings (and possible increase in reflectivity) could be made by substituting reflective Plexiglas for the aluminum reflector. If ordered in large quantities, the manufacturer could provide custom shaped Plexiglas reflecting elements that would be less susceptible to corrosion and not require the redwood frame. Introducing the cusp shape in the bottom of the reflector, as discussed earlier, would eliminate one of the Pyrex tubes, and perhaps the new oval Japanese evacuated tube would be cheaper than the Pyrex tube and piping.

The concentrator units as built by me in the garage were very labor-intensive. Proper planning of the design with mass production utilizing shop machinery could probably result in the construction of the units in four hours or less, for a labor cost of around $20 per unit. No highly skilled labor is required.

7.0 Results and Further Work

Since mounting the concentrators, detailed 1/2-hour interval measurements were available on only four weekend days. The data from these four days have been compiled into the graphs of temperature change (T) vs. input temperature (T) for the evacuated and unevacuated banks (Figure 6) and the graphs of heat collected in BTU's per minute vs. solar insolation in watts for the evacuated and unevacuated banks (Figure 7).

A problem in collecting the temperature data was the lack of precision in reading the electronic thermometer. It is possible to read the meter only to a degree Farenheit; the meter is calibrated every 5 degrees, so it was not possible to read it to a precision of fractions of a degree. Yet, the temperature differences being measured were on the order of two to four degrees. The points plotted on the graphs therefore have an artificially stratified appearance, with points being located at integer degrees, with some being located at half degrees.

Figure 6 shows the advantage of evacuation. Far more points for the evacuated collectors are above the zero temperature difference line than for the unevacuated units. Also, the temperature rise for the unevacuated collectors falls off with increasing temperature, whereas the temperature rise (ΔT) is more independent of temperature for the evacuated collectors. Negative values of T indicate cooling of the input water when clouds go across the sun, since the pumping of the water continued irrespective of the solar intensity for these tests.

The power in the incident solar radiation was calculated as follows. The insolometer is calibrated in watts per square meter. On a bright day around noon, about 1250 w/m^2 is incident. The area of two concentrator apertures is 0.859 square meters. The power arriving at the concentrators is therefore 1250 X .859 or 1074 watts. The conversion factor for converting watts to BTU/minute is 17.5796 watts per BTU/min. Therefore, the insolation expressed in BTU's is 1074/17.5796 or 61.1 BTU's/minute. This is what the concentrators would produce if they were 100% efficient.

BTU's/min can be converted to degrees Farenheit of temperature rise for a given water flow, and vice-versa. A BTU (British Thermal Unit) is the amount of heat required to raise one pound of water one degree F. One gallon of water weighs 8.345 pounds. According to my flowmeters, the flow pumping through the concentrators is 0.35 gallons/minute, or 2.92 pounds of water per minute. Thus, from our example above, 61.1 BTU's/min. should produce a temperature rise of 61.1/2.92 = 20.9°F for 100% efficiency. The reverse calculation can be done to convert temperature rise to BTU's/min, which was done for the graphs of Figure 7.

Again, the evacuated graph shows a definite increase in BTU's collected over the unevacuated, especially at the higher levels of insolation. The points under the 0 BTU line represent heat lost from the system due to constant pumping during low insolation.

A rough figure of the efficiency for the evacuated concentrators based on the highest points on the graph is 20%, 12 BTU's/min collected vs. about 60 incident. The efficiency of the unevacuated is only half that, or 10%. The advantages of evacuation are thus amply demonstrated.

It is probably unfair to take the highest point on the graph for the representative efficiency. Until much more comprehensive testing can be done, this result is only tentative. There is so much scatter in the points that a line can't be drawn representing a definite relationship between BTU/min and insolation. Much of this scatter is due to the imprecision in reading the temperatures; subtracting two imprecise numbers very close together (T) produces large random variations. In future testing, a digital temperature probe will be utilized that displays tenth degrees.

In spite of the large scatter, it is apparent that the efficiency measured is not up to the promise expected from the design. I had thought that possibly 50% efficiency would be obtained; the losses estimated under Section 2.0 combined produce a 40% loss due to reflection and absorption. Apparently, a relatively large heat leak is present. The surprising number of points below the 0 line on the graphs even for the evacuated collectors indi-

cate a loss of heat from the hot water, rather than a lack of ability to collect the heat from the sun. If the graphs in Figure 7 were displaced upwards so that few if any points on the evacuated side were below zero, the maximum BTU's/min would be about 20 for the evacuated, representing an efficiency of about 30%. This would be the case, then, if all heat leaks were found and corrected.

A possible source of a serious heat leak is contact between the inside wall of the glass tubes and the black absorbing element within. The black sheet metal is hardly thicker than aluminum kitchen foil, and therefore has a low thermal mass. The glass tube is cold, so a substantial thermal gradient exists, possibly pumping heat out of the absorber, even though the area of contact is small and glass is a poor heat conductor. It is also possible that the insolometer may not be properly calibrated, which would overestimate the solar insolation. Another source of possible error is location of the thermistor temperature sensors at the input and output of the concentrators.

Future research and testing of this design will include: calculating the proper shape for cusps, making some out of reflective mylar, and trying to install them over the lower collector tube so only one tube is operating within the concentrator. The water from flowing into the lower tube will be blocked, which should eliminate half the heat leak if it is due to the absorbers touching the walls of the glass tubes, and also if the heat leak is due to light escaping between the 2 absorbers. Five evacuated concentrators will be installed on the platform, connected in series, and tested for temperature rise. It is possible that the two evacuated collectors (or one of them) has developed another vacuum leak and has lost it's vacuum. A plumbing leak existed on the piping of one concentrator and had to be resoldered, which may have disturbed the vacuum seals. Connecting five of them in series will give much larger temperature rises, easier to measure accurately, and minimize the effect of one or two defective concentrators. An attempt to purchase a couple of the Japanese oval evacuated tubes, if they are approximately the right size to fit within a concentrator, will also be made. Industrially assembled units may produce the efficiency when within a concentrator that was not possible to obtain with homemade attempts.

8.0 Project Accounting

Hand tools: Router & accessories, table saw kit, sabre saw, electric pipe solderer, cutting guide, 5/8" drill bit, tubing pinch-off tool	$ 616.19
Solar components and instruments: Water pump, electronic thermometer, hookup wire, sensors, Thermon cement, insolometer, chart recorder, 2 Flowmeters, electronic parts	757.33
Vacuum equipment: Thermocouple gage, vacuum exopy, mechanical pump oil, diffusion pump oil, discharge gage, vacuum cement, bellows valve assembly. 648.53	
Collector fabrication: redwood lumber, Plexiglas, reflective mylar, Pyrex tubes, fasteners, black metal, caulking, foam, paint	1,593.12
Mounting platform (repairs)	112.08
Photography: Film and processing	121.78
Plumbing supplies:	133.98
Consulting: Mr. Arturo Urquieta, vacuum technology	100.00
Miscellaneous:	86.29
TOTAL	$ 4,169.30
Funds supplied by grantee	169.30
GRANT FUNDS EXPENDED	$ 4,000.00

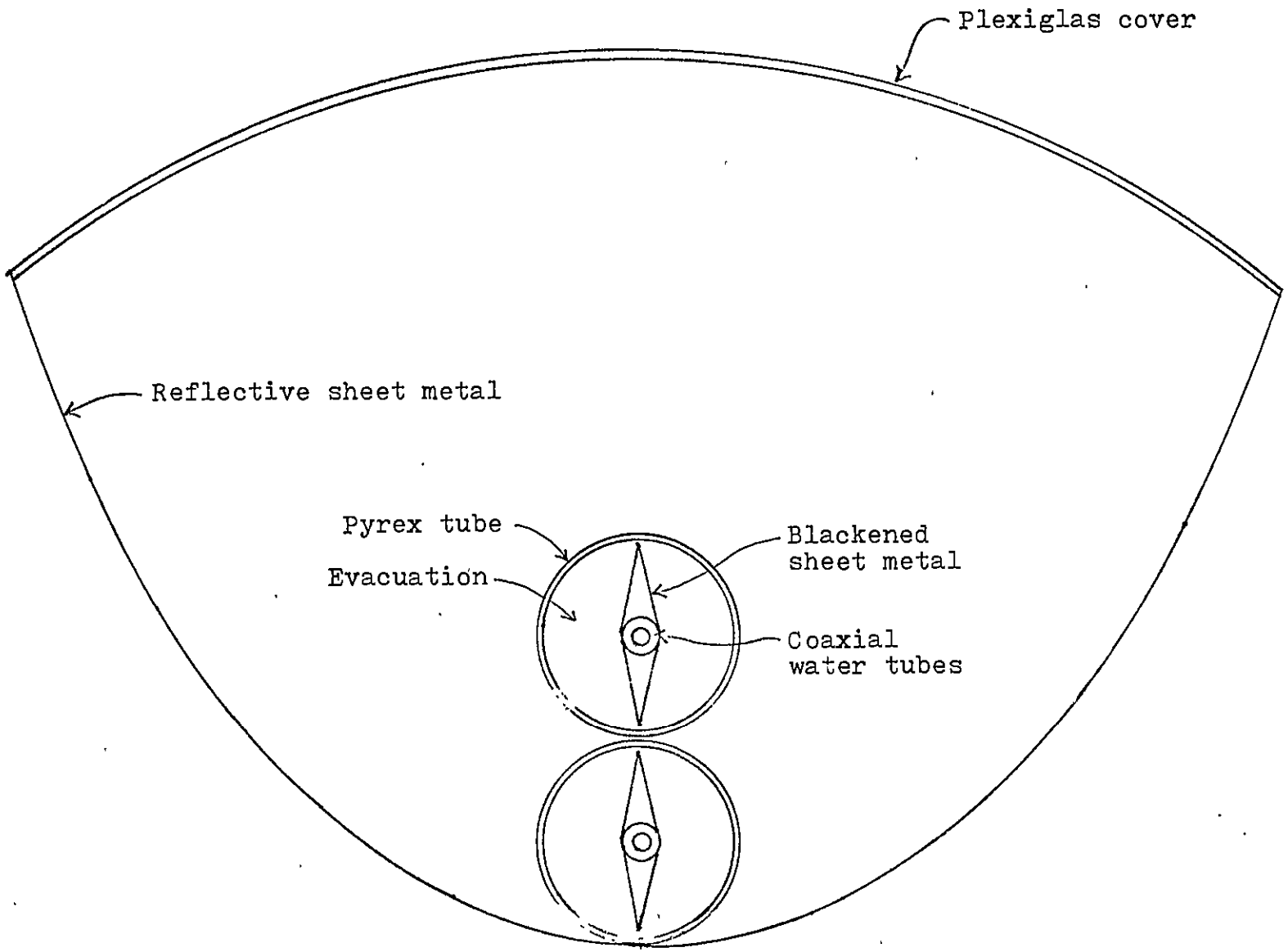

FIGURE 1 - Cross section of concentrating solar collector
(frame holding parts together not shown)

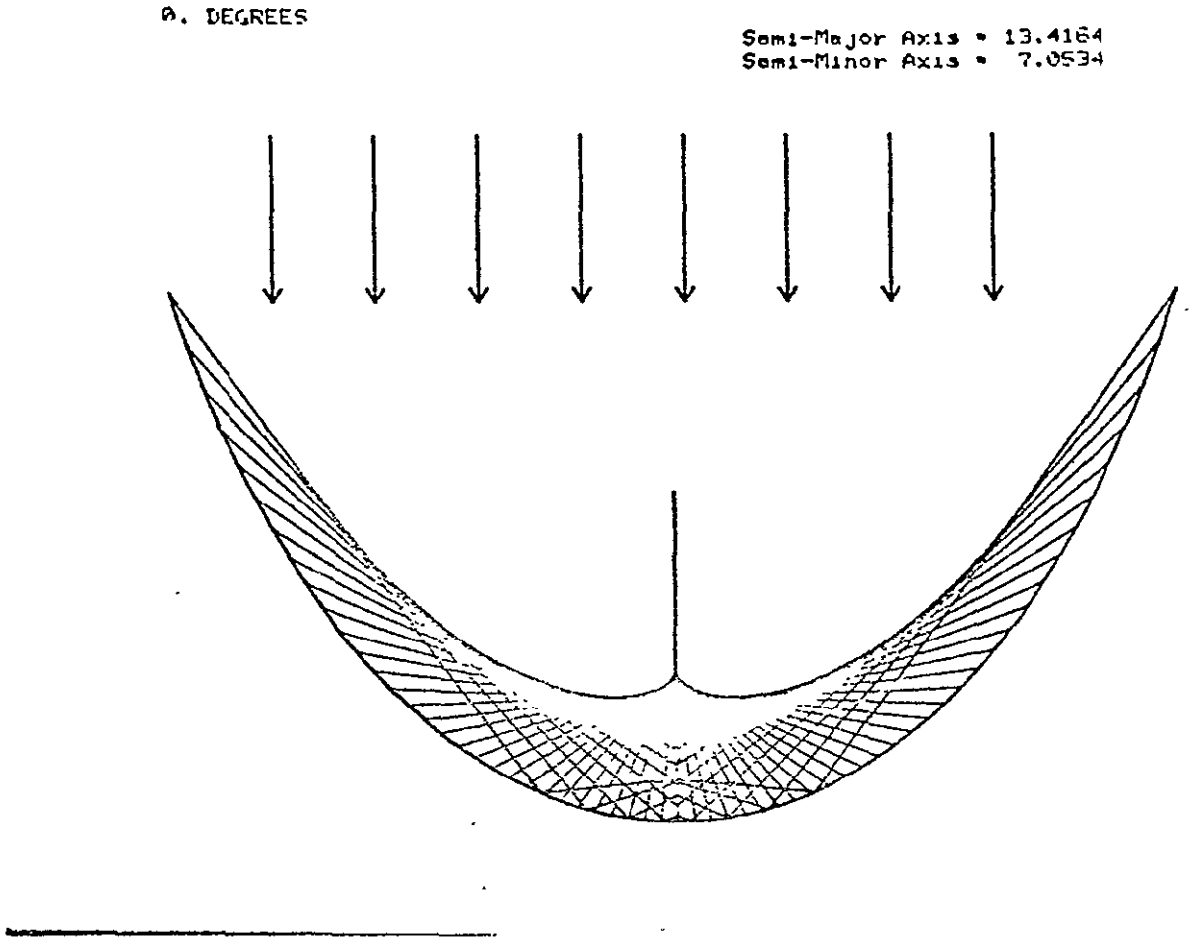

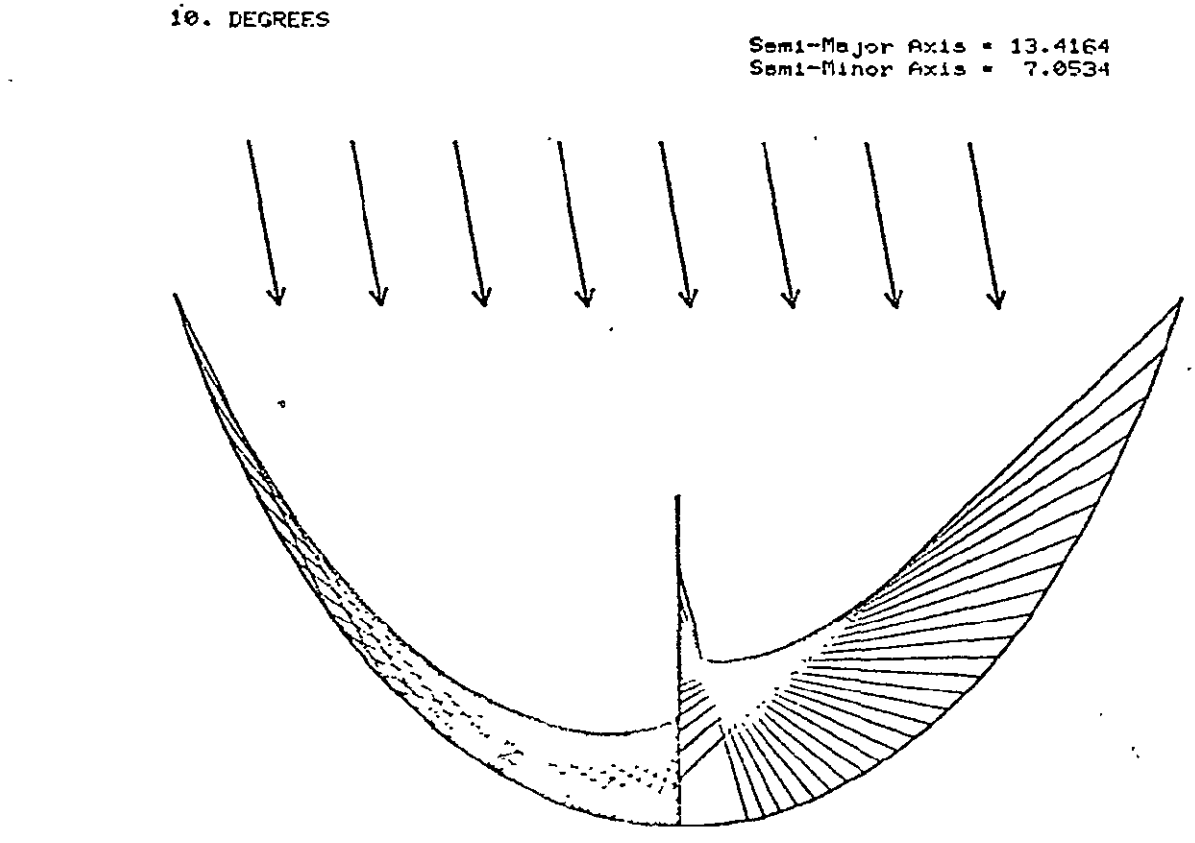

FIGURE 2 - Ray tracings for ellipse (continued next page)

20. DEGREES

Semi-Major Axis = 13.4164
Semi-Minor Axis = 7.0534

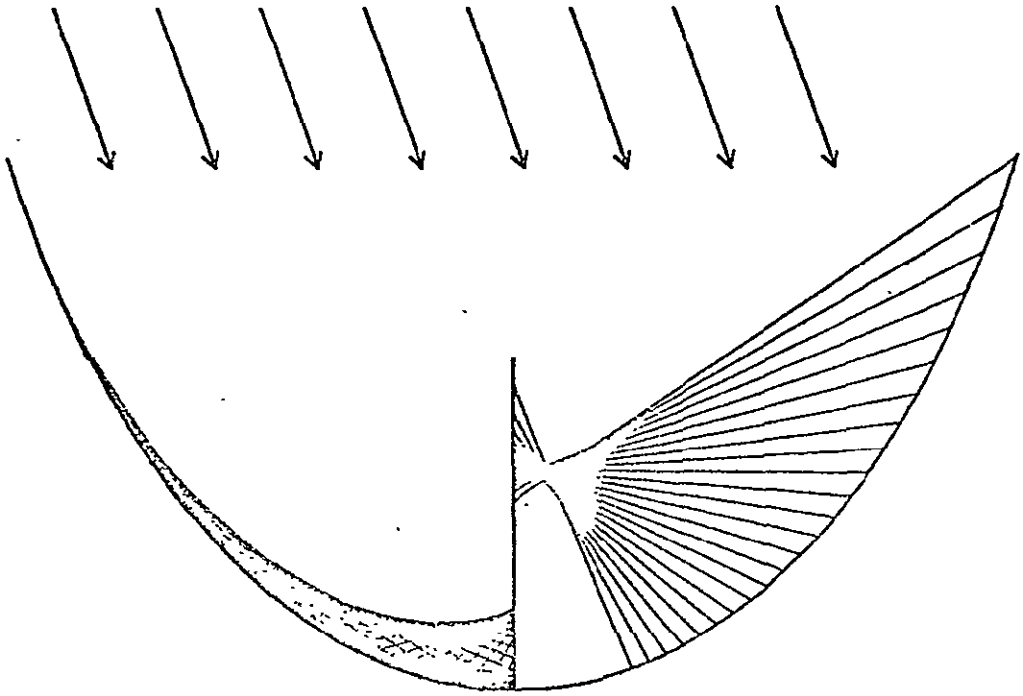

30. DEGREES

Semi-Major Axis = 13.4164
Semi-Minor Axis = 7.0534

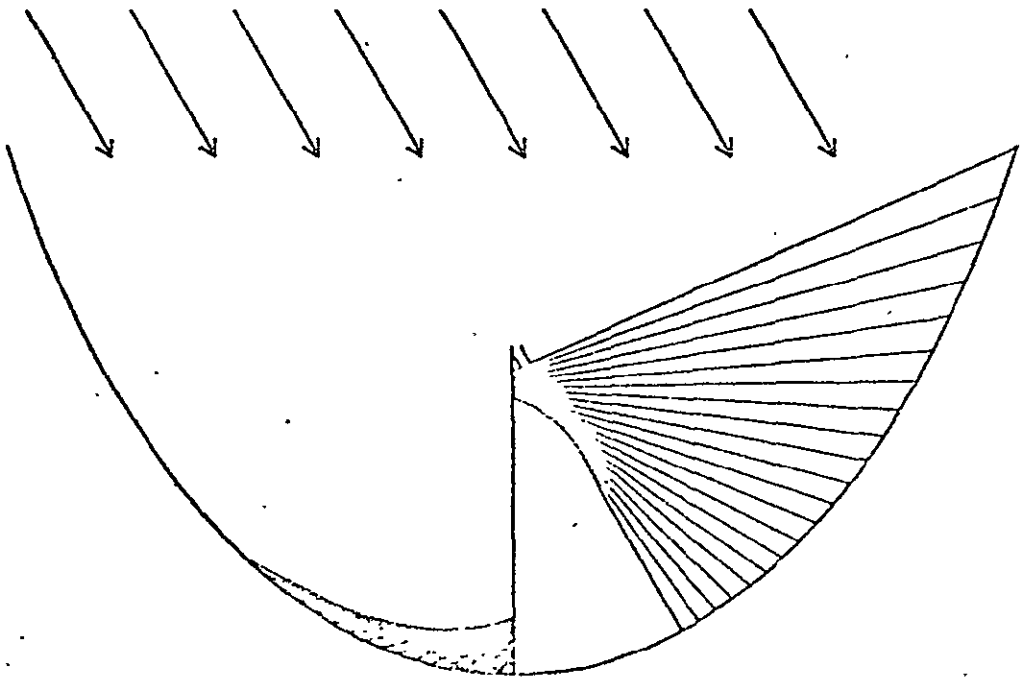

FIGURE 2 (continued)

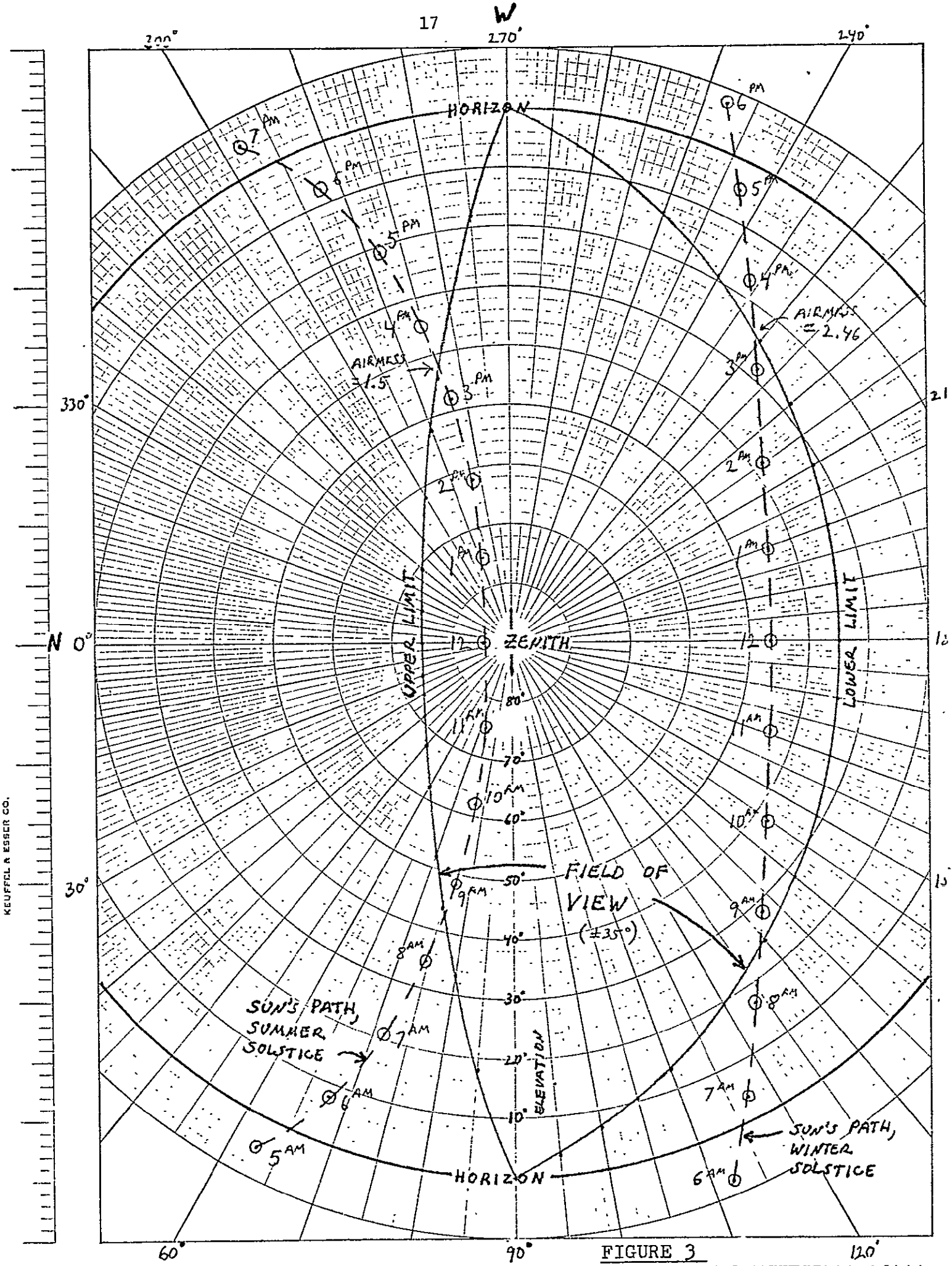
W
300°
270°
240°
HORIZON
7 PM
6 PM
5 PM
4 PM
3 PM
2 PM
1 PM
AIRMASS = 1.5
AIRMASS = 2.46
330°
N 0°
30°
60°
90°
120°
ZENITH
12
11 AM
10 AM
9 AM
8 AM
7 AM
6 AM
5 AM
UPPER LIMIT
LOWER LIMIT
80°
70°
60°
50°
40°
30°
20°
10°
ELEVATION
FIELD OF VIEW (±35°)
SUN'S PATH, SUMMER SOLSTICE
SUN'S PATH, WINTER SOLSTICE
HORIZON
POLAR COORDINATE 46 4410
KEUFFEL & ESSER CO.
MADE IN U.S.A.

FIGURE 3

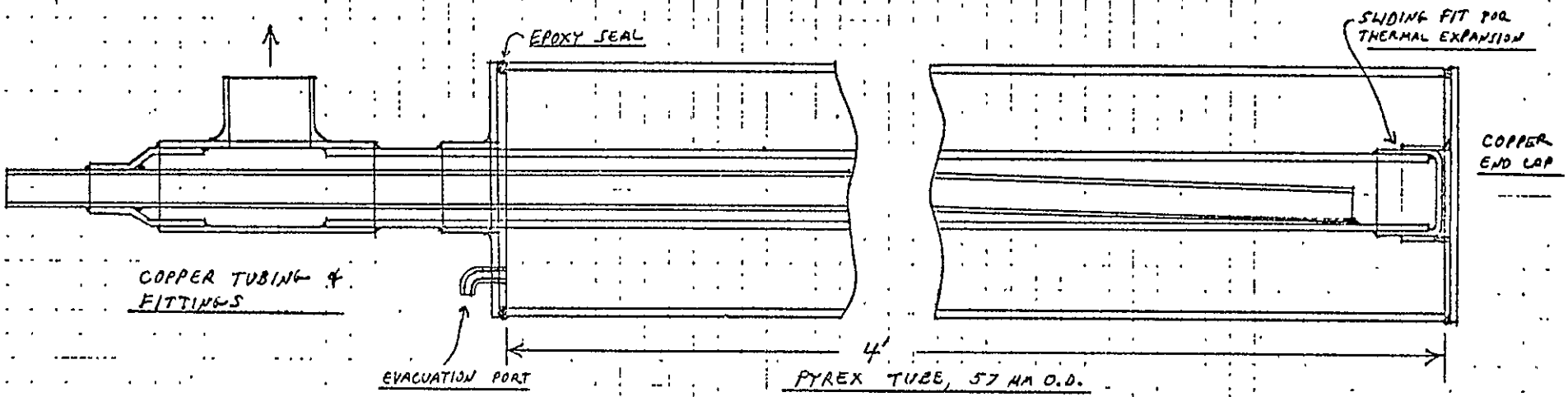

FIGURE 4: COLLECTOR DETAIL – 2 EA. / ASSY. SCALE 1:1

COAXIAL ARRANGEMENT. BLACK ABSORBER NOT DRAWN.

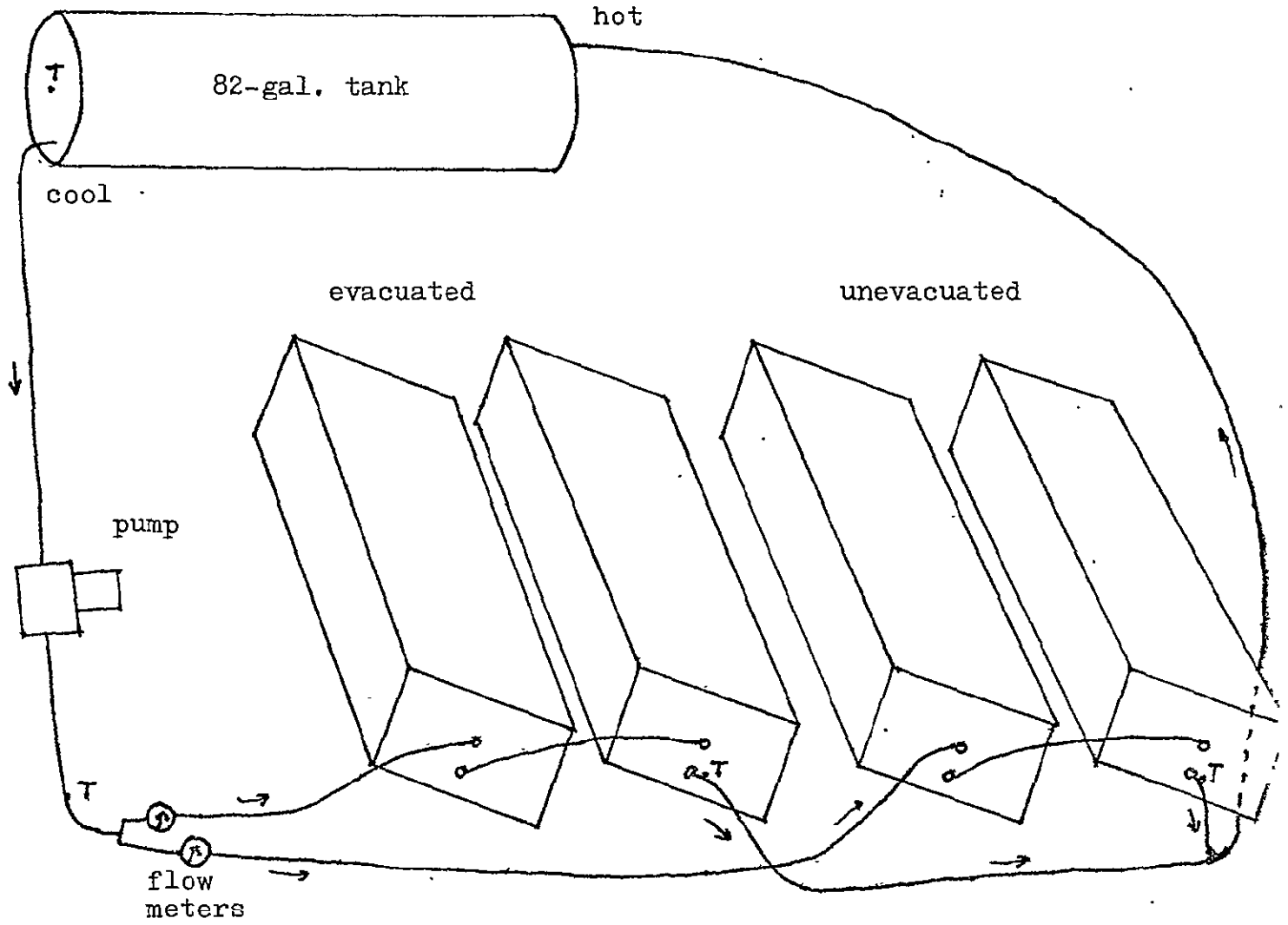

"T" = location of thermistor temperature sensors

FIGURE 5 - Experimental Arrangement

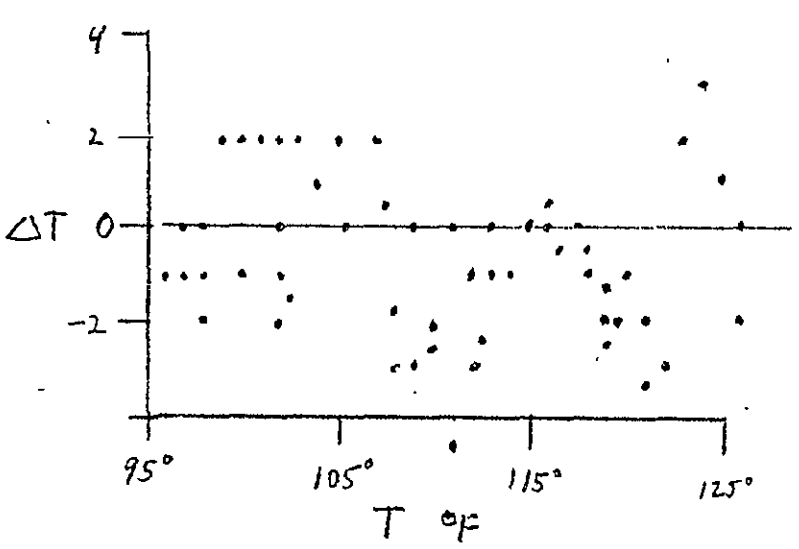

UNEVACUATED

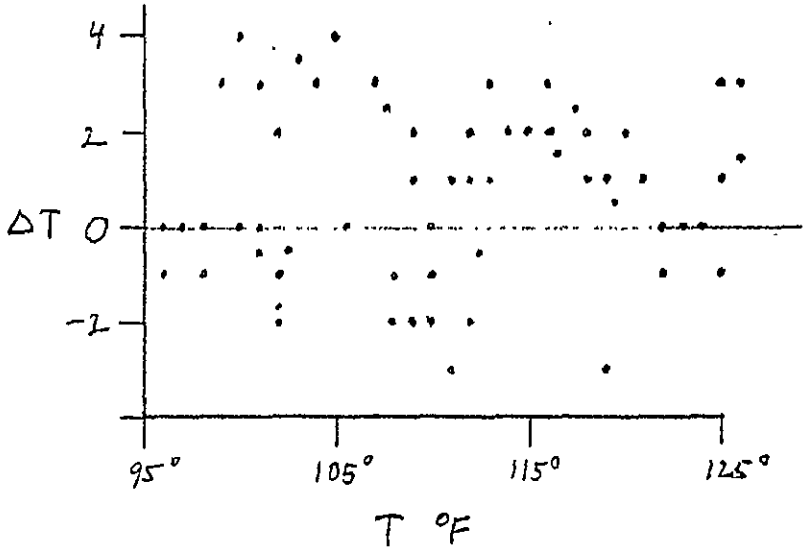

EVACUATED

FIGURE 6

FOR BRIGHT SUN, INSOLATION = 1100 WATTS;
WITH 100% EFFICIENCY, THIS IS EQUIVALENT TO 61 BTU/MIN.

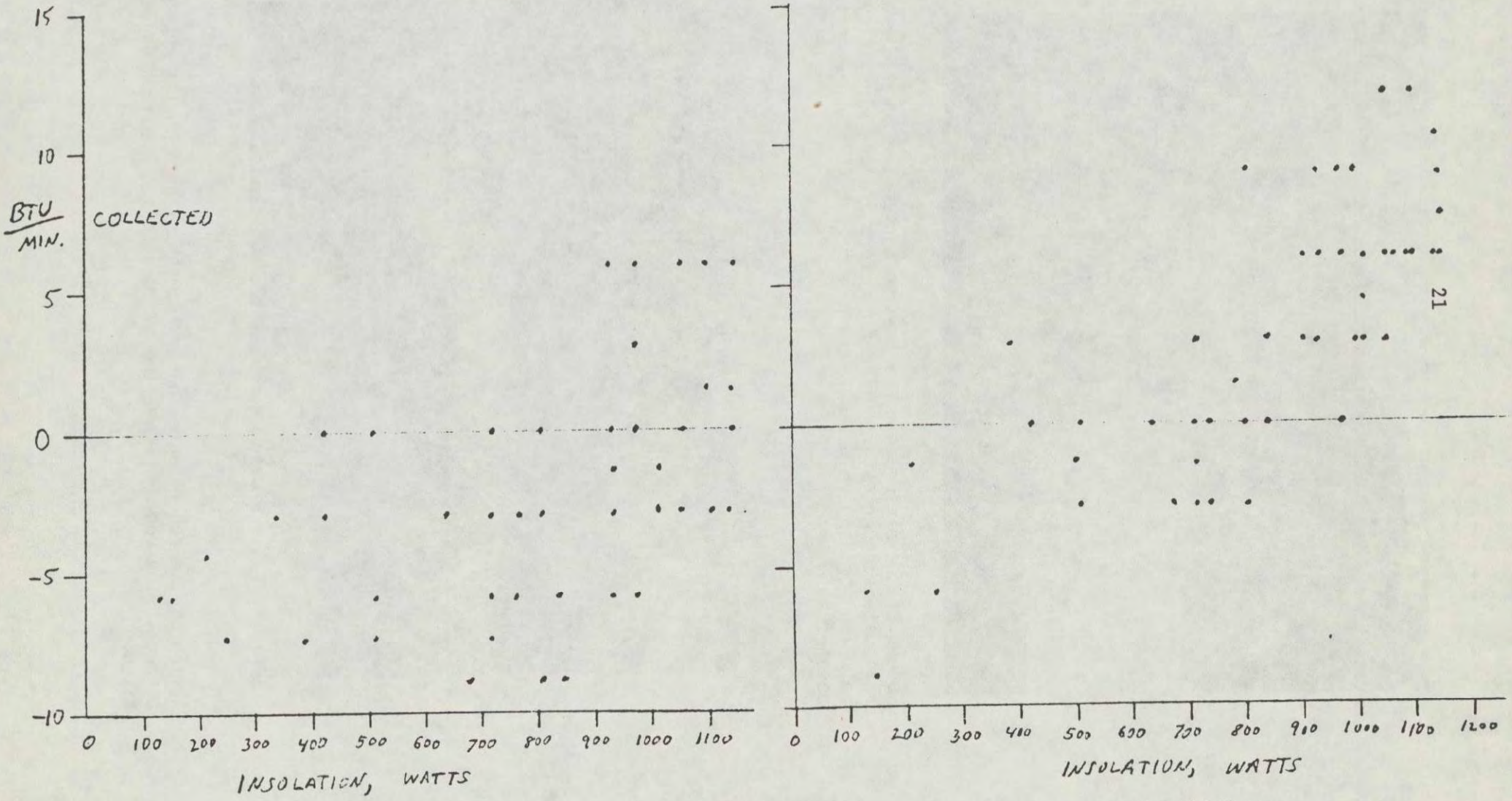

FIGURE 7

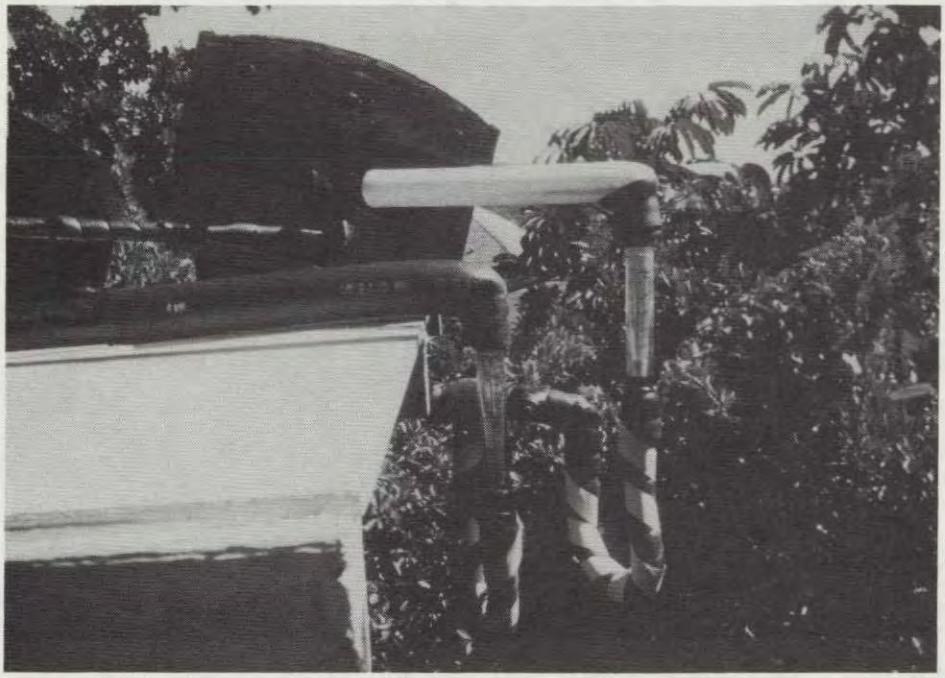

Closeup of the piping going to the two banks of evacuated and unevacuated concentrators. The flowmeters are the plastic cylinders. The white striping helps to keep me from bumping my head on the goosenecks.

A view of the concentrator banks from the stairs to the upper terrace. The roof is where the picture on the previous page was taken.

The four concentrators installed on the platform. Note how dark their interiors are. The insolometer is to the right of the right concentrator in the corner of the platform.

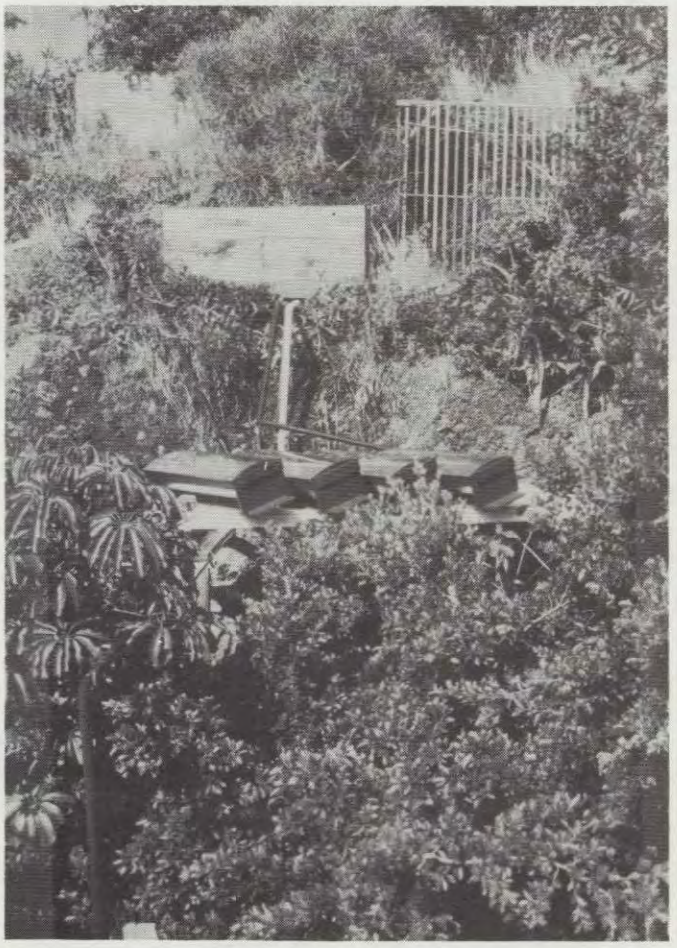

Taken from the roof of our house. The concentrators are installed on a mid-level terrace; the 82-gal. tank is on the next higher terrace for thermosyphon operation.

The pipes going down to the house are seen in the lower left.

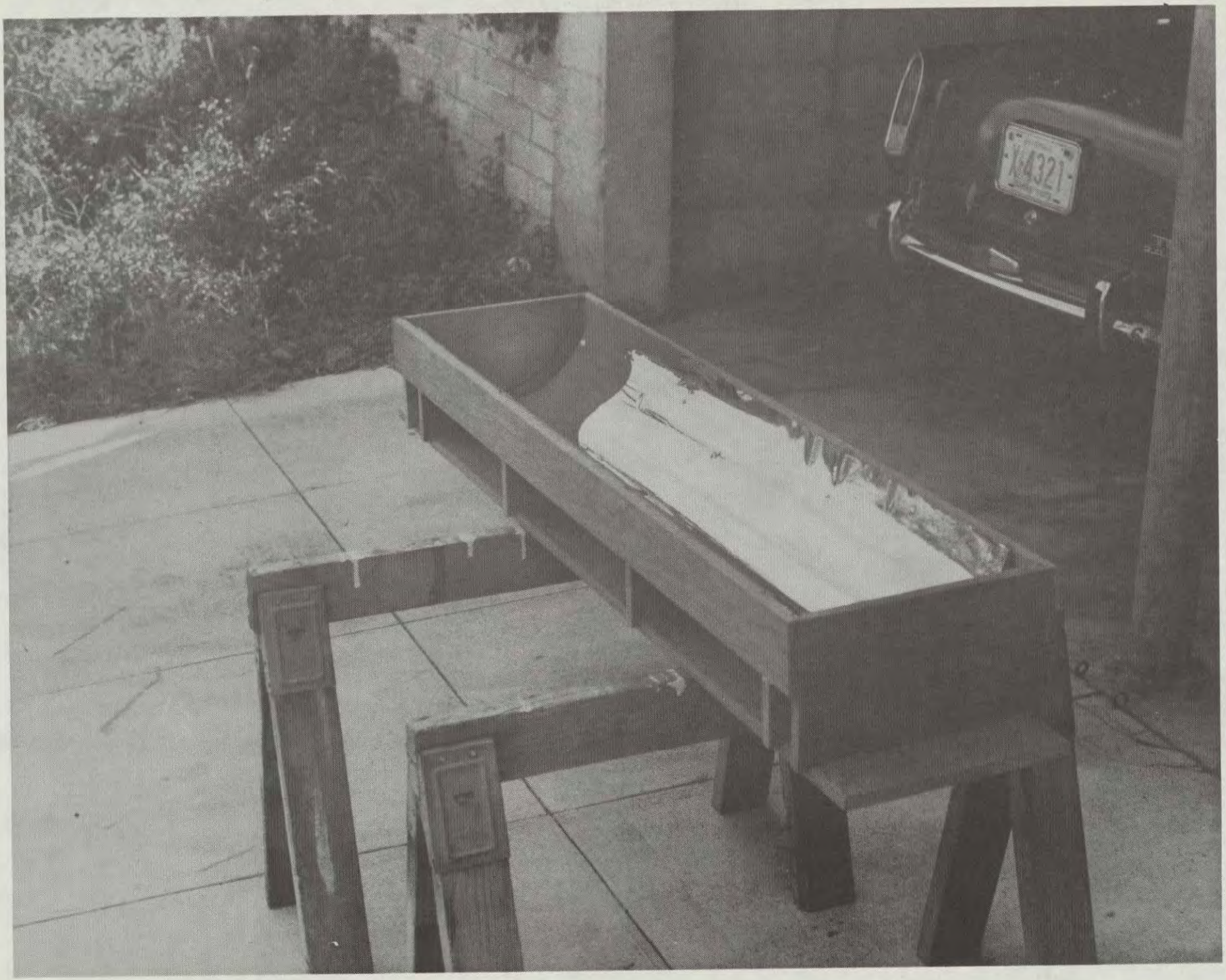

CONCENTRATOR ASSEMBLY

COAXIAL ASSEMBLY--END DETAIL

COAXIAL ASSEMBLY--END DETAIL

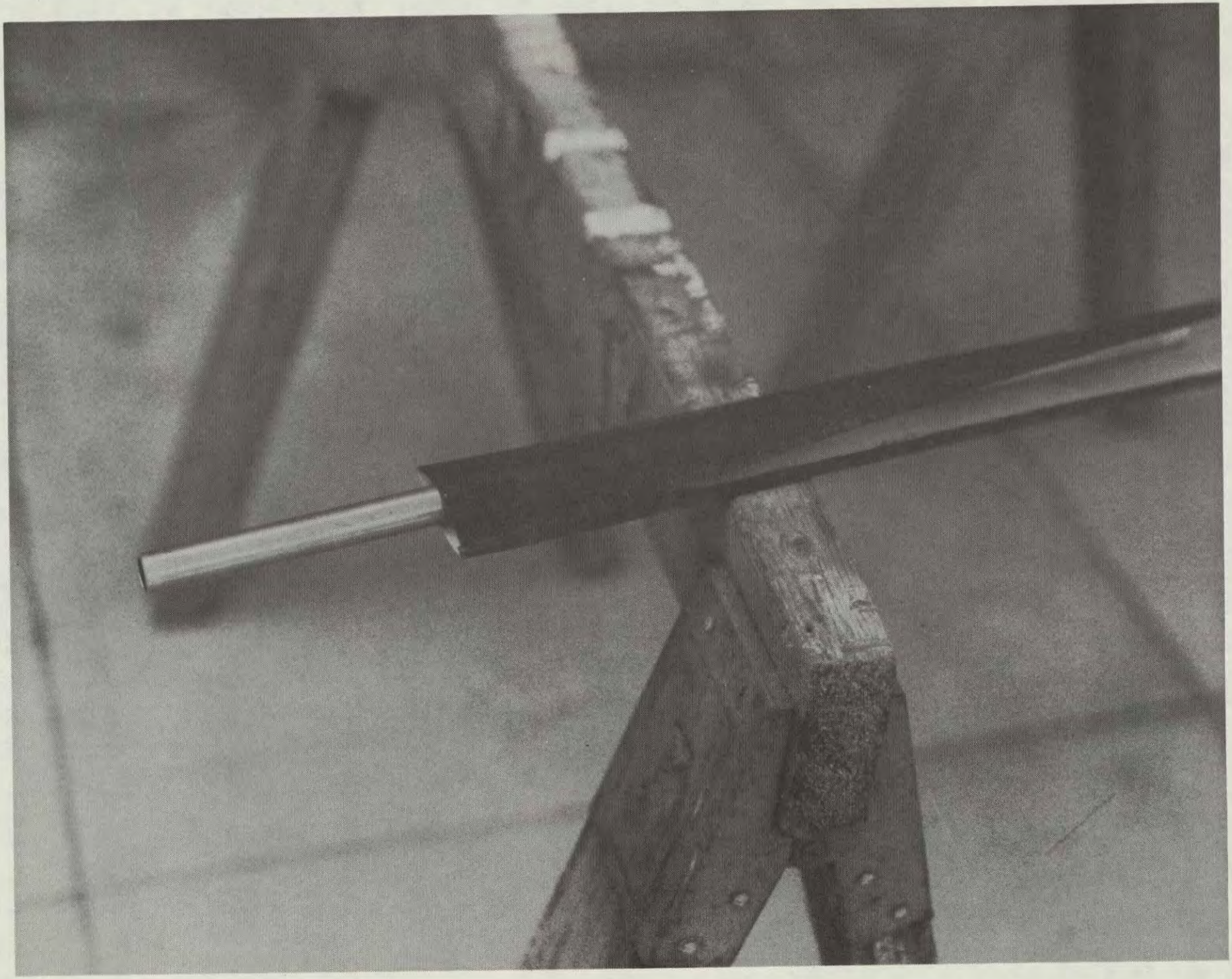

BLACK FOIL ABSORBER FOLDED AROUND COAXIAL TUBE

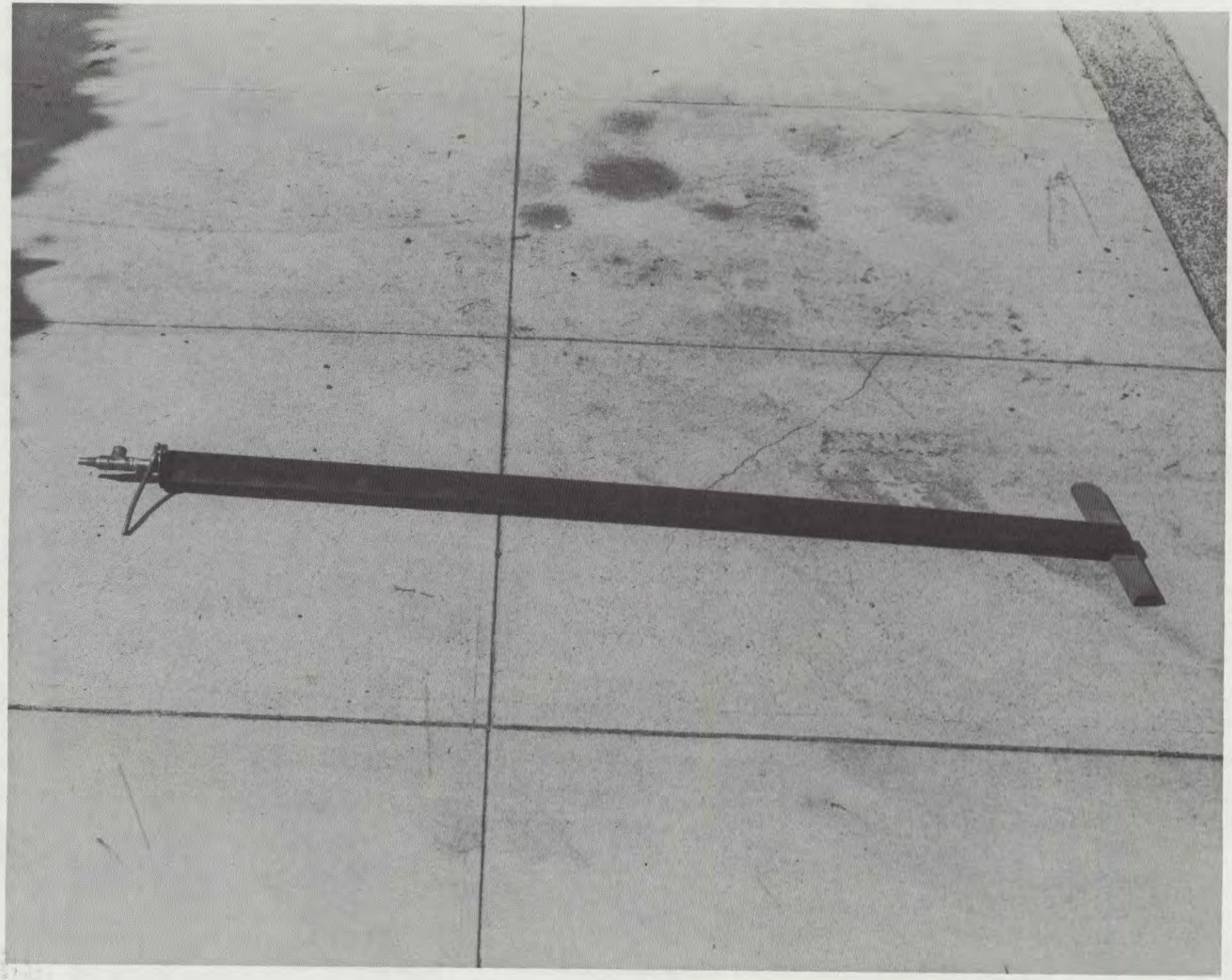

COMPLETED COAXIAL ASSEMBLY WITH BLACK ABSORBER INSTALLED

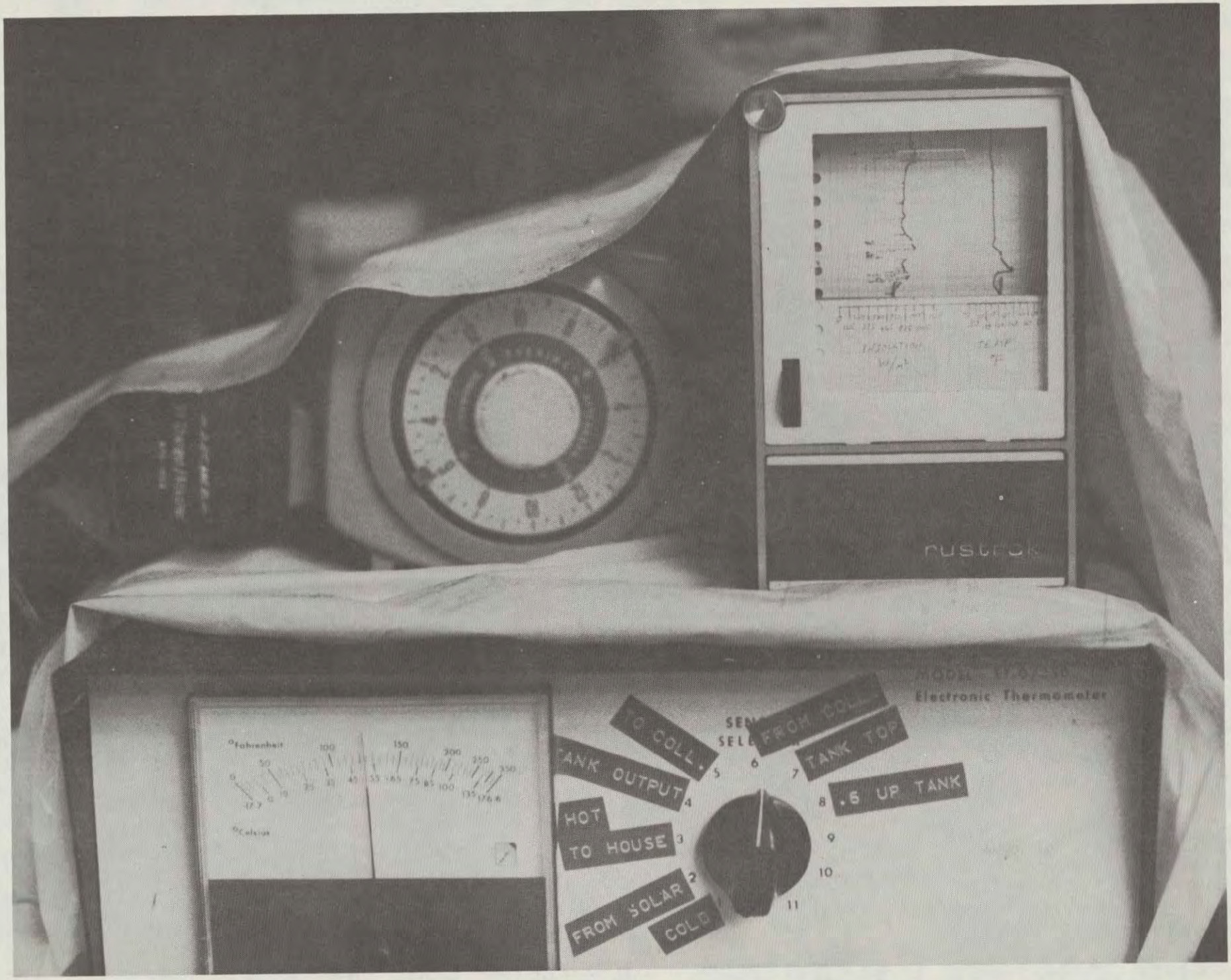

INSTRUMENTATION

III. Non-Tracking Concentrating Solar Collector Using Acylindrical Mirrors

Final Report: Grant No. DE-FG03-78SF-02009
Principal Investigators: Raymond T. Hebert
Douglas A. Reim

1.0 Introduction and Summary

This document is the Final Report on the U.S. Department of Energy's Appropriate Energy Technology Grant No. DE-FG03-78SF02009, summarizing work done from July 1, 1978 to December 15, 1980. The grant was to have funded development, testing, and demonstration of a unique, non-tracking solar concentrating collector panel for residential and commercial space heating and cooling, and for light industrial applications. (Higher efficiency at higher temperatures can result in reduced backup energy requirements for a given system cost goal, or reduced panel and storage requirements for a given system performance goal.) The design utilized acylindrical concentrating mirrors which form high-quality foci on each side of channeled flat-plate absorbers. Thermally sensitive valves at the end of each channel were to allow the panel to integrate energy and control flows for both direct and diffuse radiation.

1.1 Work Performed

Scope, schedule, and costs of the program were substantially altered as work progressed. The most outstanding reasons for these changes were the wide range of difficulties encountered with materials characteristics, fabrication methods, and performance. These are reviewed in Section 2.0 of this report. The results of work performed are summarized below:

* A prototype panel was fabricated and tested. See Section 4.0 for test results. For a number of reasons presented in Sections 2 and 4, the panel did not perform as expected. Corrective measures at this point are too costly and time consuming to be included in this program.

* A number of materials and fabrication methods were identified, documented, and tested. These are reviewed in Section 2.0 and design drawings are compiled in Appendix 3. Key materials did not perform as advertised. Others were victims of design errors. Most of the materials are petrochemical-based or energy-intensive in their manufacture. So prices have escalated dramatically since concepts were developed.

* The optical concentration ratios were measured (see data in Section 3.2) and found to be in general agreement with the theoretical expectations outlined in Appendix 1.

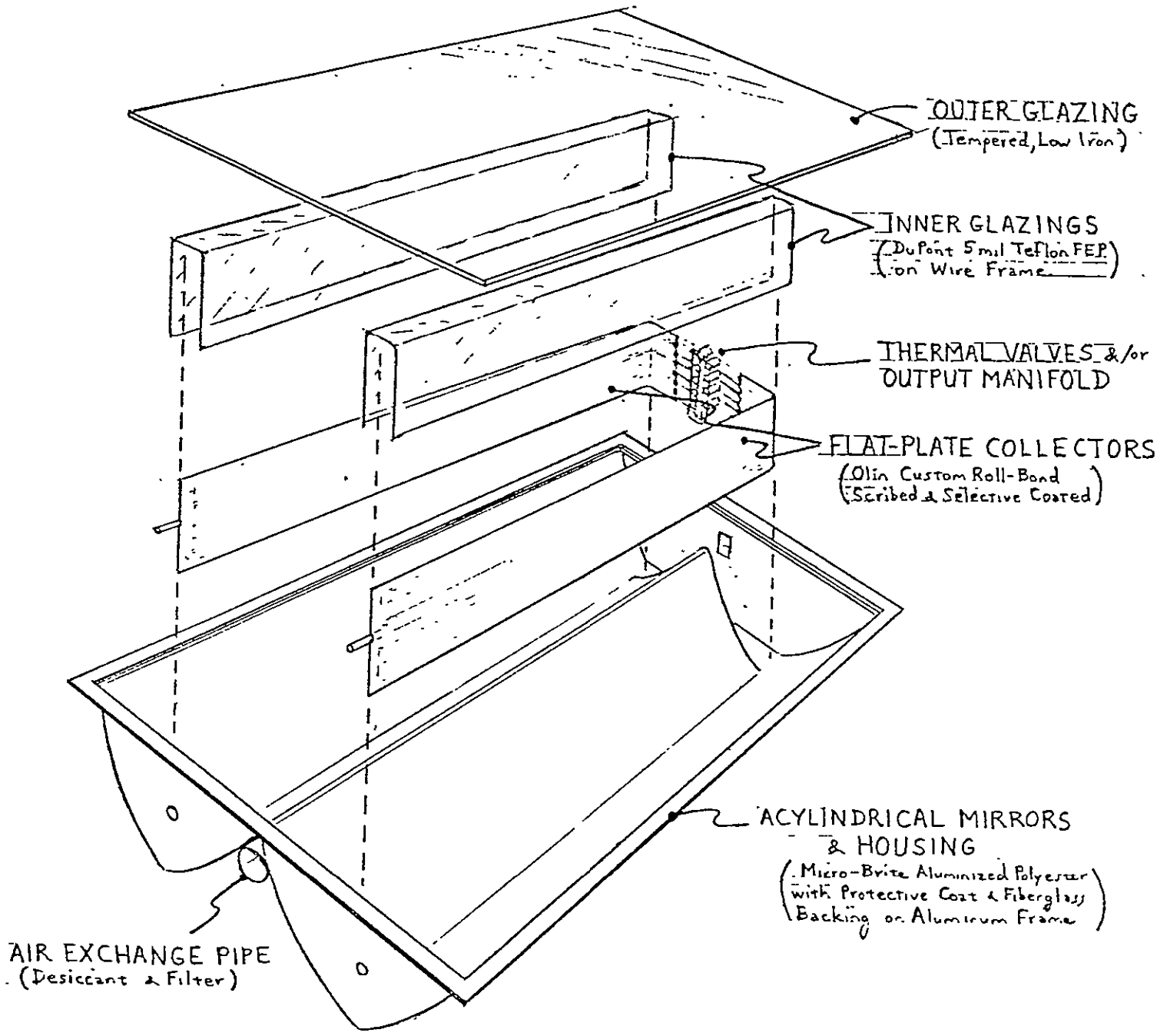

COLLECTOR ASSEMBLY AND MATERIALS

* Defects in the design have been identified and changes are proposed for improved operation in Section 4.0

* Some of the envisioned economics for material and labor are found to be impractical.

* Program schedule and budget overran. Budget deficits were absorbed by the grantee. (See Section 5.0)

* The patient application was rejected and abandoned.

Twelve panels were to be built, installed, and demonstrated in a residential system. While the materials have been purchased and partially fabricated, the additional panels were not fabricated due to performance below system requirements, and time and budget overruns.

Before the patent application was rejected and there was still hope of commercialization, plans called for one panel to be delivered to and tested by a certified testing laboratory. Under the circumstances, and due to the difficulties associated with running the tests, this was not done.

2.0 Progress Summary: Design and Fabrication

This section discusses the sequence of developments, and the materials and fabrication techniques employed for each of the major components of the panel assembly.

2.1 Optical Housing

The collector housing is a high-temperature polyester resin fiberglass mold that also forms the cylindrical mirror contours. The mold is formed around a welded rectangular frame of steel tubing which adds rigidity to the structure and provides a mounting surface for the tempered, low-iron glazing. All of these materials have low and nearly equal temperature coefficients that should result in a stable, weather-tight, reliable assembly. Fifteen such housings have been commercially fabricated using conventional chopper-gun application of polyester resin and fiberglass over a negative form.

The walls of the housing form the substrate for the optical surfaces, as shown in Figure 1. The theory involved in generating their shape is covered in Appendix 1. While the optical performance of the housing has in fact turned out to be quite satisfactory, early efforts were made to carry the mathematical expression describing the acylindrical mirror contours to a higher order in an attempt to further improve the focal quality. Howard Morrow, an employee of Lockheed, an independent optical consultant, and former coworker, was engaged to consider simulating the optical model in ACOS V (perhaps the most powerful of optical software packages) within reasonable financial limits. However, the number of variables and restraints, such as multiple reflections, packaging aspect ratios, overall daily and seasonal performance evaluation, etc., placed the cost of such an evaluation beyond the scope of this grant. However, Mr. Morrow's personal evaluation was that a higher order curvature was unlikely to yield truly significant improvements in

view of the tolerances to which the molds can be built. This opinion offered us the encouragement to continue with the existing and previously modelled design.

A set of precision templates were generated on a numerically-controlled mill according to the drawing of Sheets 1 to 4 in Appendix 3. These templates were used to check the contours of both the negative form and the housings during and after fabrication. These are shown in Figure 2.

Steps taken in the fabrication of the form are shown in Figure 3. Details and dimensions are on Sheet 7 of Appendix 3. Bulkheads cut from thoroughly dried 2" x 12" Douglas fir #1 were covered with grade A-A exterior 1/4" plywood to form the critical optical surfaces. Ends were boxed with lower quality plywood and the entire structure was mounted on a drip flange. Edges and corners were filled, assuring draft on all surfaces for a clean release of the molded part. In the process of sealing the form with a resin coat for a smooth finish, a wrong mixture was inadvertantly used, which failed to set up. Substantial rework was required, and the surface was never corrected to perfection. While it was of sufficient optical quality, some localized complex curvature would later result in difficulties in application of the reflective material. If this were to be done again, a thin sheet steel would probably form a much better prototype mold. A master form could then be made from the prototype.

A prototype housing was hand laid up on the form using a base gel coat for a hard surface finish, plus two plies of fiberglass weave and isophthalic bond-coat polyester resin. A welded 1" steel tubing frame was bonded into the outer edge to provide rigidity and a firm mount. With some difficulty, the housing was released from the form, and 3M reflective film was applied to the surfaces. The resulting prototype is pictured in Figure 1. A simple test demonstrated its ability to char black paper placed at its best focus. A more sophisticated evaluation used a laser to ray-trace reflections onto a focal-plane target for various angles of incidence (see Figure 4 and Section 3.2.1). Satisfied with its optical quality, the prototype was delivered to Vance Marine Company of San Jose, a commercial fiberglass shop, where subsequent housings were fabricated for slightly more than our materials costs; a task we gladly relinquished.

Application of a suitable reflective layer has taken considerable experimentation and effort. The originally proposed fabrication technique for the housing eliminated the secondary operation of reflective film application by directly applying the resin and fibergalss to the film, which was to be draped over the form. Used in this way, the film could also act as a release layer for easy removal of the mold from the form. The problem was to identify a material that would effectively bond to a direct application of polyester resin and fiberglass without separation, bubble entrapment, or print-through of the fiberglass weave. First experiments showed that polyester resin will not bond directly to polyester or acrylic films, as shown in the almost automatic release of Martin "Llumar" film from the sample on the left in Figure 5. It was also noticed that the minor shrinkage of the polyester resin around a fiberglass weave during curing resulted in a print-through of the weave to the reflective surface. These problems were initially overcome by using 3M "Scotchcal 3400" or FEK-244 reflective multi-layer acrylic films, supplied with a pressure-sensitive adhesive backing which appeared to be compatible with the direct application of the resin. The application of a gel-coat base, a second layer of fine-weave fiberglass tooling cloth, and

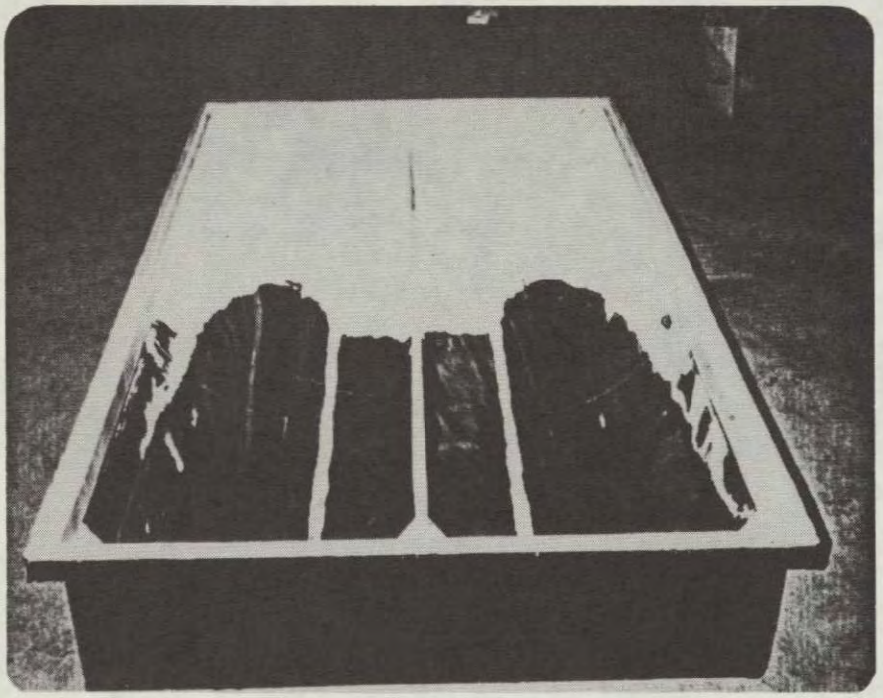

Fig. 1- Prototype housing with reflective foil.

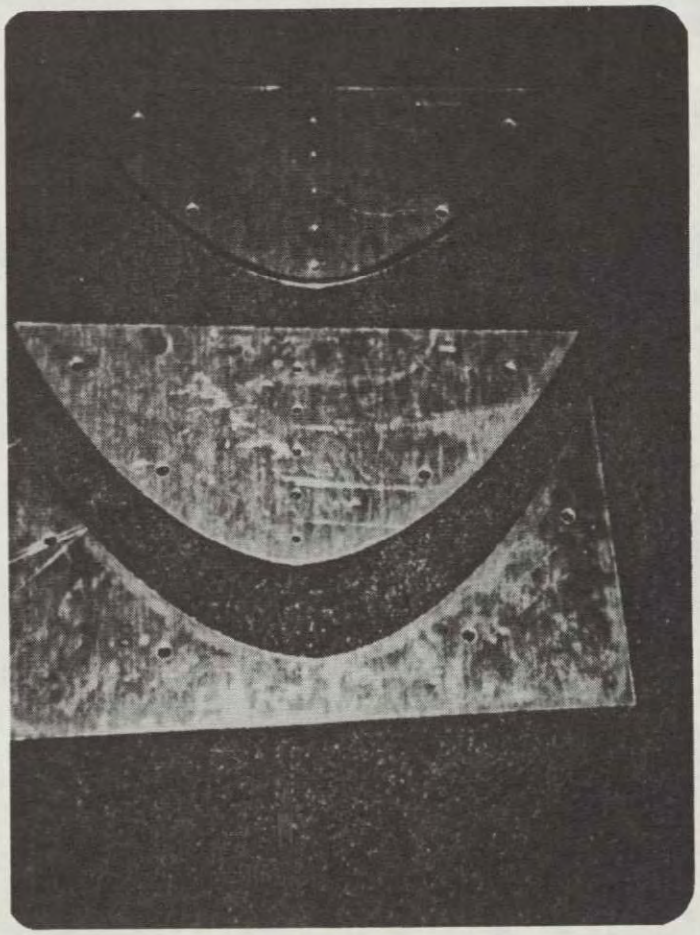

Fig. 2- Precision templates for generation and checking of form and housing contours.

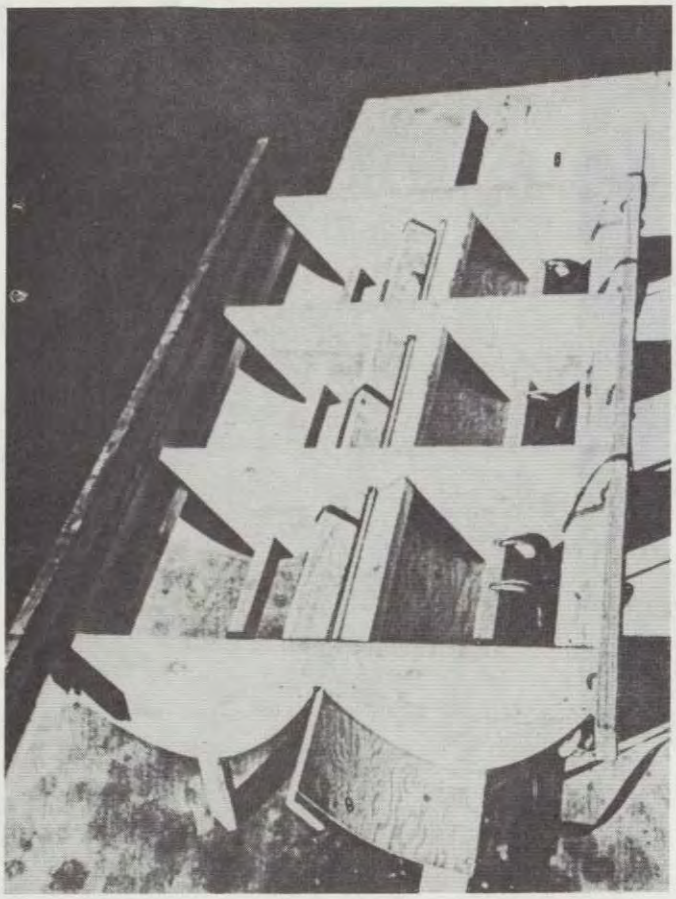

A) Form bulkheads.

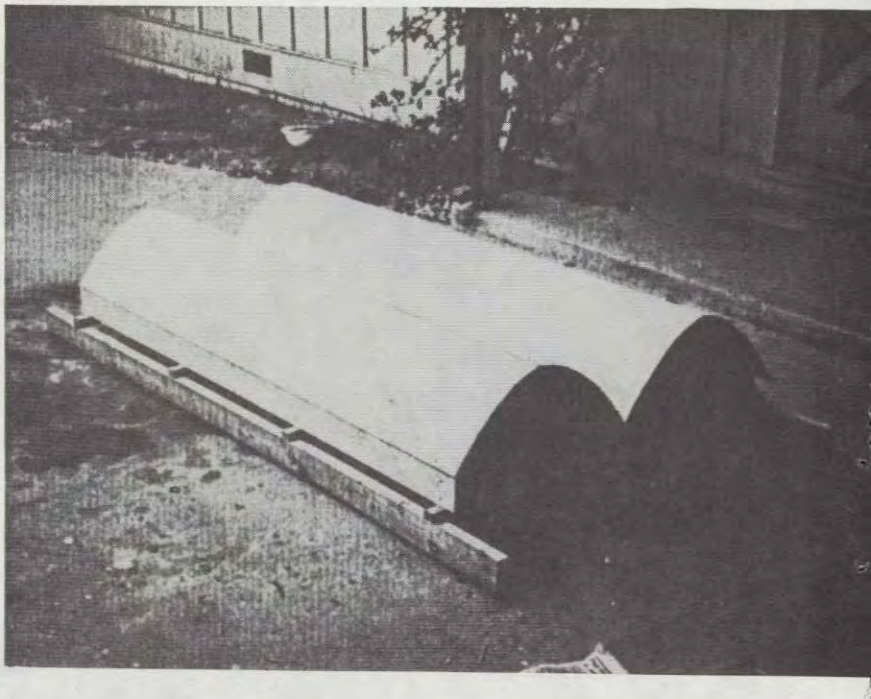

B) Plywood contours.

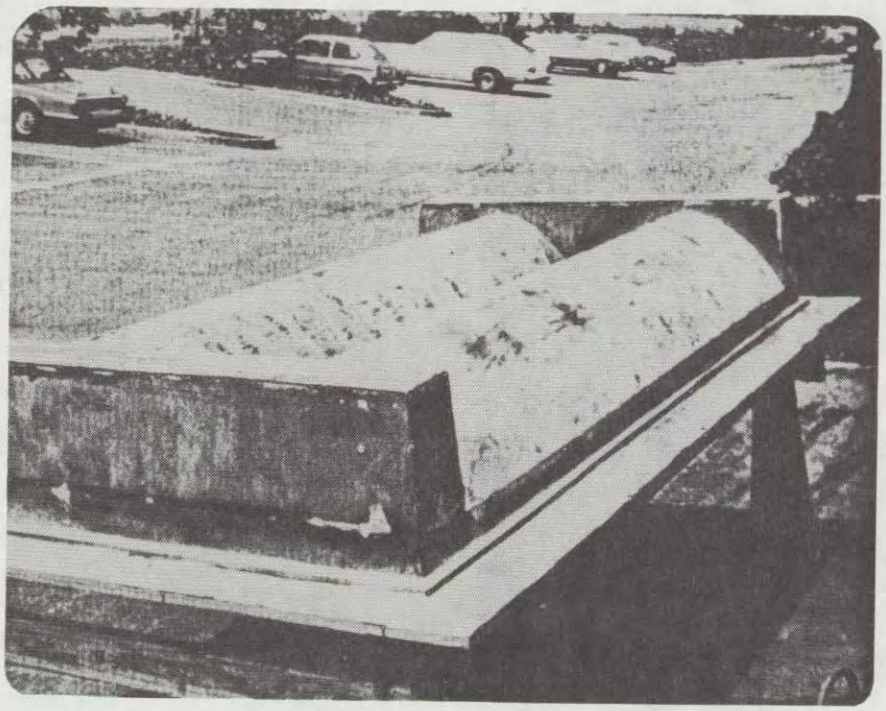

C) Form nearing completion.

Fig. 3- Housing Form Fabrication

subsequent layers of coarse or random-weave fiberglass for strength sufficiently eliminated the print-through. Destructive testing of such 3M samples exhibited excellent bond strength, with films tearing before releasing. Vendor's specifications with respect to temperature, flame spread, moisture, and fungus resistances were more than adequate for this application. Solar reflectance was a minimum average of 86% over the useful spectrum, and the product was available in a high angular resolution form (FEK-244), or the lower cost 5400 which would have been adequate for this application. However, when this technique was tried on the full-scale form, the minimal shrinkage of the polyester/figerglass during curing was enough to distort the film into a large fish-scale pattern. While an elaborate vacuum hold-down scheme may have helped, less exotic approaches proved unsuccessful, and the technique was abandoned.

The failure of the direct-application technique necessitated applying the reflective film in a secondary operation. Having had the 3M materials on hand, the most obvious approach was to use the manufacturer's recommended application technique; a detergent and water solution squeegeed out from between the film and the housing. Initial adhesion was excellent. Laser ray-tracing and solar concentrations confirmed the optical quality. Manufacturer's data suggests excellent lifetimes in direct exposures except for some slight edge-lifting in high temperature and humidity environments. But when the completed housings were convered and stored in a cool and humid environment (a garage) bubbles began to form uniformly across the surface, similar to those shown in Figure 1. Degradation continued to the point where the assemblies were totally unusable. Efforts were begun to identify the failure mechanism and corrective techniques and materials. The manufacturer's information suggested improper surface preparation, but a review of past actions and future experiments were to show that this was not the case. It was theorized that trapped soap solution from the recommended application procedures may have been a cause of failure. Cylindrical fiberglass samples of about 1 sq. ft. were prepared and thoroughly cleaned. Sample bonds were prepared using the 3M method, the originally proposed resin, distilled water, Loctite anaerobic adhesive; and various organic liquids in hopes that trapped residuals may be absorbed into the plastics and rendered harmless. In all, nine samples were temperature-cycled at 100% relative humidity between observed temperatures from 50°F to 170°F. (The chamber was a housing covered with a glass plate and placed in a sunny location with enough water to maintain a saturated atmosphere.) Most samples began to show failure within a few days. The most successful sample was the resin bond, shown in Figure 5B, which failed within a few weeks. It was found that failure was inherent to the 3M material. Further weathering showed that both the bond and the sandwiched acrylic layers failed. But the majority of the failure took place in the outer acrylic layer, even though this was partially protected from solarization by the outer glazing layer. Use of the 3M materials was abandoned.

Samples were then prepared using a conventional 5-mil metallized polyester film, consisting of a 2-mil metallized film protectively bonded with a 2-mil clear film. Such material is available from several sources, but most preferred (pending testing) is a U-V and shrinkage-inhibited version manufactured by Martin Processing, Inc., of Martinsville, VA. Bond samples were prepared using polyester resin, Loctite Super-Bonder 420, Dow-Corning Silicone Rubber Coating 8663, 8663 with 1204 primer on mildly abraded surfaces, and a

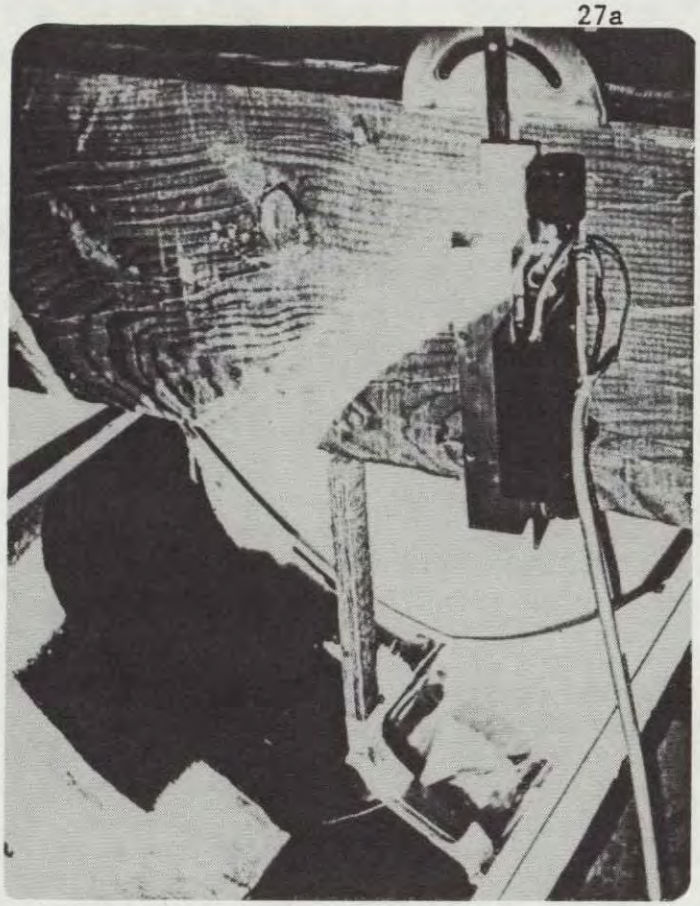

Fig. 4- HeNe laser being used for a ray trace check of the prototype reflective housing facets.

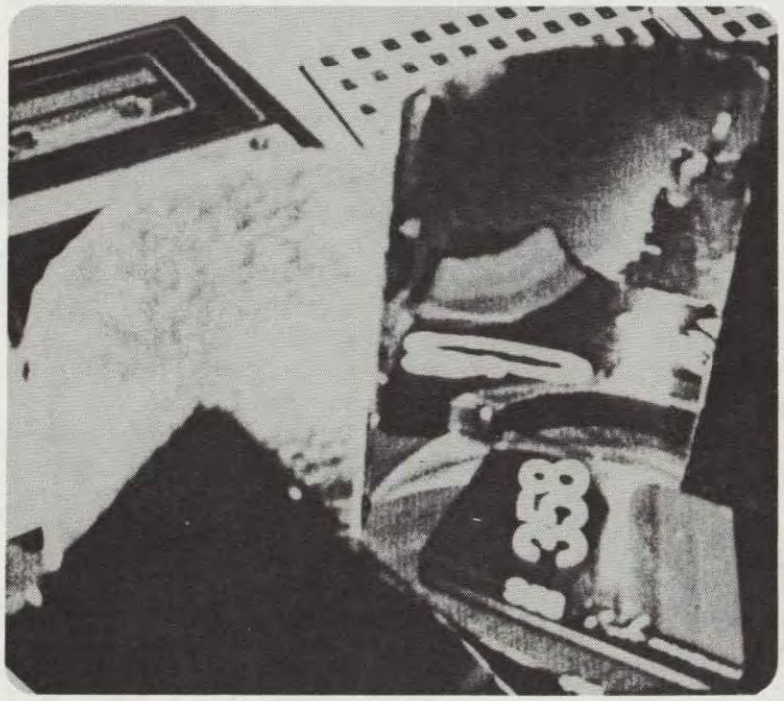

A) Reflective fiberglass sample on right made with 3M film with adhesive backing. Polyester film on left released immediately. Both had substrate molded directly to the film.

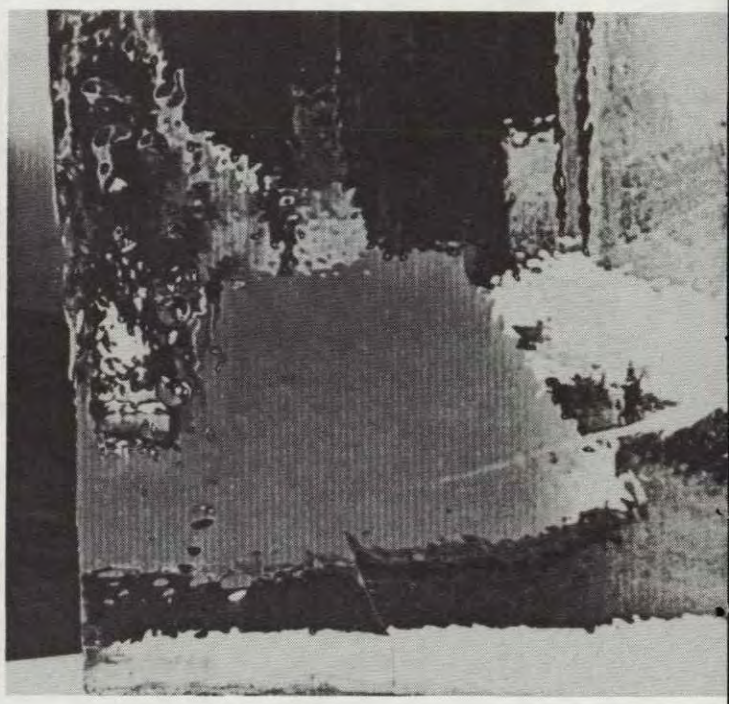

B) A resin-bonded sample after humidity tests. One of many failures.

Fig. 5- 3M Reflective Sample Experiments

A) A silicone-bonded reflective polyester sample. Both surfaces are lightly abraded and primed before applying liquid silicone.

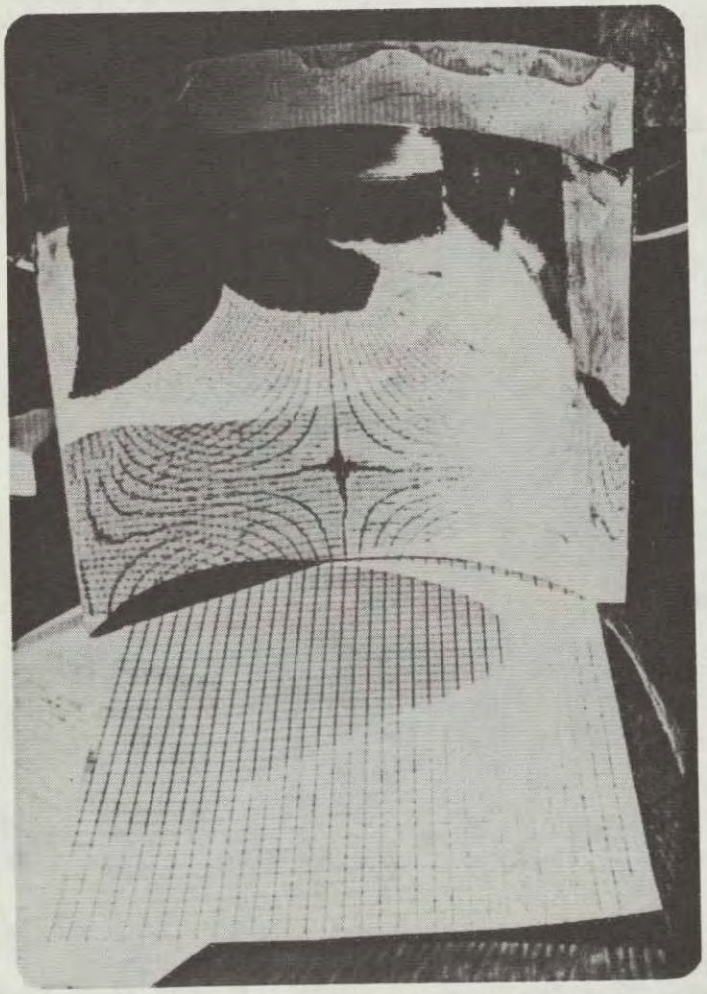

B) After ten weeks of extreme temperature and humidity cycles, the sample shows only minor degradation.

Fig. 6- Silicone Bonding Technique

grid of pressure-sensitive acrylic (3M-465) tape. Of these, the tapes showed sufficient adhesion with some distortion directly over the tape, but differentials in film and substrate temperature coefficients caused minor wrinkling of the film.

The primed 8663 silicone bond, shown in Figure 6A, has shown excellent bond strength, with the bond shearing rather than releasing from either surface when peeled off. In ten weeks of extreme temperature and humidity cycling, only minor degradation was apparent, as illustrated in Figure 6B. The recommended materials for this technique, and associated manufacturer's claims are as follows:

Material	Temp Range		Life*	Other
Material Llumar film	-70°F	350°F	10-15 yrs	R-86%
Dow-Corning 8663	-85°F	450°F	N/A	+1204 Prim.
Dion Iso 6631T Thermoset polyester resin and chopped fiberglass		275°F	N/A	Available: fire-retard. U-L approved

*Only the film is exposed. The glazing should block most of the harmful U-V and other weather-related wear factors.

This technique was used to fabricate the reflector housing for the prototype panel assembly. The technique is labor intensive, but this can be overcome. Particularly troublesome were the areas of compound curvature (due to form imperfections) where bubbles tended to form. For best results, the silicone is applied generously, with the excess being rolled out to eliminate bubbles. Care must be taken to keep the silicone off of the face of the film. Since this fabrication was a learning exercise, the results were cosmetically flawed, but the housing is optically functional and has shown no signs of degradation.

2.2 Linear Flat-Place Collector Arrays

The two collector plates in this design consist of a linear array of parallel flow channels with a common input header and a valved output header. With proper design of this configuration, any individual channel can intercept focussed radiation directed to it by the mirrored housing, and the valved output header can select the proper flow without further need of tracking the sun.

In the design of this plate, it is desirable to minimize lateral conduction between channels in order to preserve the inherent solar concentrating ability of the optics, as discussed in Appendix 1. Furthermore, it is necessary to allow for differential thermal expansion between channels in order to prevent "oil-canning" or bowing of the plate, which would cause the unit to defocus. (A 55°F differential would cause a 1" bow.) Originally, we had hoped to use an Olin "Roll-bond" or Butler "Terralite" product to avoid fabrication expense, and provide intermittent punctures or small slits between

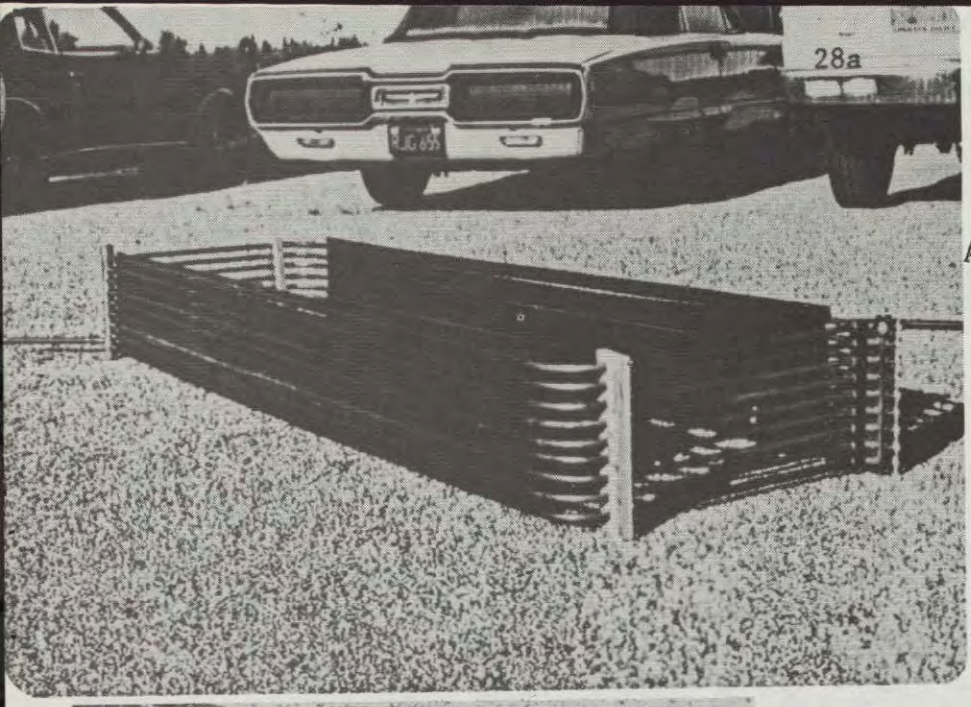

A) Early flat plate and valve assembly.

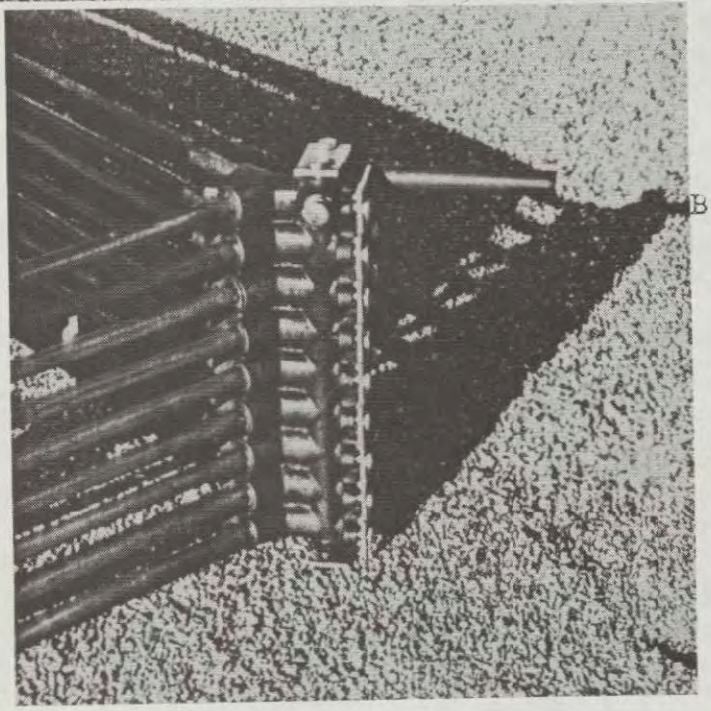

B) Closeup of the selective foil fins.

Fig. 7- Absorber Plate Configurations

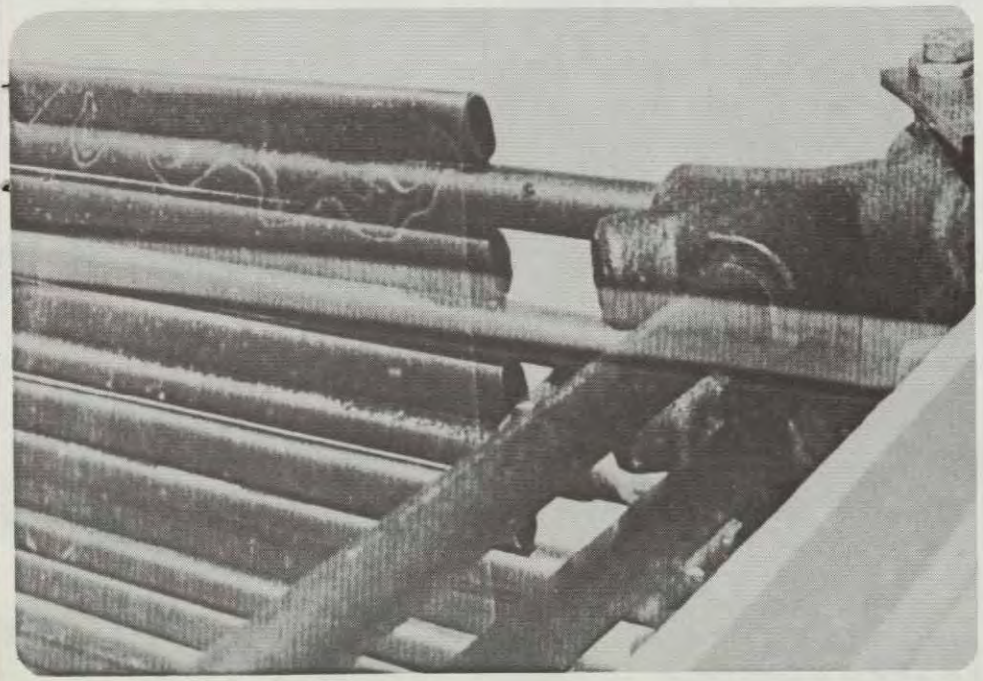

C) Closeup of the deformed pipe fin, with the inner glazing in place.

channels to discourage lateral conduction and allow for differential expansion. But the differential expansion can be so severe (especially under stagnation conditions) that the suspending web of material would be torn apart. (A 300°F differential would cause a differential length between channels of 1/4".) So the design was modified to incorporate a linear array of thin-wall copper tubes that could expand independently. Unfortunately, this requires added labor and material.

Several tubing configurations were tried over the course of the grant. Two are pictured in Figure 7. Approximate calculations of the heat loss were done for each configuration, as summarized in Appendix 2.

The first attempt (not pictured) called for 5/8" copper tubing to be flattened, plated, and mechanically tied together with slip fittings to form the array. Tooling was fabricated and samples were roll-formed at S & R Enterprises in Hayward, CA, to evaluate this approach. The results were unsatisfactory in that the samples developed excessive waviness along their length. No fault could be found in the tooling. It is theorized that the flattening of the tubing relives spiral stresses set up in the copper tubing when it was extruded. (It has since been found that tubing can be satisfactorily press-formed rather than roll-formed.)

The second approach used unmodified 3/8" Type M copper tubing wrapped with selective black-chrome plated 5-mil copper foil from Berry Solar Products of Edison, N.J. Samples prior to order were of good quality, and could be soldered (as advertised) or bonded with Loctite anaerobic adhesives with a tight wrap. While not as attractive in terms of labor and material as the original "Roll-Bond" concept, this approach was more attractive than the formed-tube method since it used less copper and provided selective plating for $50 per assembly versus $117 for the tubes. The foil was ordered in rolls, precut to 2.82" wide. However, when received after a long delay, the product was of poor quality, accompanied by a letter claiming it was "within specifications." The new foil could not be soldered without discoloring the plating, and we were having difficulty forming the foil over a long length to get a tight enough wrap for anaerobic adhesives to function properly. A dry-contact, silicone adhesive, 10-mil tape was ultimately used to make the bond. But while both theoretical (see Appendix 2) and initially measured temperature gradients were acceptable, performance quickly degraded as panel assembly tests began. A new approach was required and, as the foil was laboriously removed, bubbles and air pockets were discovered interspersed with areas of excellent adhesion. So with proper tooling and, perhaps, surface preparation, it may be possible to make this approach work.

With time growing short, the final configuration was assembled (Figure 7C) by soldering slightly crushed tubing (material on hand) to the flow channels, and painting the entire assembly flat black. The configuration is neither cost effective nor performance effective compared to what should be achievable. This is the configuration, however, that was installed in the assembly of Figure 10 so that some testing could be accomplished under this grant program.

2.3 Thermal Valves

The thermally sensitive valves automatically select the collector zones receiving focussed energy and regulate fluid flow (integrate available solar energy) to obtain desired operating temperature from any zone capable of delivering it.

The valve, as implemented, is functionally illustrated in Figure 8A. Since the two troughs of the collector assembly are identical, corresponding zones of each plate should receive equal energy, so a single valve function is shared between them. In each valve, a bleed orifice in the valve is closed to keep the valve informed of the zone temperature. When the valve's power element (an automative, encapsulated paraffin device) is elevated to a temperature in excess of 160°F, it's push rod begins to force the ball valve open against the spring pressure and allows increased flow in its channel with respect to flow in other cooler channels.

As a first step, a single valve cell was designed and fabricated to test the principle and operating characteristics. The valve was designed with a viewing port to observe the mechanism's reaction to temperature and pressure, as shown in the photographs of Figure 9. This test was completely successful within its limits. What was not recognized at the time was that this experiment simply tested the valve's response to a uniform supply of hot fluid, and did not regulate the fluid's temperature as it does in the panel. The influences on the valve's performance, as they are now recognized, are illustrated in the closed-loop control concept of Figure 8B. Lulled into an open-loop frame of mind by the test's "success" and distracted by other project catastrophes, the critical closed-loop parameters k_2 and k_3 were virtually ignored in the design of the cast valve assembly of Figure 7B and Sheets 8 and 9 of Appendix 3.

When testing of the panel assembly began, the valves were noticed oscillating (too much gain and/or too slow of a response). At this point there was little that could be done except to coax data out of the panel by manually controlling flow rate in response to the monitored output temperature of the hottest zone. Considerations for valve redesign are listed in Section 4.0.

3.0 Tests and Results

Several aspects of the integrated collector assembly were observed, tested, and measured. These have led to a good understanding of the strengths and shortcomings of the system.

3.1 Optical Efficiencies

Along with manufacturers' data, efficiencies of optical elements encountered in the light path are listed below as they were measured by laser beam and by solar power meter:

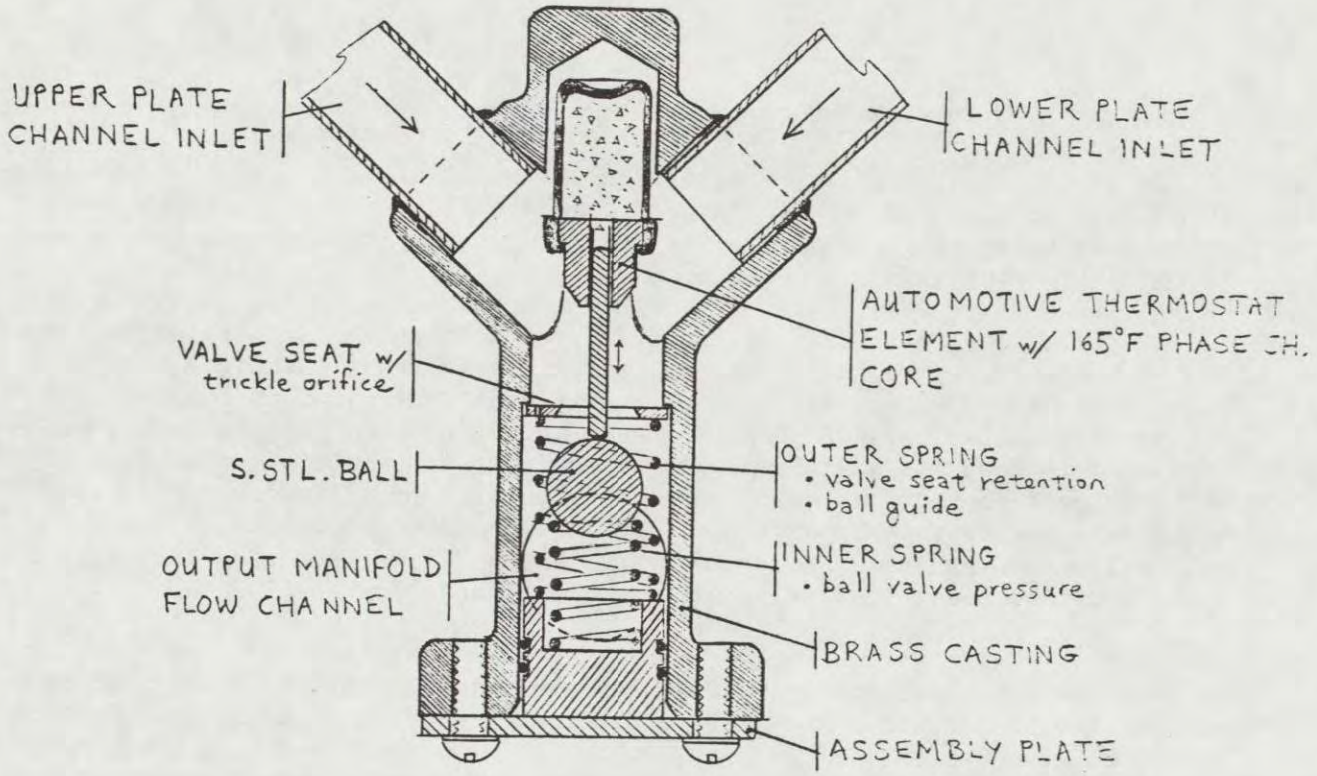

Fig 8A - Thermal Valve Cross-Section & Assembly

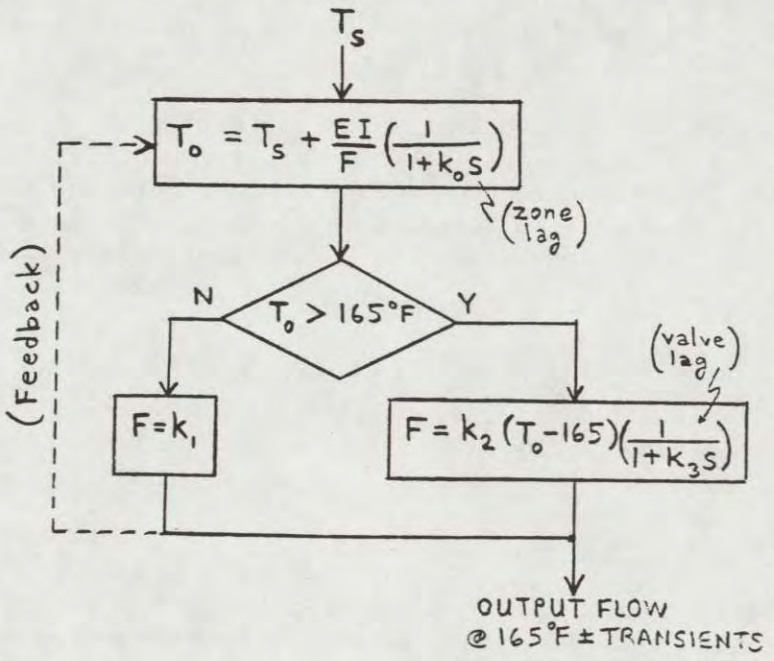

T_s = storage temperature
T_o = zone output "
I = insolation
E = zone collection efficiency
F = fluid flow rate
k_o = zone response time
s = complex variable
k_1 = orifice flow rate
k_2 = valve gain
k_3 = valve response time

Fig 8B - Model of Valve Response

Element	Transmittance/Reflectance/Absorptivity			
	laser msrmt.	solar msrmt.	mfgr's data	assumed value
3/8 Temp Gl.	.87	.84	.82	.84
Fep Inner Gl.	.94	.97	.96	.96
Refl. Polyester	.85	.89	--	.87
Black Paint	--	--	--	.95
Overall				.67

Measurements were made with a silicone photocell. Valves shown are the ratio of power measured behind the element to that measured in front of it, with the surface at near normal incidence to the source. The assumed value is the average of all data.

Absorptivity of the black paint was not measured, since such measurements are difficult to make without special equipment.

3.2 Optical Concentration

As a visual indication of the workings of the concentrating optical surfaces, Figures 10B and 10C show two interesting close-ups of the assembly. Upon close inspection, the inner glazing's specular reflections of the linear foci can be seen on the third zone from the top of each array. The foci are of good quality and are fully captured within one zone. Figure 10C observes the same inner glazing reflection back through the focussing mirror, on axis in cross-section but off-axis in azimuth to avoid shadowing. This back-reflection nearly fills the entire mirror, giving a feeling for the optical concentration at its best. A close observation of Figure 10C also shows the foci on the opposite sides of the arrays down on the bottom two zones.

Aside from appearance, solar concentration was also measured by laser ray-tracing and by photocell.

3.2.1 Laser Ray Trace

Before delivering the initial housing mold to Vance Marine Company for reproduction, a laser was used for ray-tracing across the surface to confirm its function. As shown in Figure 4, a board was placed in the plane of the exterior glazing to hold the laser jig. The angle of the laser could be adjusted to simulate angle of incidence and it could be moved along the board (along the cross-sectional axis so that the beam could enter the glazing at chosen points across the $\pm$11" aperture. A scale at the focal plane checked beam displacement.

Data is plotted in Figure 12 for 0°, 16°, and 32° angles of incidence across the aperture (outer glazing). The displacement in the plane of the array is designated by zone and in inches. Where the beam hits the scale directly, the curves are so labeled.

While a few irregularities exist in the curves, they show approximately what was expected of them from Appendix 1.

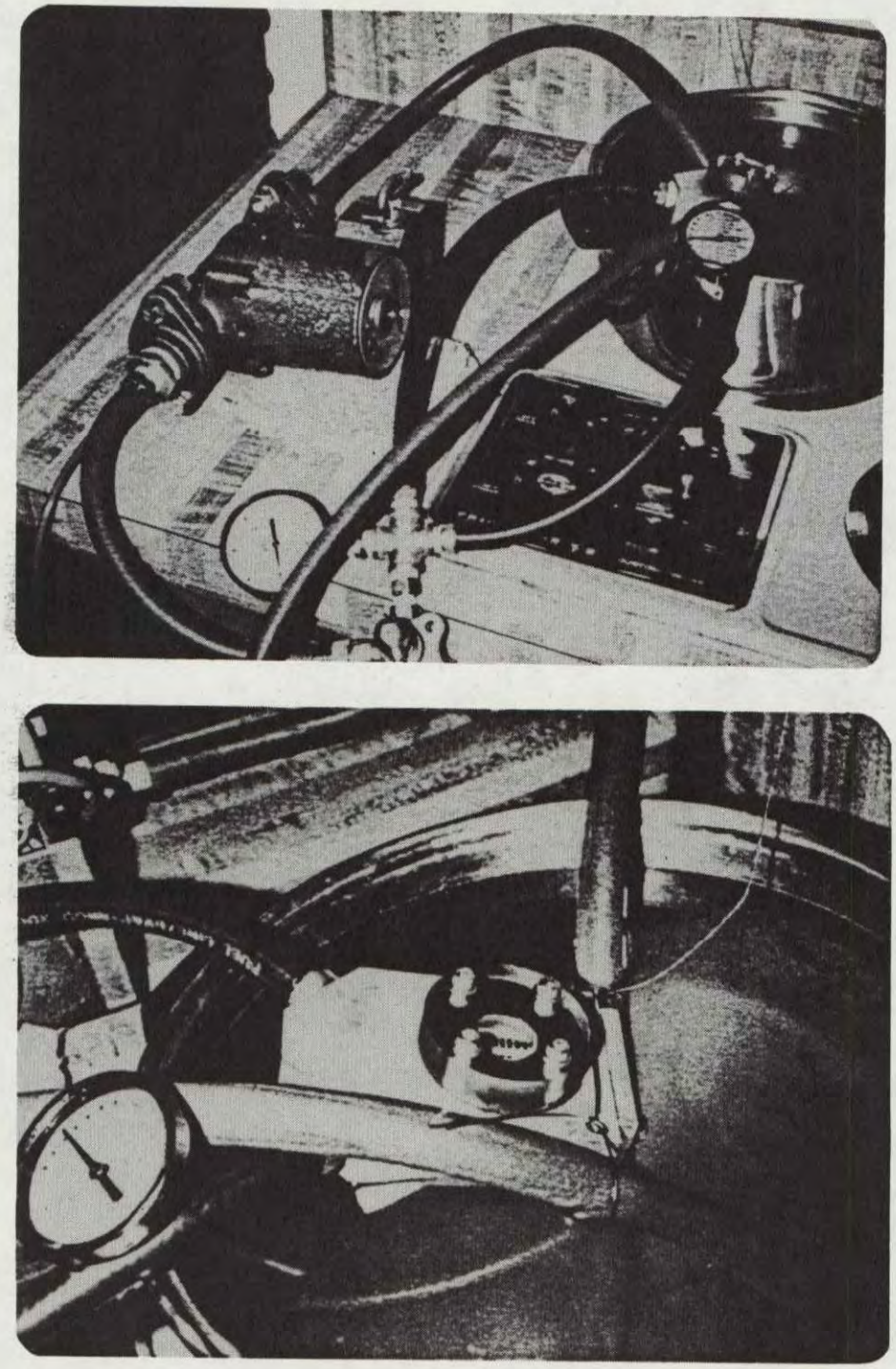

FIGURE 9 - Experimental testing of a single valve with temperature and pressure. The window on the valve allowed viewing of the mechanism

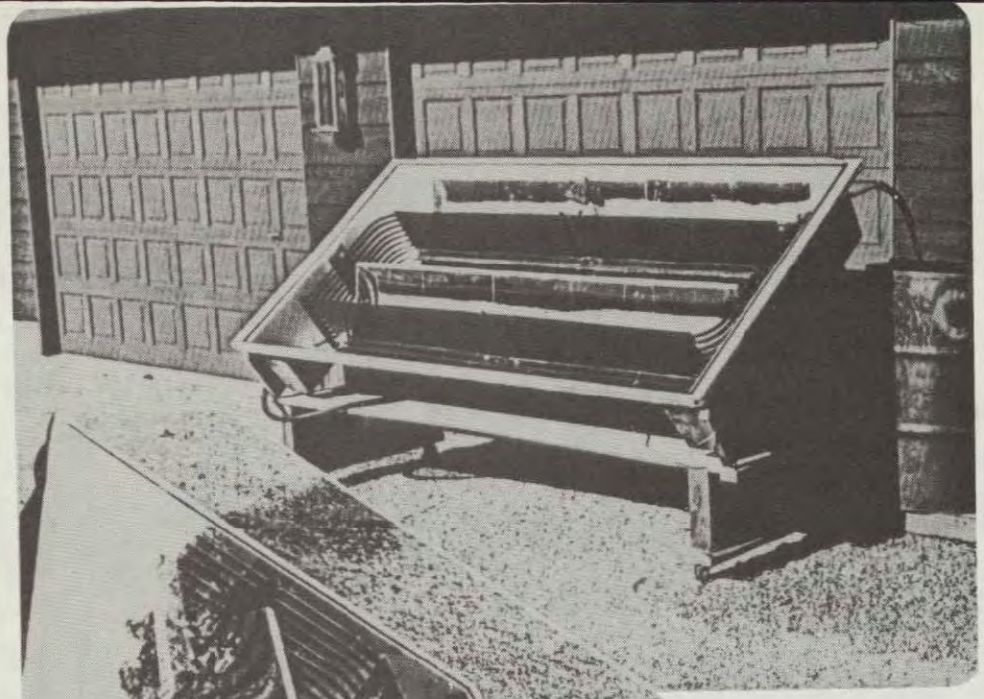

A) Final Collector Assembly.

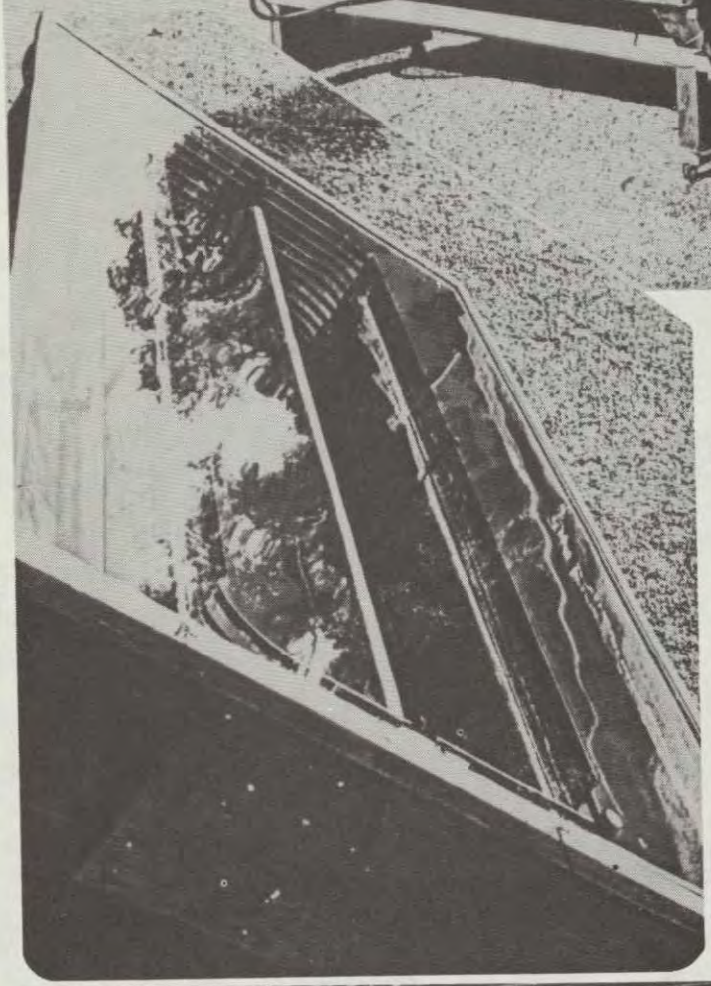

B) Upper foci can be seen on the 3rd zone of each plate.

Fig. 10- Views of the Final Assembly in Operation

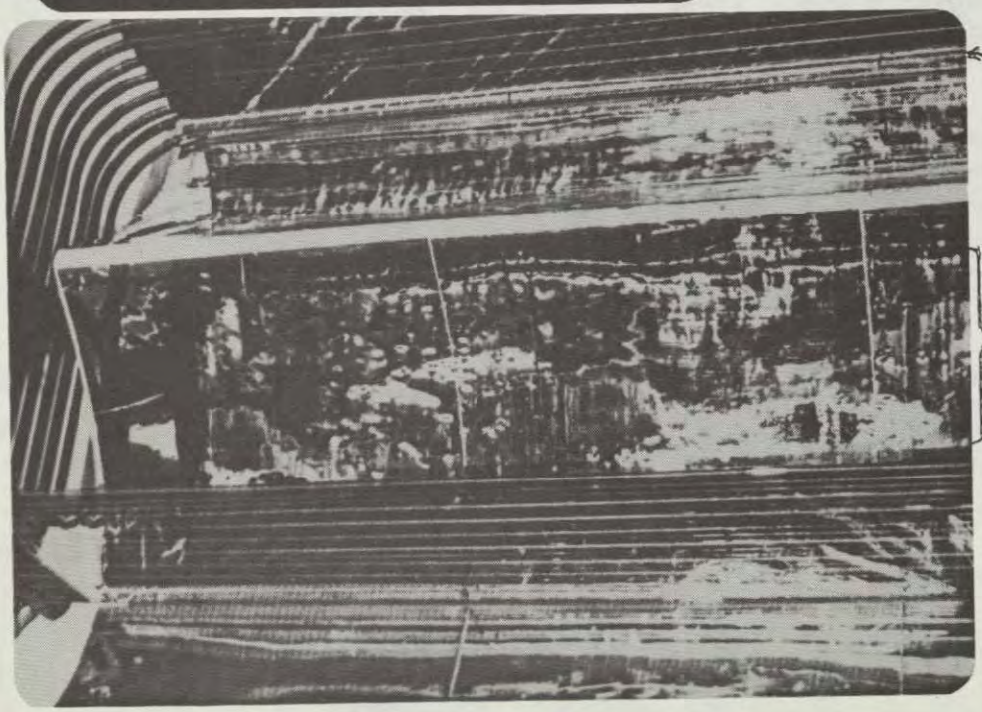

lower focus

C) Back reflection of the focus off the inner glazing, magnified as the sun sees it.

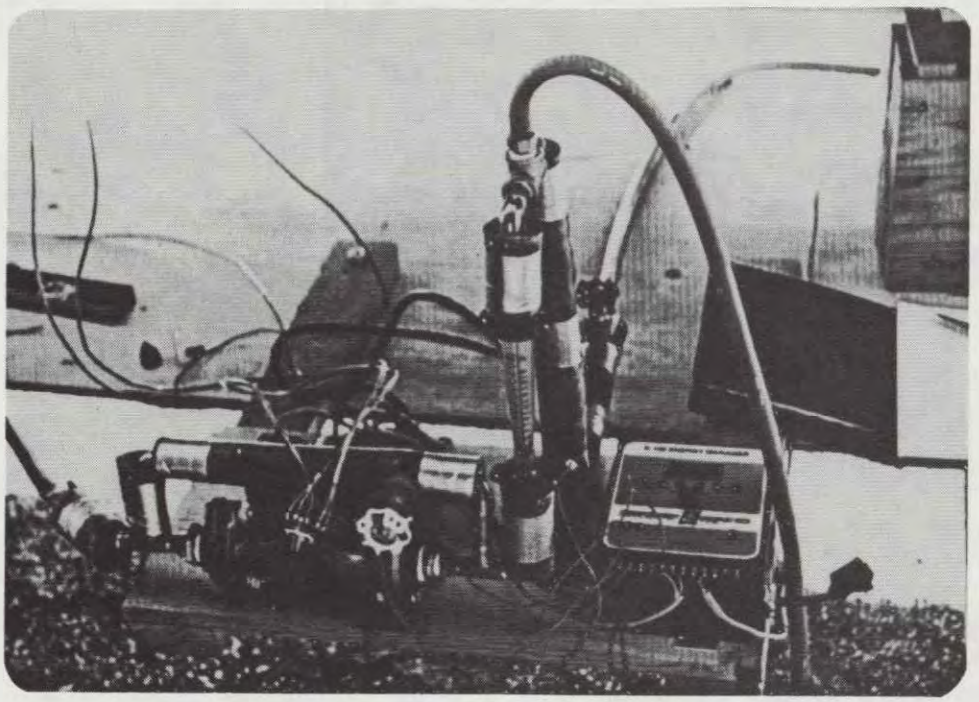

Fig. 11- Closeup of the test setup, shown schematically in Figure 13.

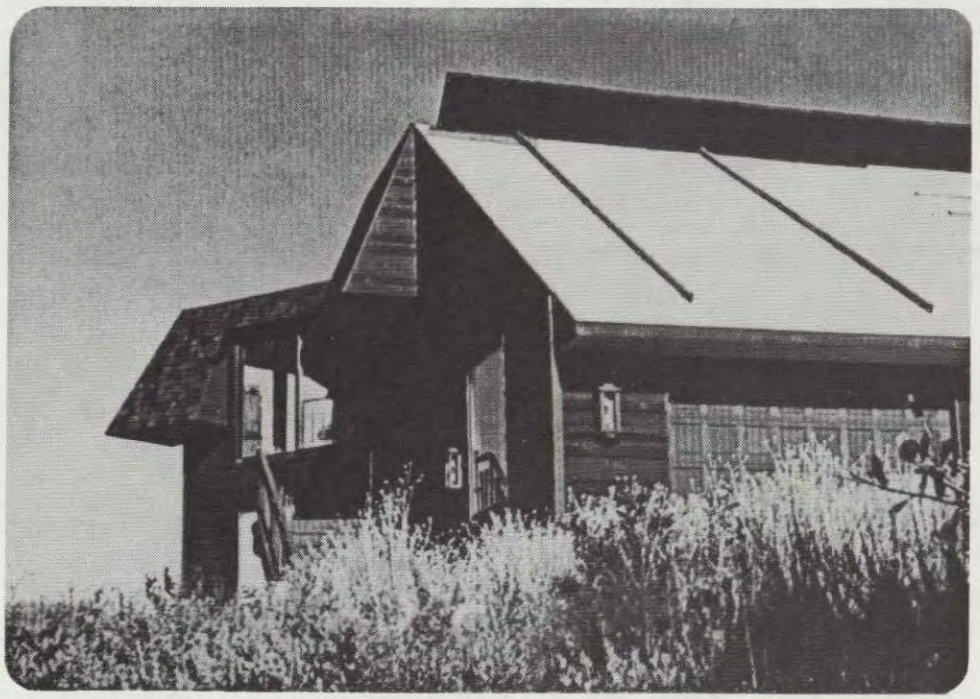

A house is not a home without solar.

3.2.2 Solar Power Measurements

Measurements were made on the completed prototype panel by moving a photocell across the array and averaging the power measurements seen within each zone. These measurements were compared to power measured on the surface of the outer glazing to determine relative optical concentration (measured data), and then divided by the overall optical efficiency to determine the geometric concentration (corrected data). The following data were taken on a clear day, with the solar radiation at a cross-sectional angle of incidence of 25° to the outer glazing's surface.

ZONE	AVERAGE CONCENTRATION			
	Top Side (measured)	Top Side (corrected)	Bottom Side (measured)	Bottom Side (corrected)
1	.20	.30	.50	.76
2	.20	.30	.60	.91
3	4.0*	6.1	.60	.91
4	.30	.45	.60	.91
5	.25	.38	.60	.91
6	.25	.38	.60	.91
7	.20	.30	4.0	6.1
8	.15	.23	2.0	3.0
9	.20	.30	1.0	1.5

* Peak observed concentration - 5.1 (7.8 corrected)

The distribution of this data appears to agree well with Figure 12 and Appendix 1. However, the top-side concentration is somewhat less than anticipated (8.2?). This may be partially explained by the photocell sensitity, which varies with the cosin of the angle of incidence. So the sensitivity when measuring direct solar radiation may be slightly higher than the average sensitivity when measuring a concentrated, low f-number wedge of radiation. Also, the cell's response may be slightly nonlinear for higher levels of radiation.

3.3 Collector Efficiency

The assembled collector unit was faced true south and tilted up 37° from horizontal for a resulting cross-sectional solar angle of incidence of approximately 25° between 11 a.m. and 1 p.m., solar time, in mid-December. The clear-day insolation incident on the outer glazing for this same period was computed to be 232 BTU/hr-ft^2, for a total of 5450 BTU/ hr over the 23.5 ft^2 active aperture of the collector. Fortunately, we had a succession of very clear days at the site.

When the assembly was initially tested with the old selective-foil fin arrangement, flow control was attempted using the proportional or on/off pump controls of the C100 unit used for temperature monitoring. It was found that, no matter what temperatures were monitored for control (input vs. panel output, vs hottest fin, vs hottest zone, etc.), a stable electronic flow control loop could not be established due to the dynamic and unstable flow through the oscillating valve mechanisms, as discussed in Section 2.3. While it was hoped that the improved heat flux of the new fin configuration would improve valve stability, this was not to be the case. Further tests were conducted using the manually-controlled test setup, shown schematically in Figure 13 and pictured in Figure 11.

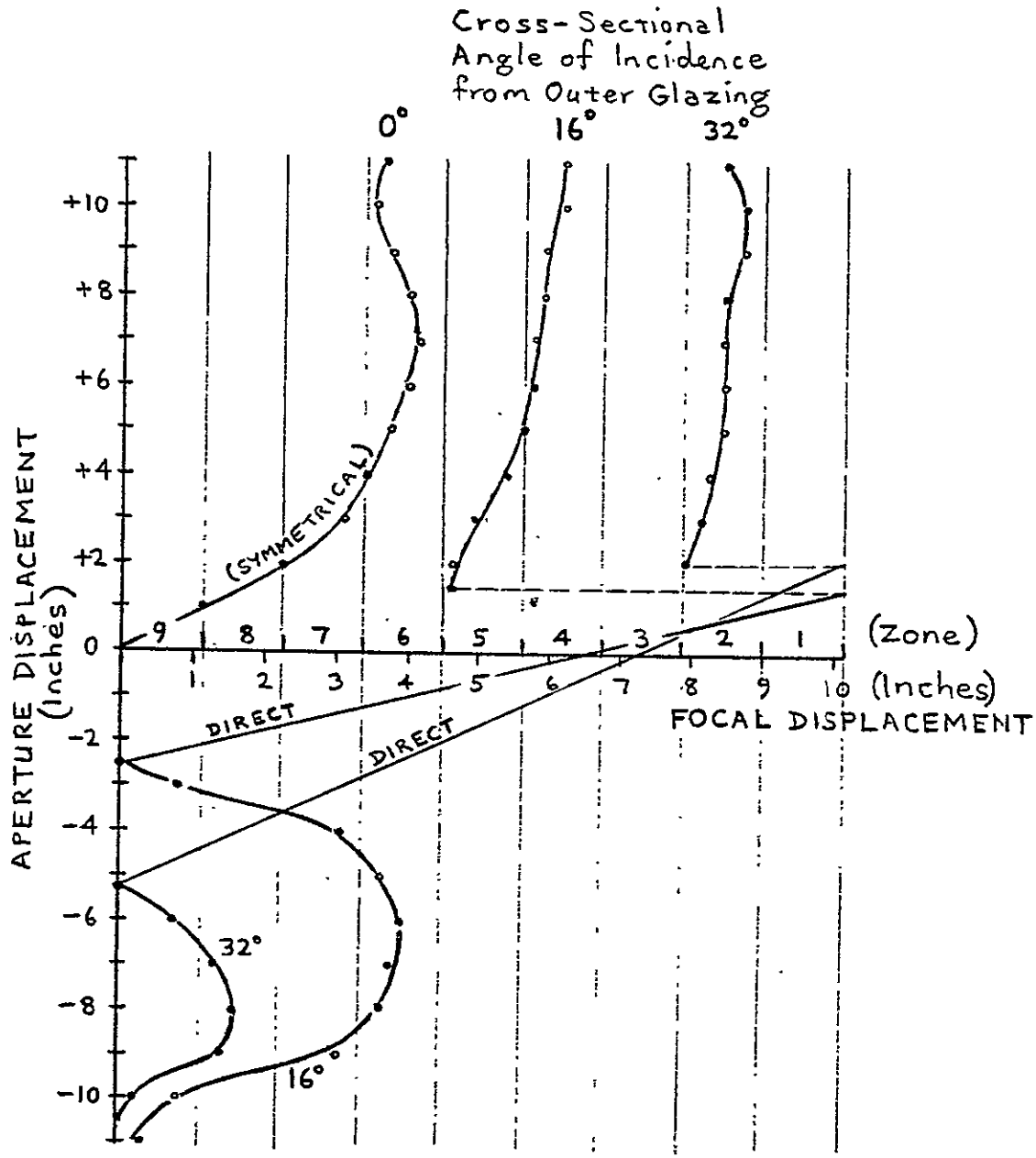

Fig 12 - Laser Data Plot

Day and Conditions	MEASURED DATA T_s (°F)	Time (hr/min/sec)	T_{03} (°F)	$\bar{T}_o$ (°F)	CALCULATED DATA $(\bar{T}_f - T_a)/I$ (°F·hr·ft²/BTU)	Incremental Efficiency
	90	11/25/50	104	105		
	103	11/37/50	119	116	.140	64%
X	114	11/49/00	130	122	.184	58
15 DEC	121	11/58/58	137	127	.216	42
(Clear, Lt. Breeze)	126	12/07/48	143	131	.238	34
T_a = 71°F	130	12/18/12	149	133	.254	22
	132	12/25/55	152	141	.272	15
3.3 GPM	141	12/34/32	156	147	.299	61

Switch from Diffuse Mode to Concentrating Mode

Fig 14 – Diffuse Mode Data

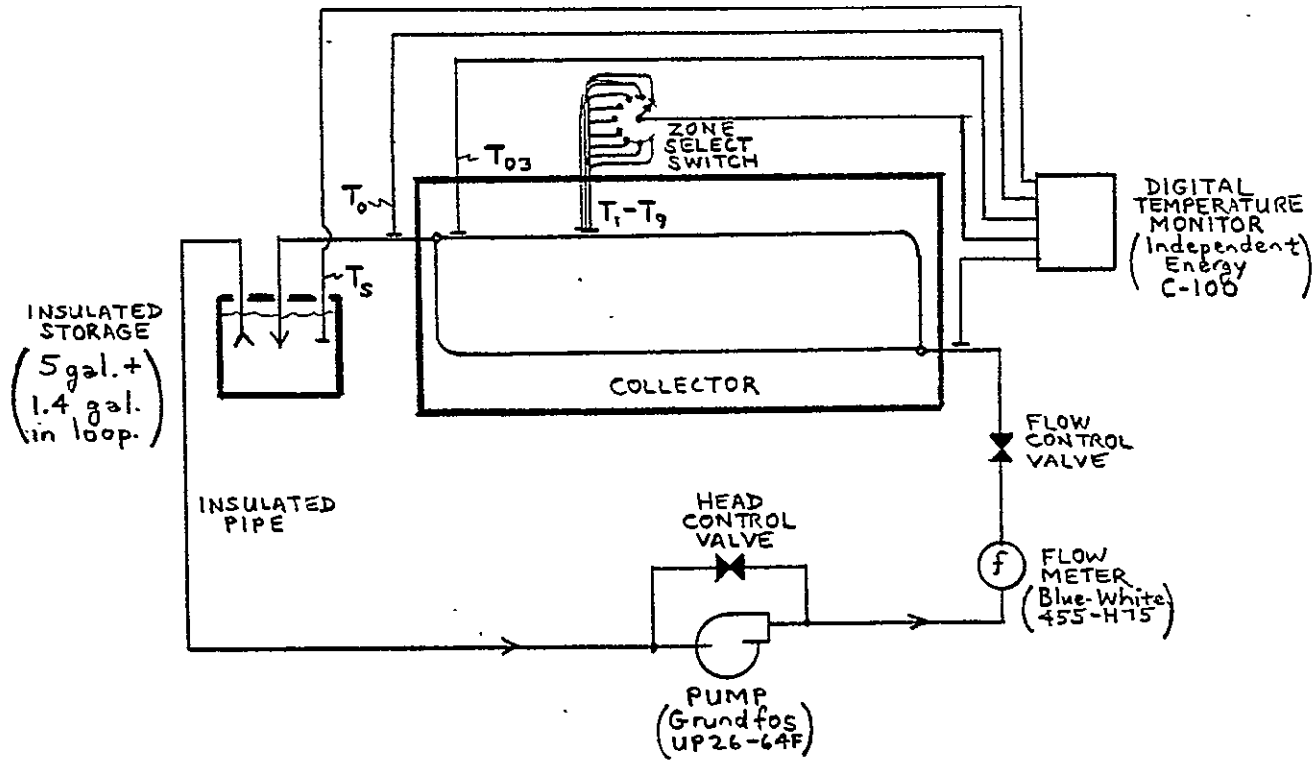

Fig 13 – Collector Test Schematic

The objective of the tests was to determine the efficiency of the collector in both the diffuse and concentrating modes by monitoring the rate of increase of temperature of a known mass of fluid. For the 6.4 gallons of water in the system, 53.4 BTUs would be required from the collector for every 1^{o} F increase. Measuring the corresponding period of time for this to occur, and having computed the insolation, the incremental efficiency could then be calculated by the following equation:

$$E_i = \frac{(53.4 \text{ BTU}/^{o}\text{F}) \quad (T_{s2} - T_{s1})}{(t_2 - t_1)(5450 \text{ BTU/hr})(.0167 \text{ hr/min})}$$

By monitoring the output temperature of the zone receiving the most concentrated radiation (zone 3 for these tests) flow rate was manually controlled to maintain approximately 165^{0} (the opening temperature of the valve) to assure operation in the concentrating mode. By maintaining a high steady-state flow rate with fluid pressures that overcome the values' spring forces the collector was also operated in the diffuse mode (where operating all zones below 155^{o}F assures that no zone gets preferential flow).

To avoid effects of the test setup on the performance measurement of the collector, the storage container, pump, and tubing were insulated to minimize their heat loss. Data are presented in Figures 14 and 15 for diffuse and concentrating modes, respectively. All data are plotted in Figure 16, and compared to the anticipated performance of an ordinary glazed flat-plate collector. The wide scattering of data points is due in part to the cycling and interactions of the thermal valves, which could not be controlled, and to thermal currents within the insulated storage container, which should have been mixed. It is unfortunate that data were restricted to such a narrow range of fluid parameter $(T_f - T_a)/I$, since this prevents us from predicting the shape of the curve and higher temperature performance with any good degree of certainty. This restriction results from a number of factors:

* On the low end, very low flow rates allowed heat gains to be dissipated in the pipes, which adds uncertainty to the efficiency calculations.

* Unusually warm December ambient temperatures kept fluid parameter values low.

* The use of the fixed-temperature valve mechanism in combination with the boiling point of water tightly constrained the operating temperature of the collector. (Water was used as a fluid since, as shown in Appendix 2, high temperature fluids would have exhibited too great a temperature differential for the chosen flow channel diameter.)

Barring some unrecognized flaw in this test strategy, performance is obviously far below expectations. Since optical performance was at least close ot expectations, the majority of the problems lie within the absorber plate and valve assembly. Likely causes and solutions are addressed in the following sections.

Day and Conditions	T_s (°F)	Time (hr/min/sec)	T_{03} (°F)	$\overline{T_o}$ (°F)	$(\overline{T_f}-T_a)/I$ (°F·hr·ft²/BTU)	Incremental Efficiency	Avg. Effic 90° to 140°
		MEASURED DATA			**CALCULATED DATA**		
● 12 DEC (Clear) T_a=68°F	69	10/50/00	81				
	75	11/01/34	162				
	80	11/09/58	165	130			
	90	11/23/31	165	[132]	.172	43.4%	
	100	11/36/24	168	134	.196	45.7	
	105	11/43/12	164	136	.221	43.2	
	110	11/49/35	168	138	.236	42.1	
	120	12/01/00	167	140	.252	51.5	46.3%
	130	12/12/48	168	[141]	.278	49.8	
	140	12/27/00	169	143	.302	41.4	
	150	12/45/10	169	145	.328	31.8	
■ 13 DEC (Clear, Lt Breeze) T_a=66°F	80	11/10/00	89				
	90	11/20/00	158	133			
	95	11/26/48	173	[134]	.212	43.2 %	
	100	11/32/56	163	135	.215	47.9	
	105	11/39/09	167	136	.227	47.3	
	110	11/44/54	174	137	.240	51.1	
	115	11/49/22	172	138	.253	65.8	
	120	11/55/53	168	139	.266	45.1	45.7%
	125	12/02/06	174	140	.279	47.3	
	130	12/10/05	170	[142]	.294	36.8	
	135	12/16/21	173	143	.307	46.9	
	140	12/24/39	170	144	.320	35.4	
	145	12/33/00	172		.330	35.2	
	150	12/43/56	176				
▲ 14 DEC (Clear, Med. Breeze) T_a=63°F	75	11/05/00	150	121			
	80	11/13/45	160	123	.156	33.6	
	85	11/23/13	160	125	.171	31.1	
	90	11/29/38	155	127	.187	45.8	
	95	11/33/36	163	[129]	.202	73.5 X	
	100	11/38/53	165	131	.217	55.6	
	105	11/43/06	170	133	.232	69.7 X	52.0%
	110	11/48/29	170	135	.247	54.4	
	115	11/54/16	170	137	.262	51.1	
	120	12/02/21	175	139	.277	36.4	
	125	12/08/30	171	142	.292	47.6	
	130	12/14/00	172	[145]	.307	53.4	
	135	12/18/31	169	147	.327	65.3	
	140	12/26/05	175	149	.342	38.7	
	145	12/34/29	177				
							AVG = 48.0%

Fig 15 – Concentrating Mode Data

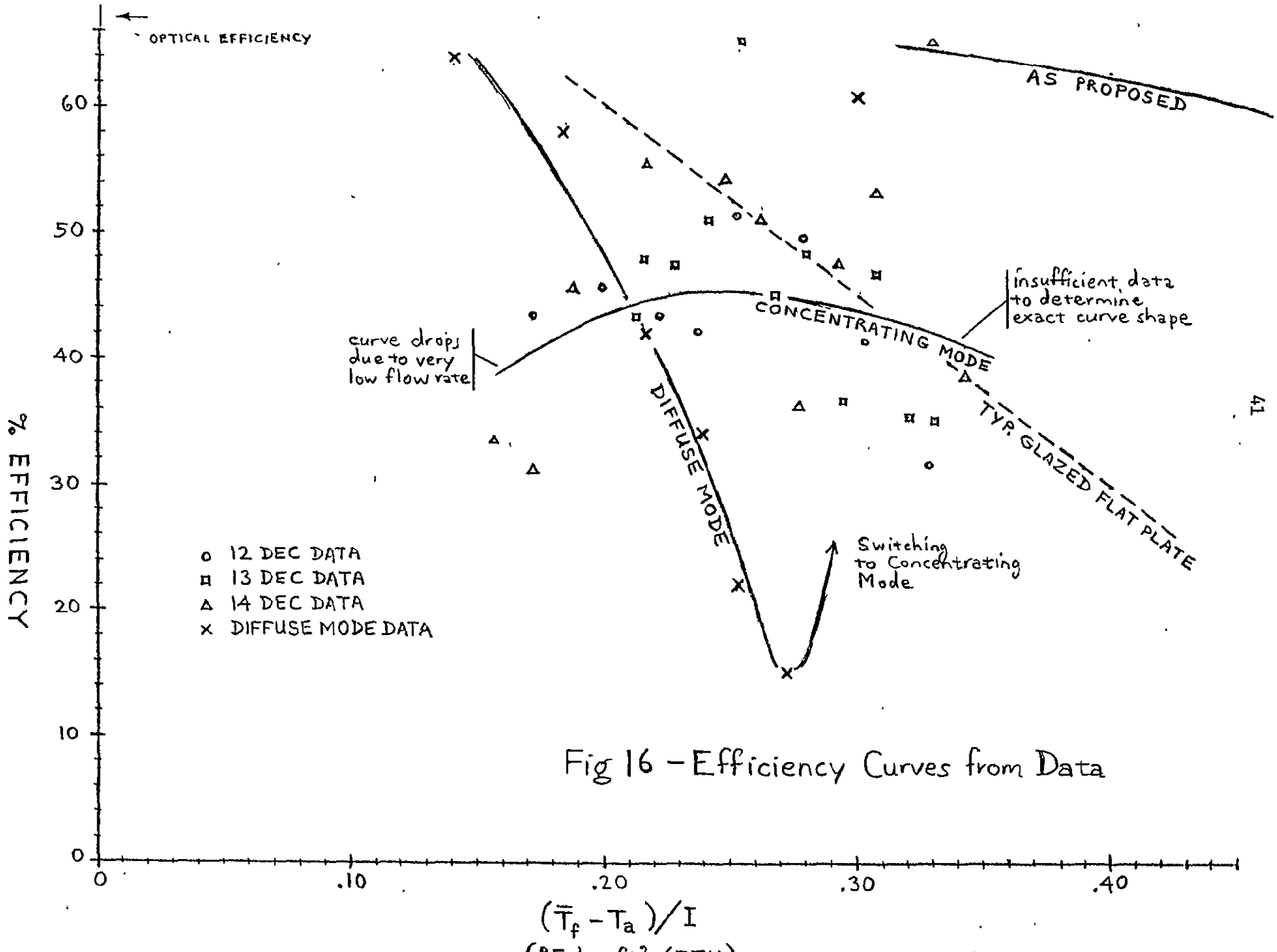

Fig 16 – Efficiency Curves from Data

4.0 Budget Summary

Exclusive of approximately $2,500 privately spent on patent efforts, the following chart summarizes project expenditures:

ITEM	As Proposed	As Spent
Debits	$19,680	$18,968 to date
Credits		
* Labor	(11,740)	(5,977)
* Collector Materials		(4,999)
* Fabricated Components and services	(7,700)	(7,560)
* Experimental and Assembly Materials		(1,262)
* Test Materials		(825)
* Administrative and Report Materials	(240)	(608)
NET	-0-	($2,262)

Scrap value of materials on hand is approximately $900.

Major overruns were encountered in the areas of minimum orders of materials, replacement materials for alternative designs, and machine shop services. To counteract these, labor expenditures were cut substantially, even though time spent was far beyond that proposed.

5.0 Conclusions and Recommendations

What was intended to be a high performance, low cost solar collectior design is, at this point, neither. Even if the design had performed as expected, the proposed materials were either petrochemical-based or energy-intensive in their manufacture. In light of the tremendous cost escalations of such materials since the design's inception, its cost-effectiveness would certainly require careful analysis even if all technical and manufacturing problems were overcome.

With regard to the technical problems and solutions, the following observations can be made, in order of priority:

* The thermal valves must respond quickly to fluid temperature. A spiral bimetallic element operating a butterfly-type valve would probably be much more effective than the phase-change cylinders that were used in this program.

* The gain of the valve (backpressure vs. temperature) must be controlled by design, which can also be accomplished with a bimetallic element. This should probably be done in conjunction with an inversely proportional controller for low flow rates at low storage temperatures (high T).

* Rather than incorporating the valves into the output header, place them in and near the outputs of the absorber channels. In this way, they can operate by solar absorption rather than by trickle flow. This will avoid their "stalling out" when there is no flow, and will prevent diluting flows from concentrating zones with the trickle flows from all other zones.

* Use smaller flow channels to promote better fluidic heat transfer by inducing turbulent flow. This is particularly important for high-temperature fluids, which are required to take full advantage of the design's intentions.

* Return to a selective absorber coating. This is desirable for higher temperature concentrating mode operation where the unfocussed back side of the channel can radiate away some of the gains from the focussed side.

* Use the unit for higher temperature operations or in colder environments, where the inherently greater optical losses of this concept are overcome by the greater thermal losses of conventional designs.

* Despite the fairly respectable optical performance of this design, it could probably be better. A higher-order image analysis should be performed.

* For the sake of better material and labor economies, return to an Olin "Roll-Bond" type of absorber plate. While inherently flimsier separated zones would require more slip-joint supports, this type of product is even more advantageous when used with the separate valves proposed above. Elimination of the common headers can take advantage of the integrated headers of the "Roll-Bond" product. Perhaps expansion stresses can be relieved by a gentle 90° bend of the plate at the input end. Perhaps gasketed, clamp-on valve castings could be used. Both the plate and the castings could be aluminum.

* Consider the optical concepts of this program for a single-sided, non-tracking concentrator/tracking absorber channel design. Such a design would have a low-mass, environmentally to protected, potentially inexpensive servomechanism optimally focus the single absorber channel. The focal track could be linear or non-linear. The absorber channel structure could incorporate a small secondary reflector or lens to highly optimize concentration.

The stationary primary reflectors could be incorporated as part of a structure (as a roof, for example) or firmly anchored to earth as an independent structure.

* Work with manufacturers to perfect a reflective film product. Martin's "Llumar" polyester film appears to be a good product in itself. The 3M products initially apply with good optical quality, with their uniform contact-adhesive backing. Dry-contact silicone products are available, and should withstand humid, moderate temperature environments.

Appendix 1: Acylindrical Reflector Theory

The primary objectives in the design of the optically reflective surfaces for the collector were to define a stationary surface that forms an optimal line focus of direct solar radiation. As the sun tracks across the surface, the focus is to track in a plane. In azimuth, the surface is to face true south, and the surface elevation is to be defined by site latitude.

The cross-section of the surface curvature lies in the vertical north-south plane. For solar altitude, B, and solar azimuth, , the equivalent, B_e, of the sun above horizontal as projected into the cross-sectional plane is:

$$B_e = \tan^{-1} \frac{\tan B}{\cos}$$

For fully effective year-round operation between 9 A.M. and 3 P.M. solar time, B_e will have a range of $\pm 31.5^\circ$ to either side of an elevation equal to site latitude. In other words, for a panel assembly having a tilt angle equal to site latitude, the objective surface must form an acceptable focus over an angular deviation of $\pm 31.5^\circ$.

The above requirements can be met only by a surface having a higher order curvature, herein referred to as an "acylindrical" surface. In the coordinates of the cross-sectional plane, this surface is of the form:

$$y = \frac{x^2}{2F + Q}$$

where:

$$Q = \sqrt{(2F)^2 - (K+1)\,x^2}$$

F = nominal focal length

K = conic constant

The slope at any point is then:

$$\phi = \tan^{-1} \frac{dy}{dx} = \tan^{-1} y \left[\frac{2}{x} + x \frac{(K+1)}{Q\,(2F+Q)} \right]$$

A secondary objective was to utilize the above equations in a way that would result in a panel of acceptable dimensions. To conform to construction industry standards, the panel was to be 4 feet by 8 feet, with a depth preferably less than one foot. To accomplish this, it was necessary to use two reflective troughs per panel assembly.

Within the limits of the above acceptance angles and geometry, focal length and conic constant were iteratively adjusted for least blur widths (best foci) lying in a single plane. Once this plane was defined, the surface was tipped and decentered so that the plane lay on the y-axis, and was then made symmetrical about that axis. These procedures are illustrated in Figures A1-1 and A1-2 for optimal values fo F and K. The resultant descriptive equation is:

$$y = \frac{x^2}{\sqrt{7.5 + 56.25 - .25\,x^2}}$$, rotated 10° about x=0, y=12

The resultant blur widths vary from about 1.2 inches to 1.5 inches over a plane that is 10 inches high. Therefore, nine zones across the width of this plane should sufficiently resolve the foci. (More zones would better resolve positional ambiguities, but in the interest of least complexity, nine were favored.)

For the resultant 23 inch wide trough and the 9 element, 10 inch plat, the maximum direct solar concentration ratio per side is:

$$C_1 = \frac{23"/2}{10"/9} = 10.4$$

If the blur width equally straddles two elements, the concentration ratio is:

$$C_2 = C_1/2 = 5.2$$

For effective solar elevations greater than or less than site latitude (normal incidence to the panel), there is some obscuration of the reflective surface by the shadow of the absorber plane. This radiation is absorbed directly without concentration, and therefore reduces the average overall concentration. This obscuration varies from 2% for direct normal incidence to 33% for 31.5°.

Taking the above effects into account, the instantaneous average concentration of direct radiation varies with angle of incidence from a minimum of about 3.8 to a maximum of nearly 10. Diffuse radiation experiences almost no concentration (11.5"/10" = 1.15).

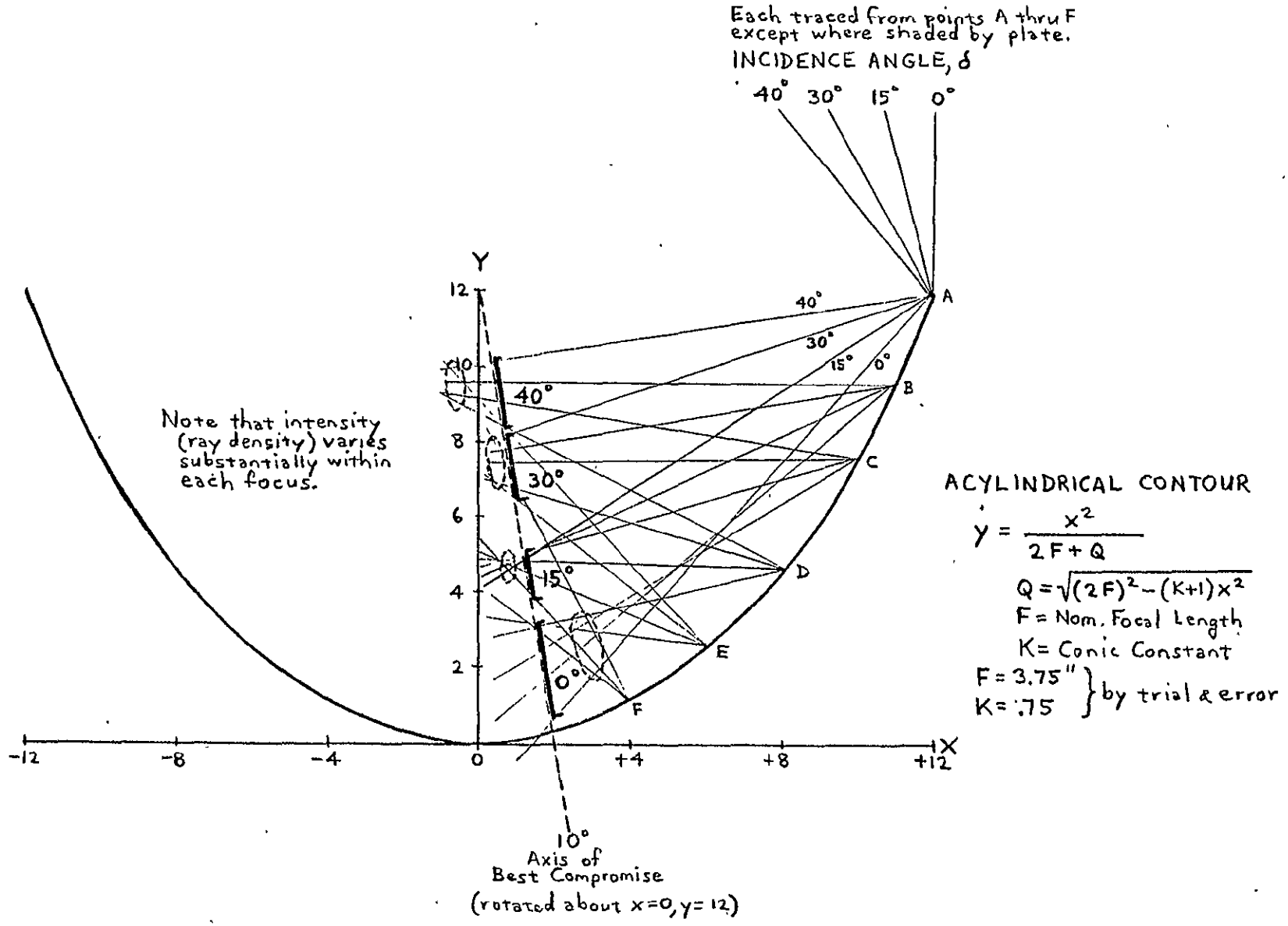

Fig A1-1 – Process for Identification and Optimization of Focal Plane

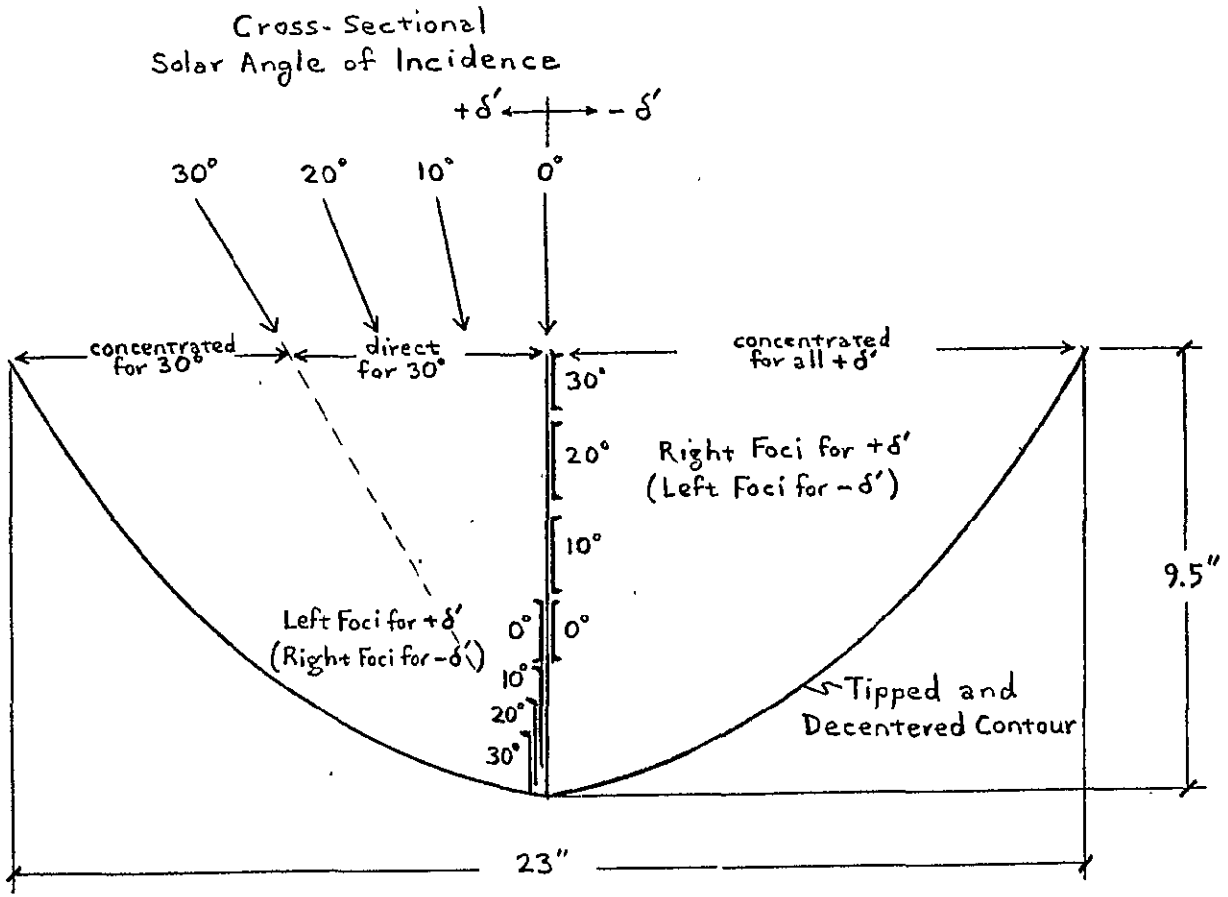

Fig A1-2 – Assembly of Contour and Formation of Double-Sided Foci

Appendix 2: Absorber Plate Theory

The flat plate collector array is placed in the focal plane of the reflective housing. Each array consists of nine thermally isolated longitudinal zones to selectively accept focussed direct solar radiation without laterally diffusing the heat to cooler zones.

Two configurations of zone tubes have been fabricated and tested, as described in Section 2. The following sections summarize the thermal efficiencies of each configuration.

A2.1 Selectively-Plated Foil Fin

A selectively-plated, 5-mil copper foil was wrapped around a 3/8 inch, Type M copper tube flow channel, and bonded to it with a 10-mil dry-contact silicone adhesive tape. This configuration is shown in Figure A2-1. Had the tape been applied totally free of air bubbles, and had it adhered without selectively separating, the following performance could have been expected:

A2.1.1 Fin Loss

K_c = conductivity of Cu = 220 BTU:ft/hr.ft.^{2} F
I = max incident isolation = 325 BTU/hr.ft^2
E = overall optical efficiency = 0.65
C = optical concentration = 5 typ
e = efficiency, selective dbl-glazed flat plate, T = 150°F .7
t_c = fin thickness, each side = .0005" = 4.2 x 10^{-4}ft.
w_c = fin width = .625" = .052 ft.

For a uniformly irradiated fin with T_f small with respect to its absolute temperature, the average temperature differential from fin to channel bond line is:

$$\Delta T_f = \frac{0.67\ hwc}{k_c t_c} = 14.6F$$

where h is the fin's heat flux remaining after convective and radiative losses:

$$h = I \times C \times E \times e \times w_c = 38.4 \text{ BTU/hr ft}$$

A2.1.2 Bond Loss

k_s = conductivity of silicone tape = .096 BTU ft/hr ft^2°F
t_s = tape thickness = .010" = 8.3 x 10^{-4} ft
w_s = tape width = .5" = .042 ft

The temperature drop across the bond is:

$$\Delta T_b = \frac{h\ t_s}{K_{sws}} = 7.9°F$$

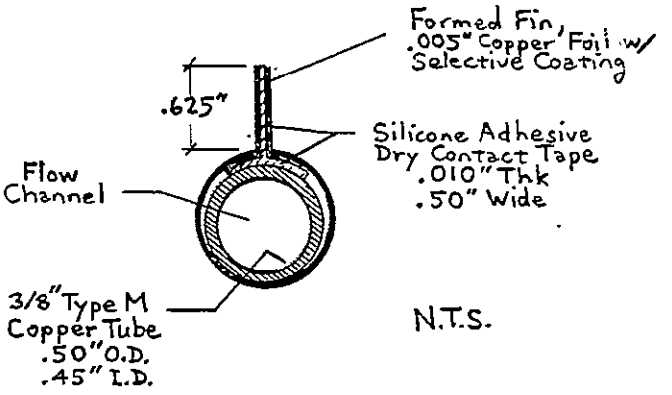

a.) Selectively-Plated Foil Fin

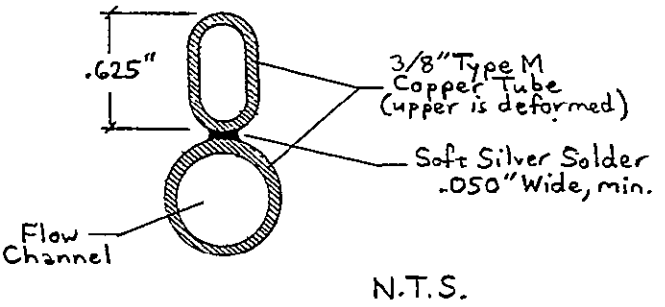

b.) Deformed Pipe Fin

Fig A2-1 – Flat Plate Absorber Zone Configurations

A2.1.3 Flow Channel Loss

k_f = conductivity of fluid = .38 BTU ft/hr ft^2°F (water)
.073 " " (BRAYCO 888HF)
d = pipe I.D. = .45" = .038 ft
N = Nusselt number for laminar flow, uniform heat flux
= 4.36

The average temperature differential from the pipe wall to the fluid for a uniform heat flux, h, over fin and pipe is:

$$\Delta T_c = \frac{h\,(w_c + d)/w_c}{N\,k_f}$$

= 13.3°F for water
= 64.3°F for BRAYCO 888HF

Obviously, a synthetic oil fluid is not appropriate for such a large size flow channel.

A2.1.4 Fin Temperature

Fluid flow rate should be controlled by a combination of head and valve back-pressure so that fluid at the valve is approximately 165°F, since this is where the valve begins to function. Therefore, fin temperature near the valve should be:

$T_f \simeq 165°F + T_f + T_b + T_c$ = 201°F for water
= 252°F for BRAYCO 888HF

A2.1.5 Fluid Flow Rate

L_c = length of channel = 6.4 ft
c = fluid specific heat = 1 BTU/16°F for water
= .58 " for BRAYCO 888HF
p = fluid density = 62.4 lb/ft^3 for water
= 50.1 " for BRAYCO 888HF
v = fluid kinematic viscosity = .32 x 10^{-5} ft^2/sec
= .4 x 10^{-4} "
T_{in} = fluid temperature at channel inlet
T_{out} = fluid temperature at channel outlet = 165°F
R = Reynold's number = 2000 (laminar limit)

The required coolant velocity in the channel receiving concentrated radiation is:

$$V_f = \frac{4L\ ch(w_{c+d})/w_c}{\pi d^2 cp(T_{out} - T_{in})(3600\ sec/hr)}$$

$$= \frac{1.74°F\ ft/sec}{165°F - T_{in}} \quad \text{for water}$$

$$= \frac{3.73°F\ ft/sec}{165°F - T_{in}} \quad \text{for 888HF}$$

Critical velocity for laminar flow is:

$V_c = \frac{vR}{d}$ = .168 ft/sec for water
= 2.11 " for 888HF

So flow will remain laminar ($V_f < V_c$) if $T_{out} - T_{in}$ 10^o for water and $> 18^o$ for 888HF. This satisfies the assumption made in Section A2.1.3.

Required flow rate to establish 165°F output is:

$$F = \frac{\pi d^2 V \text{ ft}}{4} \quad (60 \text{ sec/min}) \times (7.48 \text{ gal/ft}^3)$$

$$F = \frac{.89^oF \text{ GPM}}{165^oF - T_{in}} \quad \text{for water}$$

$$= \frac{1.90^oF \text{ GPM}}{165^oF - T_{in}} \quad \text{for 888HF}$$

A2.2 Deformed Pipe Fin

Because the silicone adhesive bond line in the above configuration was delaminating and differential temperatures were becoming excessive, a second fin configuration was implemented so that the evaluation of the unit could proceed. This configuration, shown in Figure A2.1b uses a deformed 3/8" Type M copper pipe as a fin, soldered to the same flow channel. This method was not intended to be economically attractive, but was intended to make use of materials on hand in the least amount of time.

Expect as noted, variables are the same as for the prior configuration.

A2.2.1 Fin Loss

e = efficiency, flat black dbl-glazed flat plate,

T_a @ 130°F ≃ .58

t_c = fin thickness, each side = .025" = 2.08 x 10^{-3}ft
For this fin, with a substantial conduction path over the top and through the back wall, the average temperature differential from fin to solder joint is:

$$\Delta T_f = \frac{.39 \, h w_c}{k_c t_c} = 1.4^0$$

where h, after losses, is 31.9 BTU/hr per ft length of channel.

A2.2.2 Bond Loss

k_s = conductivity of solder = 20 BTU.ft/hr. $ft^2{}^oF$
t_s = solder line thickness = .020" max = 1.7×10^{-3}ft
w_s = solder line width = .050" min = 4.2×10^{-3}ft

Temperature drop across the solder line is:

$$\Delta T_b = \frac{ht_s}{k_s w_s} = .65^oF$$

A.2.2.3 Fin Temperature

Channel loss for this fin configuration is essentially the same, except for the slightly reduced heat flux:

$$\Delta T_c = 11.1$$

So the fin temperature near the valve should be:

$$T_f \simeq 165^oF + \Delta T_f + \Delta T_b + \Delta T_c = 178^o$$

Appendix 3: Drawings

Pages 52 and 53 - Template drawings and coordinates for machining the template for generating the housing's wooden form framing.

Pages 54 and 55 - Template drawing and coordinates for machining the templates for inspecting the wooden form finish and the molded fiberglass housings.

Page 56 - Drawings and parts specifications for the prototype valve assembly. Parts 2, 3, and 7 are used in the final valve assembly, except material is brass. Parts 8 and 10 are also used in the final assembly.

Page 57 - Input manifold for the flat plate assembly.

Page 58 - Drawings for housing form, housing frame, and molded housing.

Page 59 - Casting drawing for the final valve assembly.

Page 60 - Machining drawing for the valve casting. Its assembly uses nine sets of parts including those noted above for page 5, plus Parker-Ideal 73166 thermostat power elements, plus counterwound, concentric pair springs.

Note: Drawings have been reduced for this report. Do not scale.

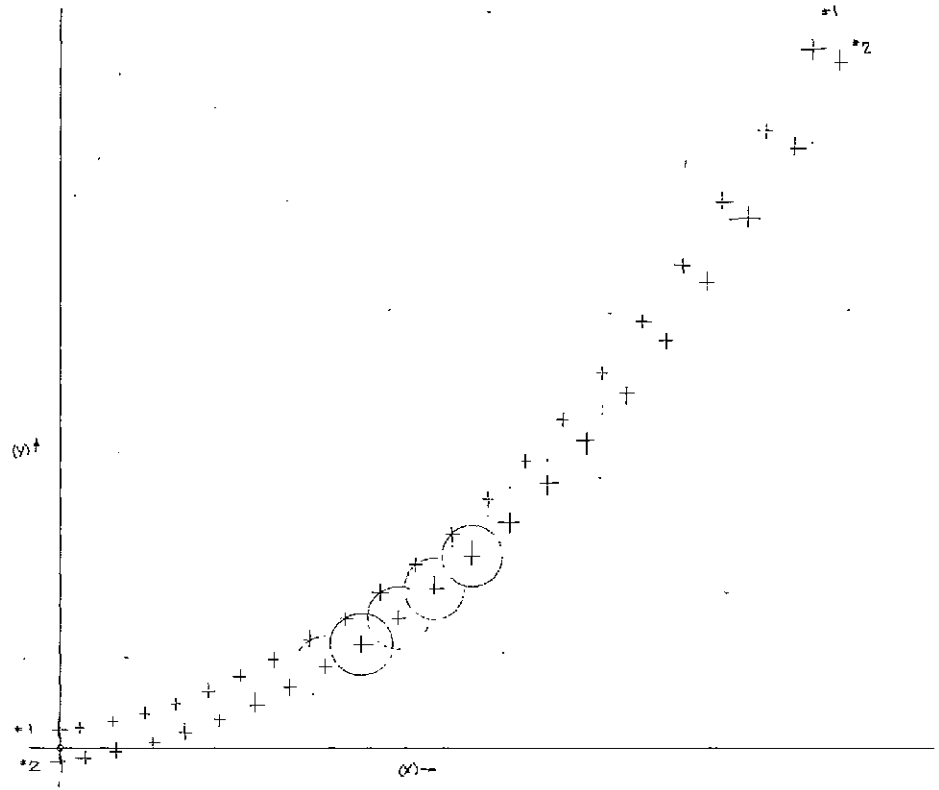

(x)	(y)	ϕ°	(x')	(y')
-.0260	.2788	95.300	.0226	-.2868
.5270	.2274	90.675	.4893	-.1664
.6646	.4218	102.207	.5703	-.0472
1.3753	.5424	103.637	1.5140	.0681
1.9010	.7121	106.958	2.0634	.2592
2.4800	.9105	112.168	2.6187	.4477
2.9665	1.1464	115.264	3.1752	.6242
3.5018	1.4212	118.246	3.7304	.8507
4.0631	1.7564	121.116	4.3214	1.0668
4.6237	2.0939	123.880	4.9018	1.6758
5.1930	2.4260	126.541	5.4807	2.0342
5.7713	2.9449	129.106	6.0547	2.5569
6.3595	3.4447	131.584	6.6912	3.0707
6.9575	3.9930	133.982	7.3047	3.6392
7.5665	4.6115	136.310	7.9260	4.2661
8.1874	5.2681	138.577	8.5623	4.9575
8.8214	6.0353	140.784	9.2068	5.7196
9.4686	6.8626	142.974	9.8688	6.5615
10.145	7.7795	145.180	10.5447	7.4933
10.8180	8.8018	147.280	11.2387	8.5315
11.5239	9.9483	149.444	11.9645	9.6941
12.2570	11.2477	151.651	12.6970	11.0102

TEMPLATE EDGE CO-ORDINATES #1

CUTTER CO-ORDINATES FOR CONVEX TEMPLATE #2 1.000 DIA. CUTTER

ACYLINDRICAL FRAME TEMPLATE
-LAYOUT-

By 9/10-70

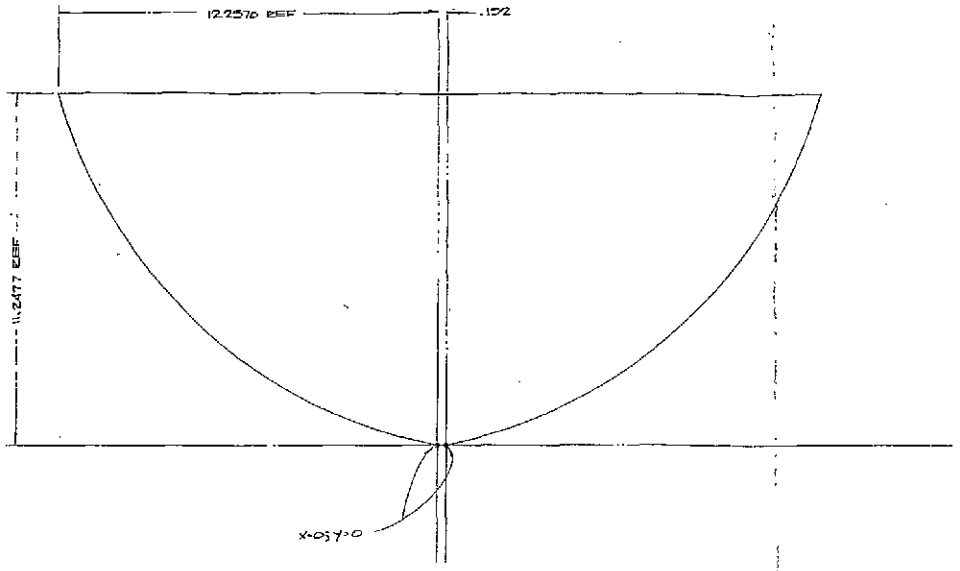

*2 CUTTER CO-ORDINATES
ACYLINDER FRAME TEMPLATE

③ TEMPLATE
.25 THK 6061-T6 AL ALY

FRAME TEMPLATE - OUTLINE
JJ 8/12-78

TEMPLATE CO-ORDINATES ARE FROM DWG. INDICATED AND MACH. AS A COMBINED RT & LEFT W/ .192 OFF-SET.

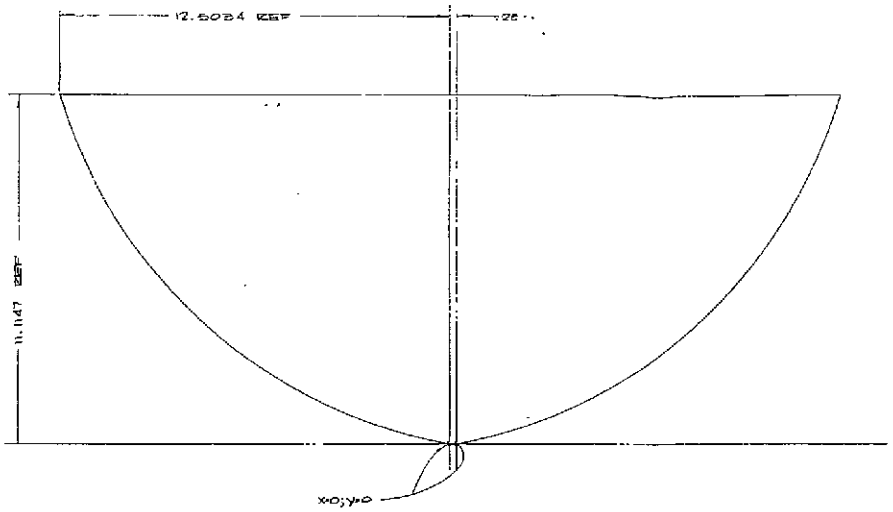

*2 CUTTER COORDINATES
ACYLINDRICAL INSPECTION TEMPLATE - CONVEX

① TEMPLATE
.25 THK 6061-T6 AL ALY

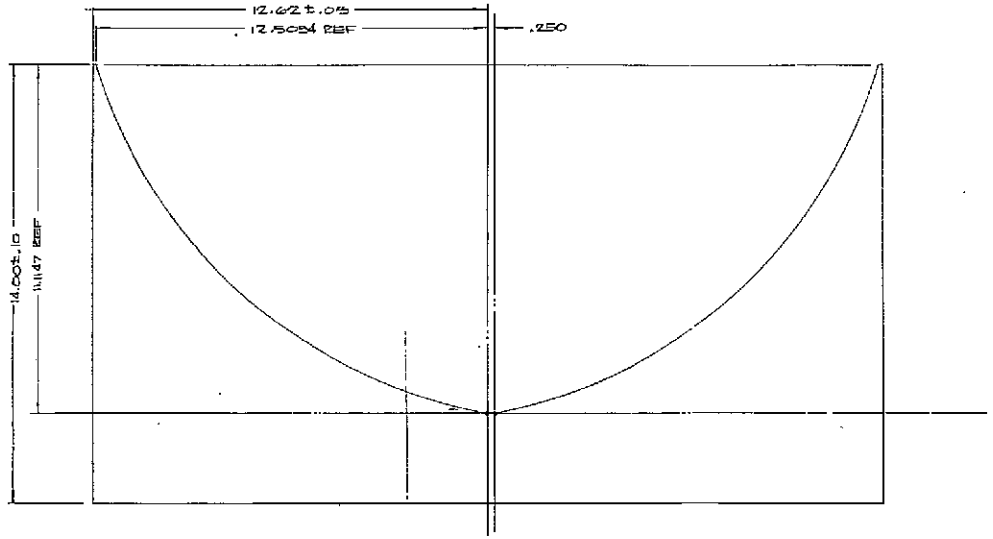

*3 CUTTER CO-ORDINATES
ACYLINDRICAL INSPECTION TEMPLATE - CONCAVE

② TEMPLATE
.25 THK 6061-T6 AL ALY

INSPECTION TEMPLATES - OUTLINE
JP 8/12-78

TEMPLATE CO-ORDINATES ARE FROM DIMS. INDICATED & ARE MACH. AS A COMBINED RT & LEFT W/ .250 OFF-SET

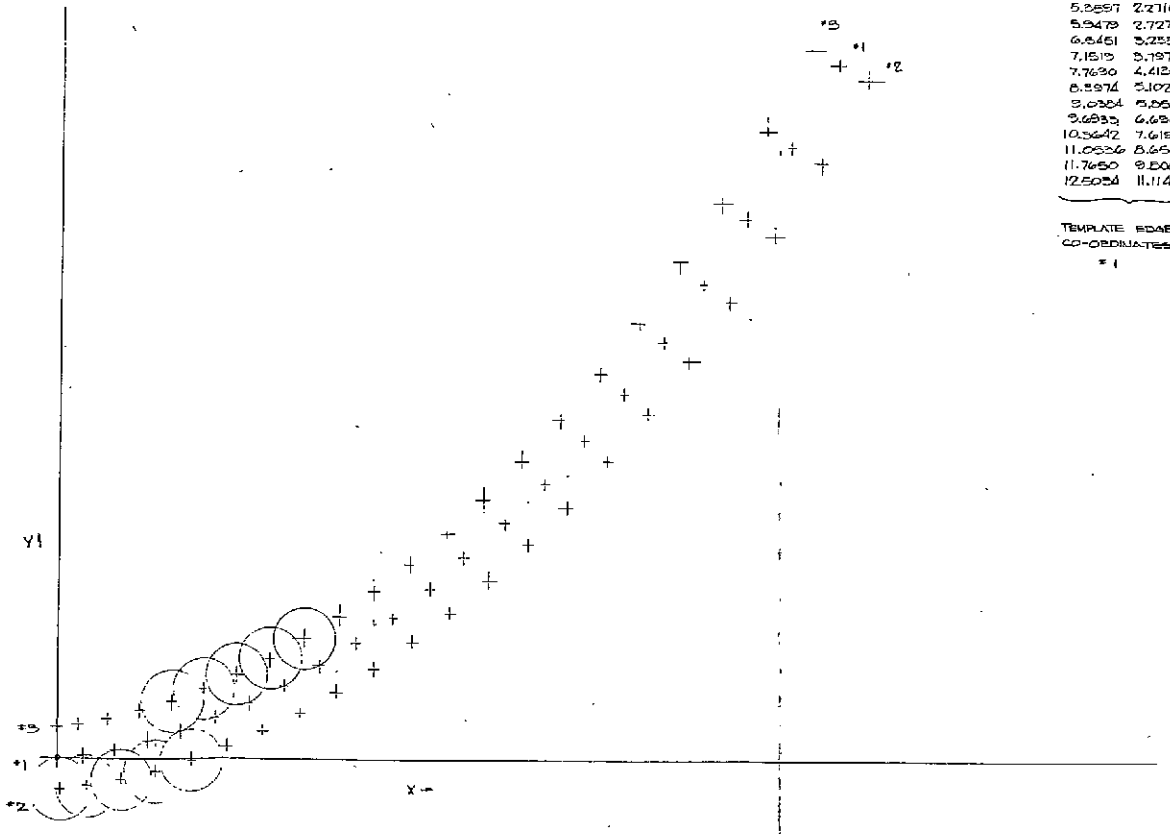

X'	Y'	∠°	X"	Y"	X"	Y"
0	0	95.300	.0514	-.1542	-.0227	.4975
.2986	.0508	90.678	.4744	-.4434	.3236	.5450
.9235	.1678	92.307	1.025	-.3436	.8160	.4364
1.4548	.2560	95.637	1.5695	-.2014	1.3200	.7614
1.9820	.4475	102.956	2.1544	-.0265	1.8295	.9201
2.5357	.6515	112.146	2.7242	.1654	2.3470	1.1145
3.0860	.8852	115.264	3.2893	.4410	2.8726	1.3453
3.6433	1.1745	116.246	3.8795	.7340	3.4066	1.6149
4.2076	1.4967	121.116	4.4661	1.0656	3.9494	1.9247
4.7758	1.8614	123.560	5.0608	1.4462	4.5010	2.2765
5.3597	2.2710	126.541	5.6575	1.8692	5.0620	2.6727
5.9479	2.7276	129.106	6.2632	2.3396	5.6325	3.1155
6.5451	3.2553	131.584	6.8769	2.8613	6.2132	3.6093
7.1515	3.7975	133.962	7.4891	3.4377	6.8047	4.1573
7.7630	4.4121	134.310	8.1305	4.0727	7.4076	4.7655
8.3974	5.1026	138.677	8.7725	4.7719	8.0225	5.4356
9.0384	5.8668	140.794	9.4258	5.5428	8.6509	6.1749
9.6853	6.6940	142.974	10.0924	6.3925	9.2941	6.9950
10.3642	7.6187	145.150	10.7744	7.3338	9.9527	7.9065
11.0526	8.6505	147.280	11.4742	8.3802	10.6329	8.9207
11.7450	9.8060	149.444	12.1955	9.5618	11.3344	10.0601
12.5054	11.1147	151.681	12.9434	10.8772	12.0633	11.3521

TEMPLATE EDGE CO-ORDINATES #1

CUTTER CO-ORDINATES FOR CONVEX TEMPLATE #2

CUTTER CO-ORDINATES FOR CONCAVE TEMPLATE #3

1.000 DIA CUTTER

ACYLINDRICAL INSPECTION TEMPLATE(S)
- LAYOUT -

DJ 9/10-75

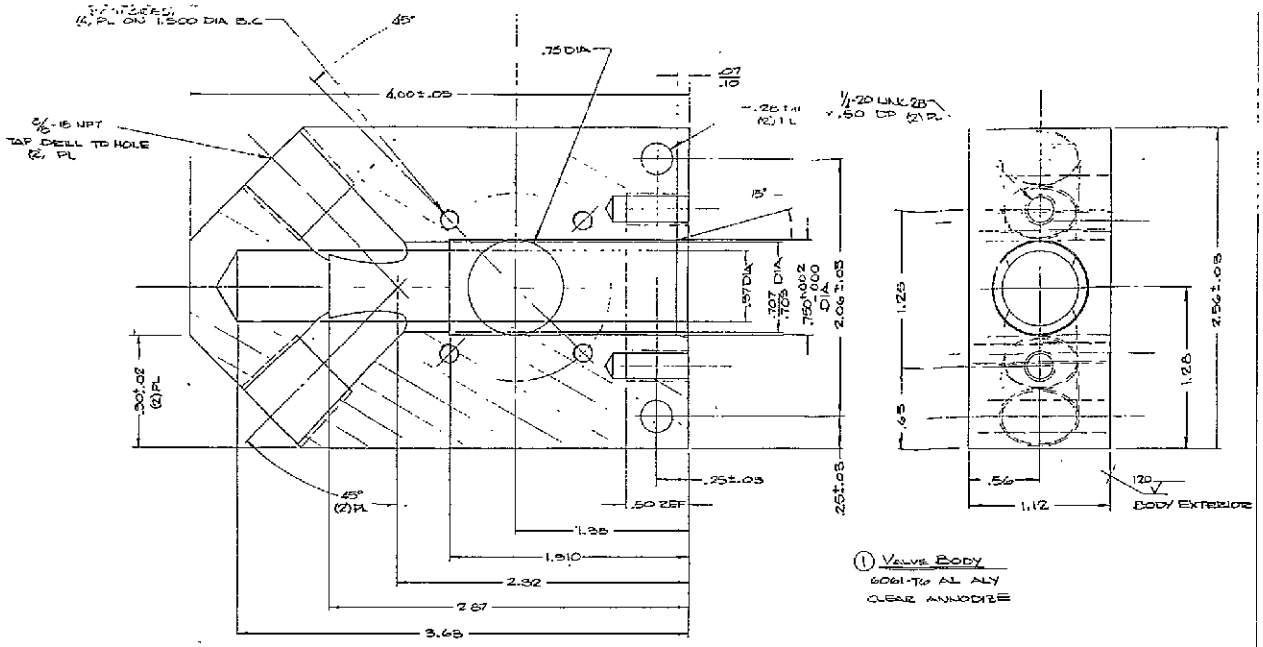

① Valve Body
6061-T6 Al Alloy
Clear Anodize

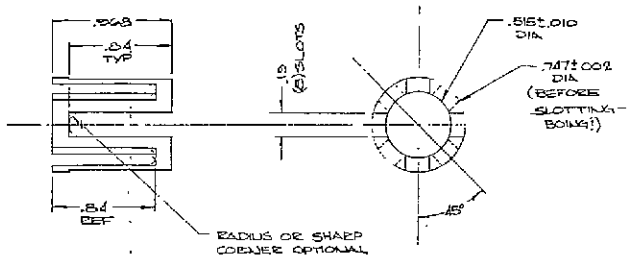

④ Spacer
6061-T6 Al Alloy
Clear Anodize

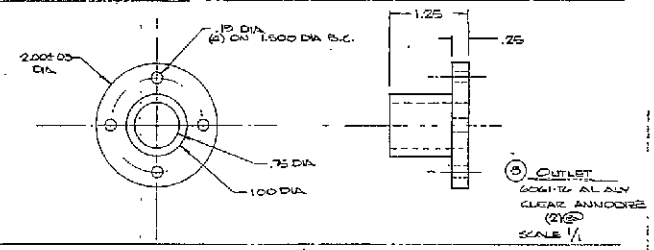

⑤ Outlet
6061-T6 Al Alloy
Clear Anodize
(2) req'd
Scale 1/1

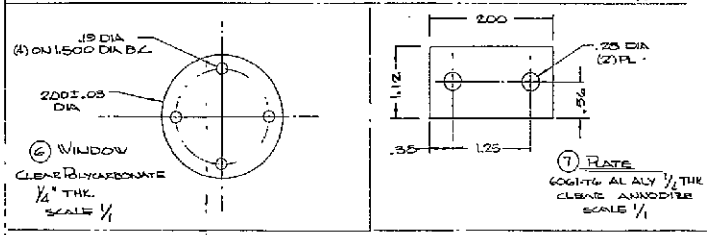

⑥ Window
Clear Polycarbonate
¼" THK.
Scale 1/1

⑦ Plate
6061-T6 Al Alloy ¼ THK
Clear Anodize
Scale 1/1

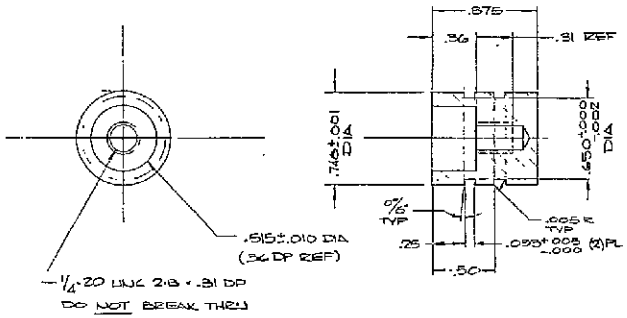

② Cap
- 6061-T6 Al Alloy
Clear Anodize

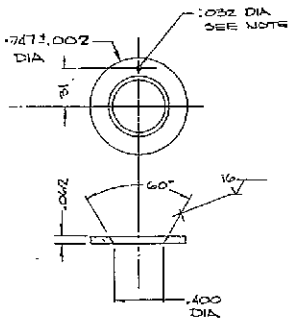

③ Seat
Brass
(2) req'd ((1) without .032 DIA)

⑧ .500 DIA St Stl Ball
⑨ Assoc Spring # C0480-065-1750-S
⑩ Parker 'O' Ring #2-16 (.754 O.D. x 1/16 sec.) (2) req'd
⑪ Assoc Spring # W0734-009-S (2) req'd

Valve - Prototype II

Scale 2/1 Noted, Qty/Unit 1 Noted
Tol: .XX±.01, .XXX±.005, ∠±1°, 32√

19 8/20-78

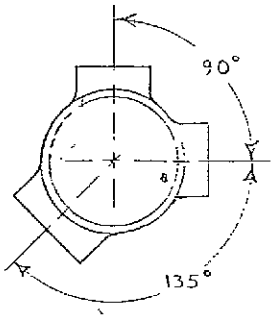

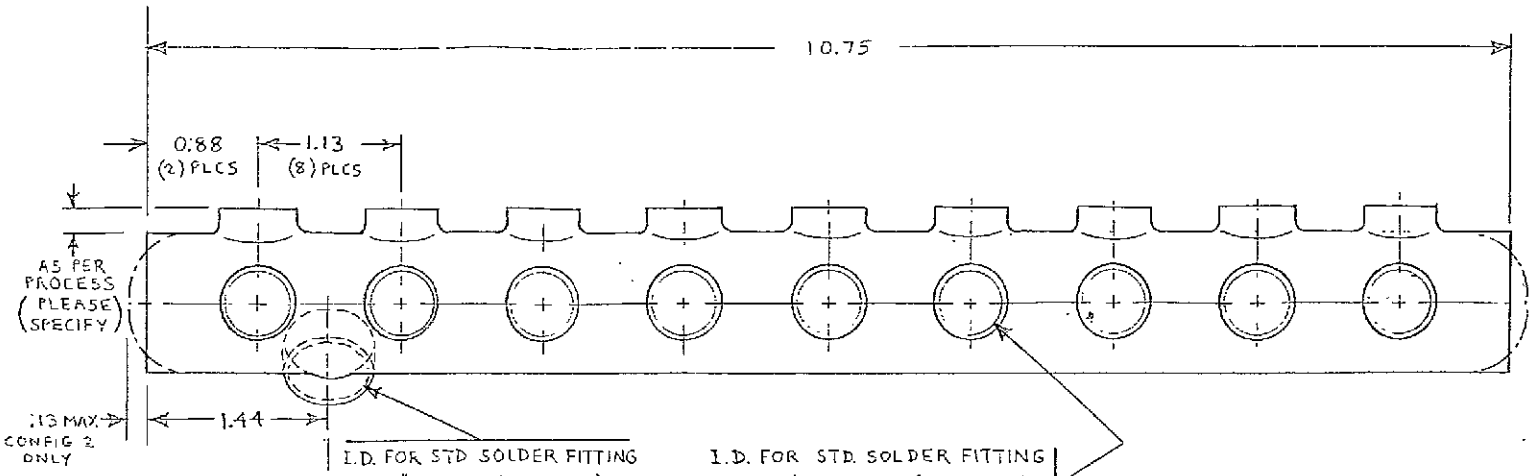

CONFIGURATION 1 :
OPEN END (2) PLCS
CONFIGURATION 2 :
SPIN CLOSING (2) PLCS.

RAYMOND T. HEBERT
CONS. ENGR / GEN. CONTR. 350449
P.O. BOX 134
SARATOGA, CA 95070
(408) 378-5821

-57-

INPUT MANIFOLD FAB

CA-235 COLLECTOR

REV —
DATE 3/15/79
SCALE: 1/1
PAGE 1 of 1

MAT'L: TYPE K or L 1" CU TUBING
TOL: .xx ± .01 EXC. AS NOTED.
∠'s ± 1°

SHEET 6
RT

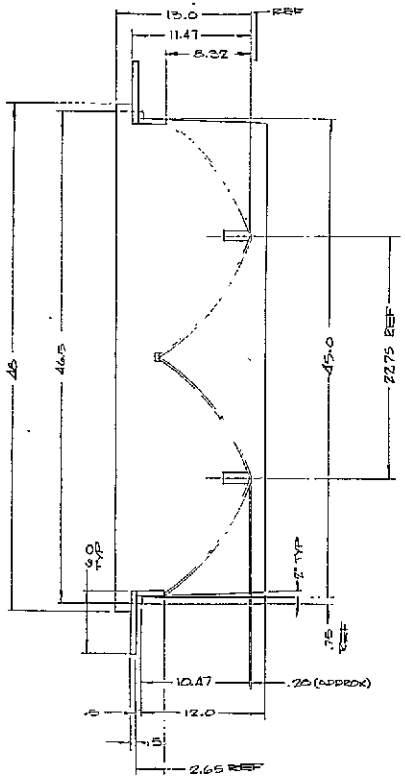

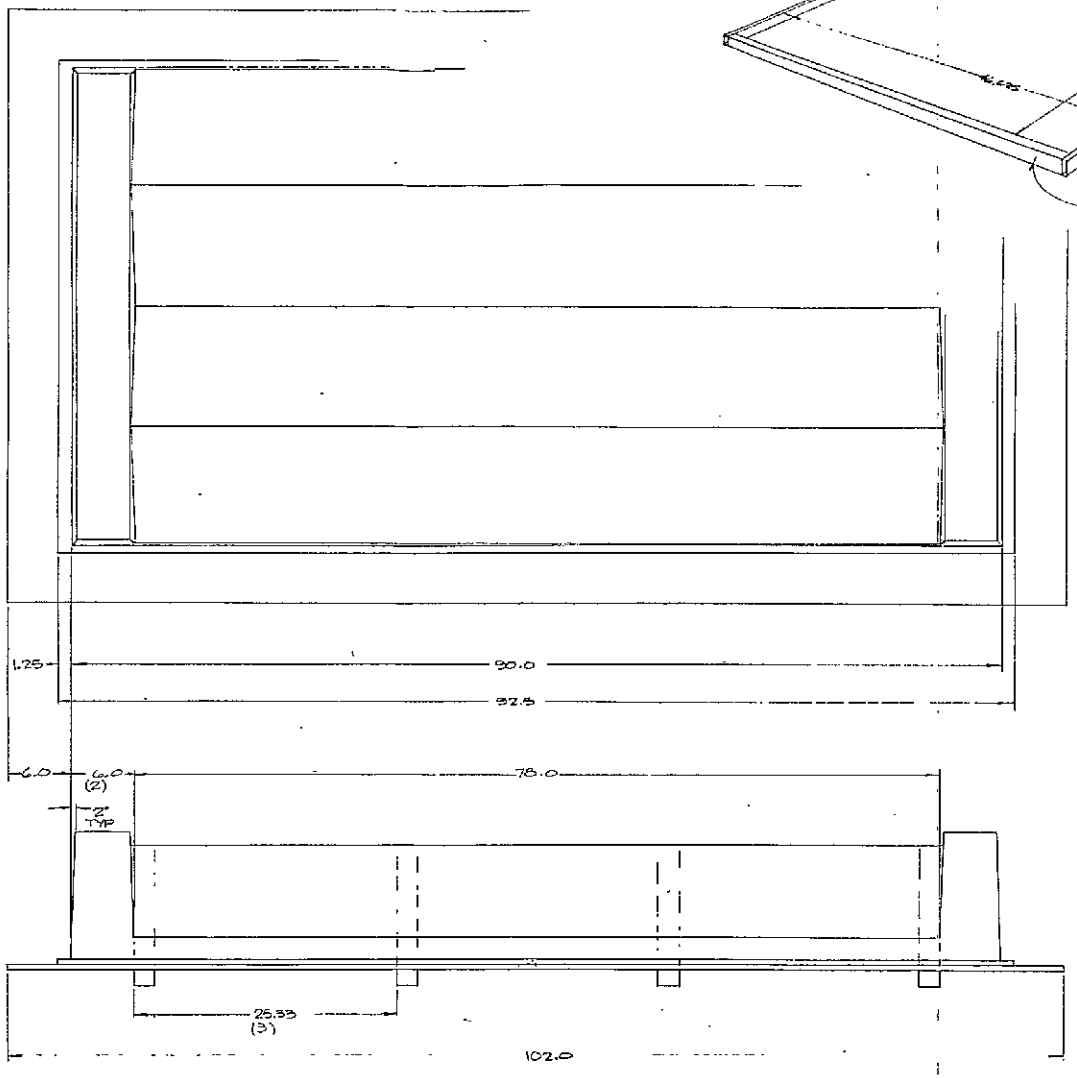

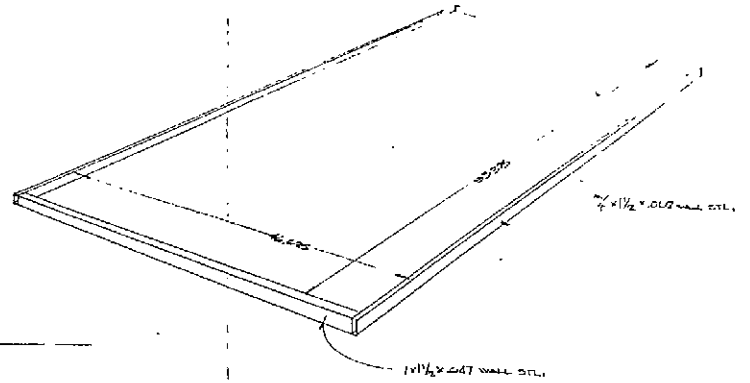

-58-

MOLD-COLLECTOR II

DR 1/17/78 SCALE 1/2

SHEET 7

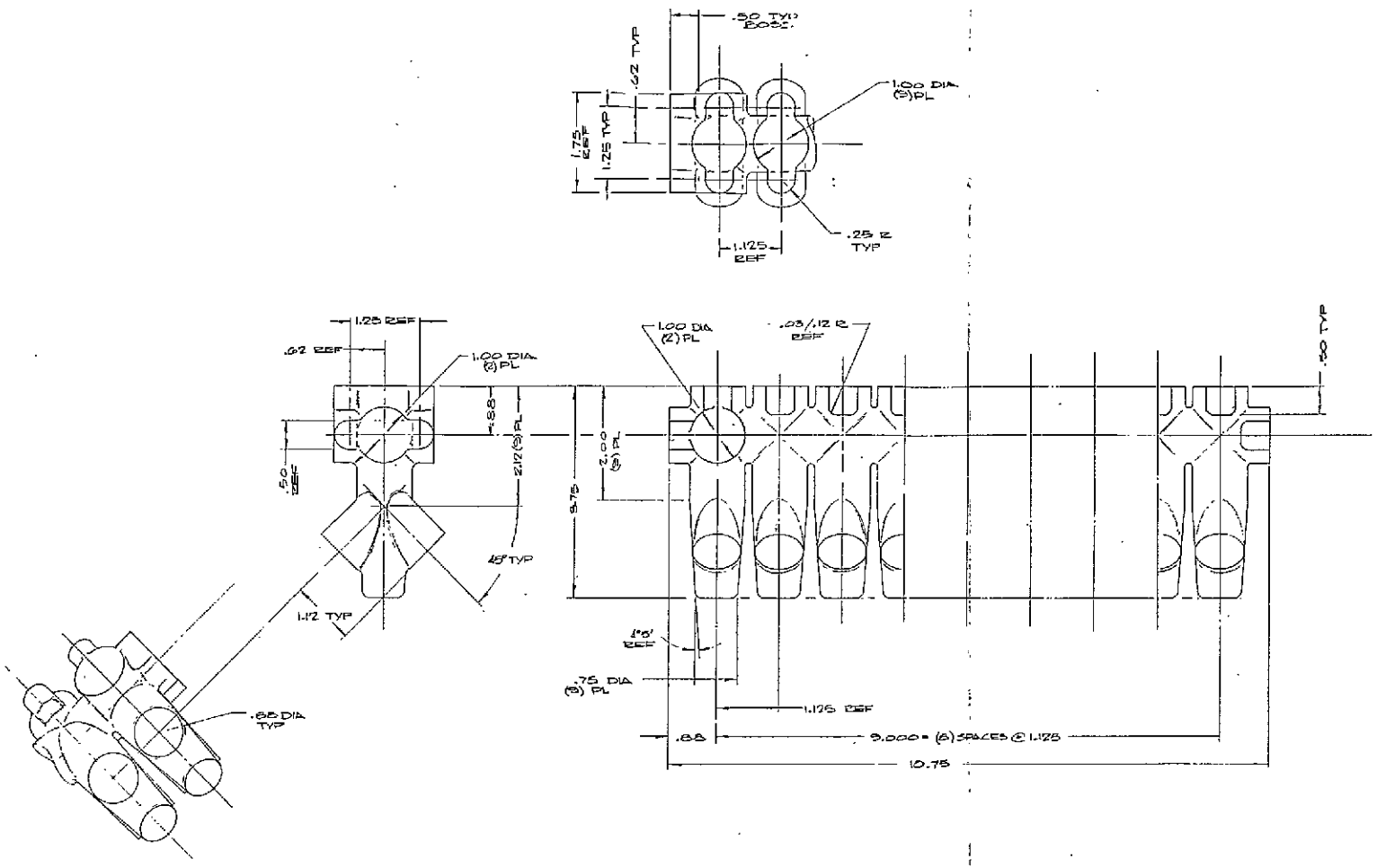

NOTES:

1. UNLESS OTHERWISE SPEC:
   A. UNDIMENSIONED RADII .03/.12 R
   B. DRAFT IS ADDED @ 2° MAX.
   C. CASTING IS TO BE SOUND & FREE OF VOIDS & INCLUSIONS

VALVE MANIFOLD CASTING

JB 8/10-78 SCALE 1/1

MATL: BRASS - SAE NO 44

TOL: .XX ± .03 ; .XXX ± .015

Doug Ellis (408)-736-8126

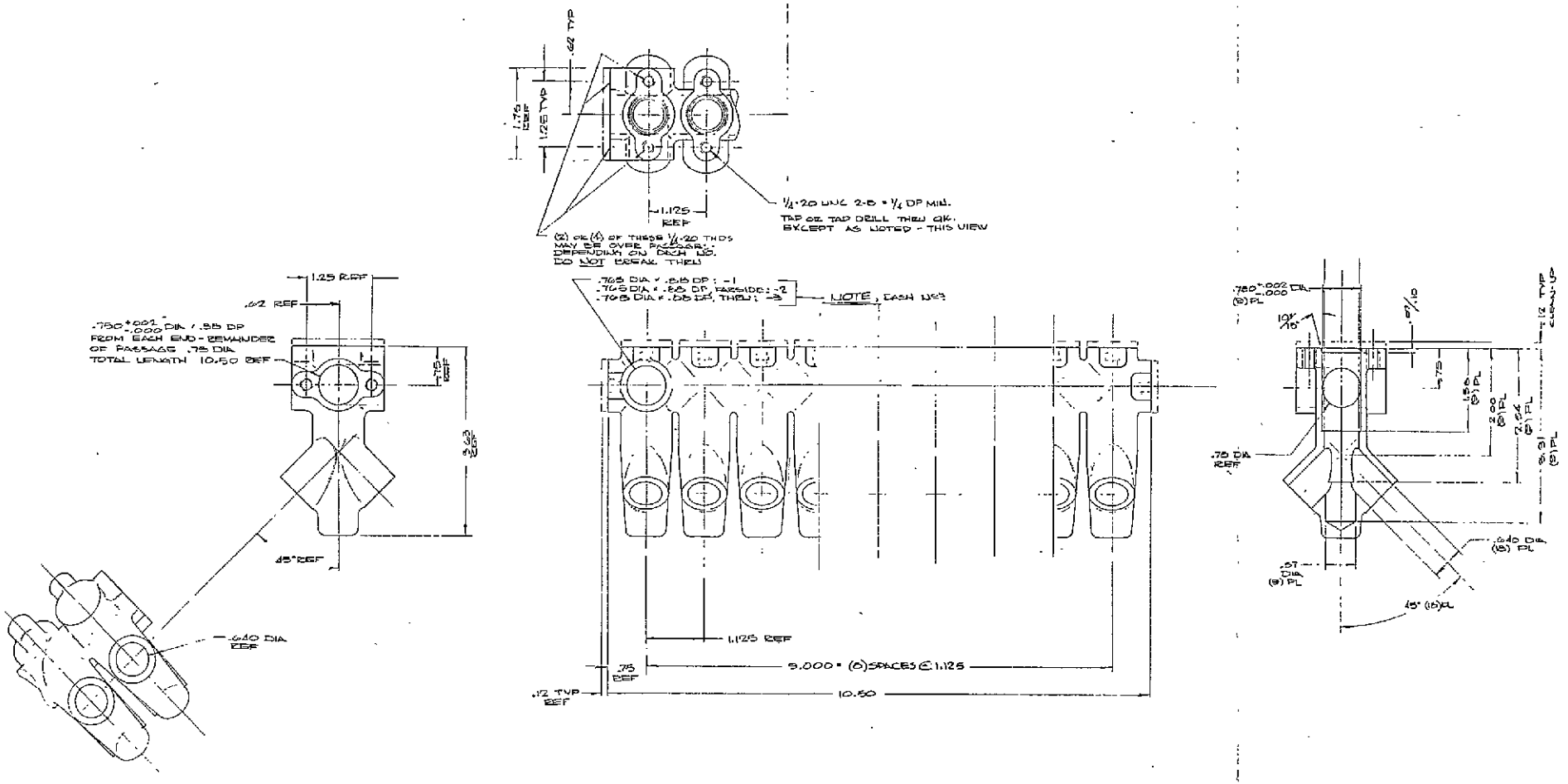

VALVE MANIFOLD
MACHINING

DWG 1/22-78 SCALE 1/1

TOL: .XX ± .01, .XXX ± .005
X° ± 1°

DWG ROOM (408) 725-8636

IV. Nitinol Tracking Devices For Concentrating Solar Collectors

Final Report: Grant No. DE-FG03-78SF01970
Principal Investigator: Charles Raymond*

1.0 Description of Concept and Research

One approach to increasing the cost-effectiveness of concentrating collector systems is to develop an inexpensive self-regulating control mechanism for tracking the sun. Preliminary experiments in Nitinol (Nickel Titanium -- a shape memory alloy) indicate that Nitinol will go through transition from the heat supplied by direct insolation. The primary purpose of this project was to construct and test a mechanism using Nitinol of the proper transition temperature range, so that a focusing collector will track seasonally (i.e., North-South) with precision. A second objective was to provide a simple East-West tracking system for flat-plate collectors, in order to increase system efficiency at minimal additional cost.

Basically, development of the nitinol tracking system consists of constructing two simple Nitinol heat engines, each of which is only required to cycle once per day. This is probably the simplest of engines, where a Nitinol element elongates when cool (at night) and contracts when it encounters the heat from solar insolation. The following is a brief description of the tracking device for the focusing collector (see Figure A): A Nitinol ribbon, wire, or spring is placed on a shadow line of the collector with an orientation parallel to the axis of rotation. The Nitinol is fixed at one end and connected to a ratchet handle at the other. Opposite the Nitinol, also connected to the ratchet handle, is a spring that pulls against the Nitinol with a force sufficient to elongate the Nitinol a distance x when the Nitinol is cold (at night or in shade). Under sunlight the Nitinol transforms and contracts to its annealed length with a force that overcomes the spring and also drives the ratchet. The ratchet turns a screw (or double screw such as a turnbuckle) which rotates the collector. The system is designed so that every time the Nitinol transforms it drives the collector through approximately 30 minutes of arc. Thus whenever the collector gets out of focus by 15 minutes of arc or so, the sun will hit the Nitinol and move it back into the shade. The only criterion for the tracking mechanism to work then, is that sunlight strikes the Nitinol at least once within every two or three days for the collector to stay in focus; even if there is a longer cloudy period, it would eventually catch up and come back into focus. The precision of tracking depends upon how fine one makes the shadow line and upon the magnitude of motion of the Nitinol element. This device uses only a small amount of Nitinol since the motion is very slight.

To provide East-West tracking of a flat plate collector, on the other hand, large Nitinol springs will be required, with the strength to withstand windloading and also provide a large displacement. (See Figure B.) The springs should be made from plate and annealed sinusoidally so that when they are heated they become very short and when cooled, long. The tracking flat plate collector, then, will be as follows: the collector is pivoted on

---

* Mr. Raymond has recently turned over all records, drawings and models involved in this project to Mr. Tom Flynn (P.O. Box 734, Marshall, CA 94940). Mr. Flynn will continue to promote research in this field.

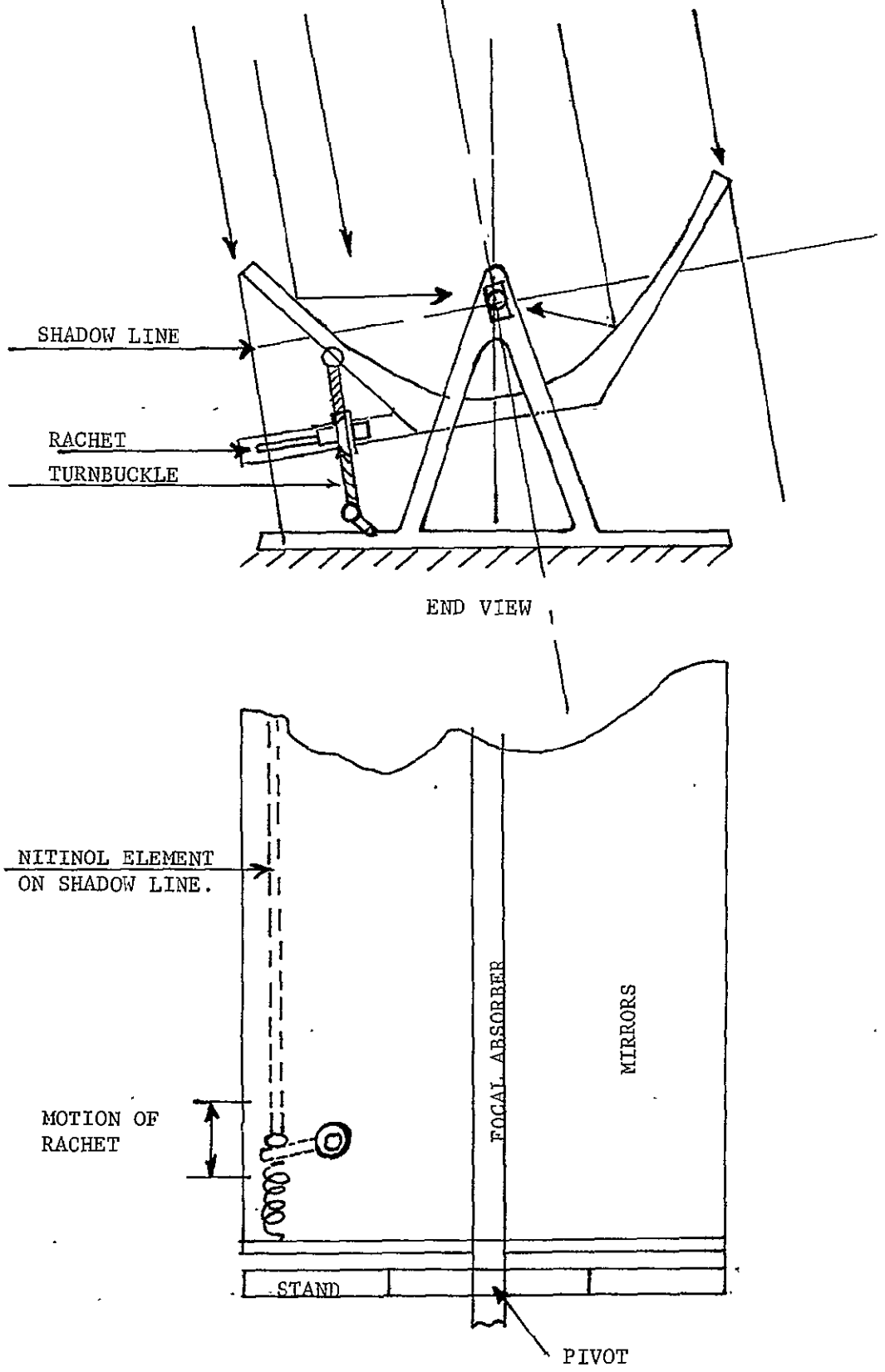

FIGURE A: NITINOL POWERED SOLAR TRACKING DEVICE FOR SOLAR COLLECTORS.

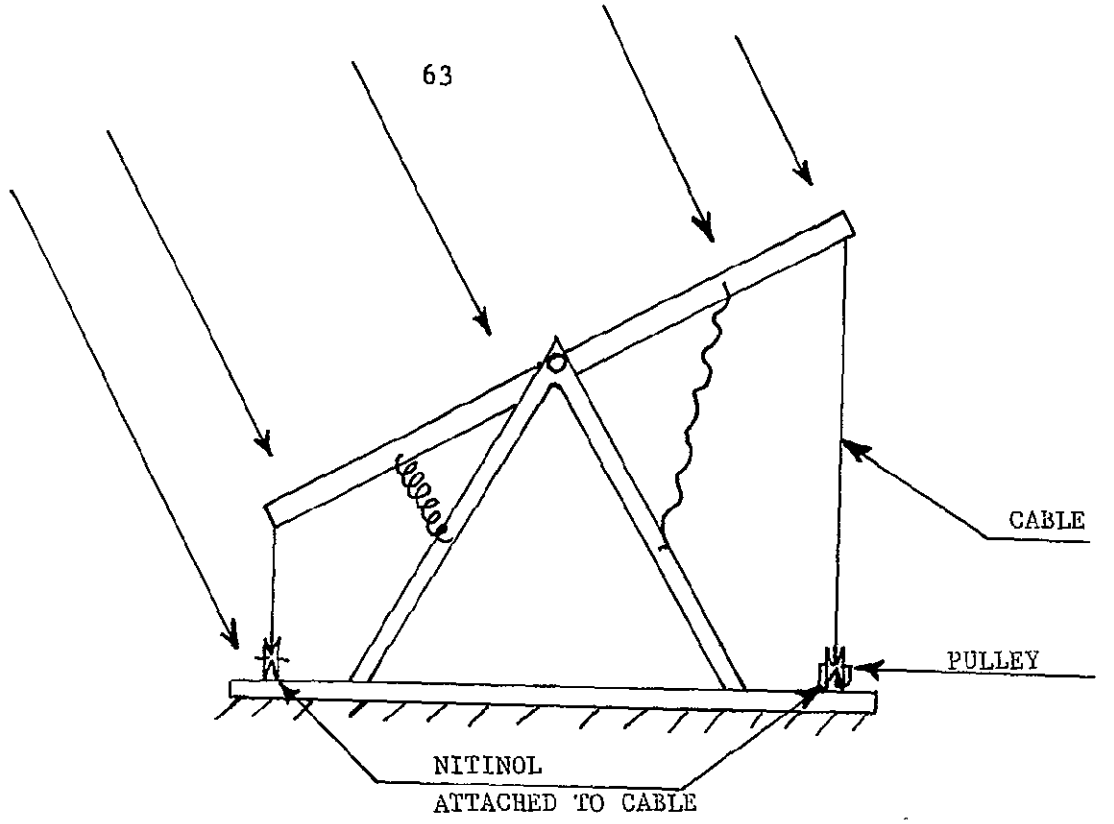

The Nitinol element is fixed to the stand so that it may have glazing for insulation. It is connected to collector by a cable linkage.

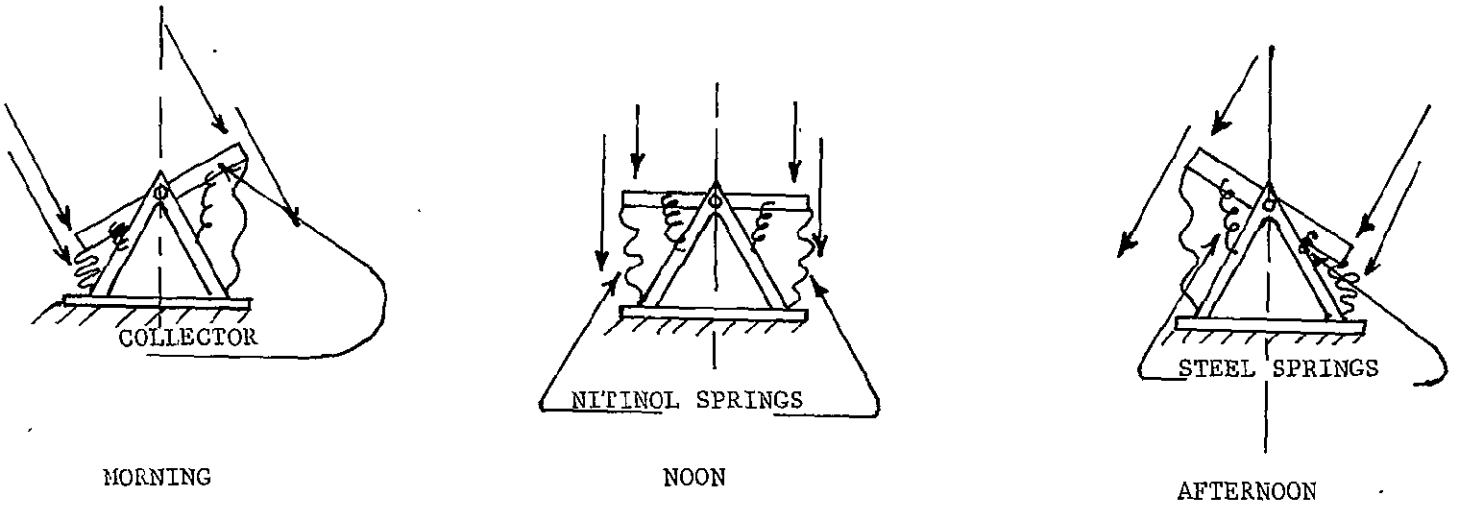

FIGURE: B SCHEMATIC OF MECHANISM TO TILT FLAT PLATE COLLECTORS.

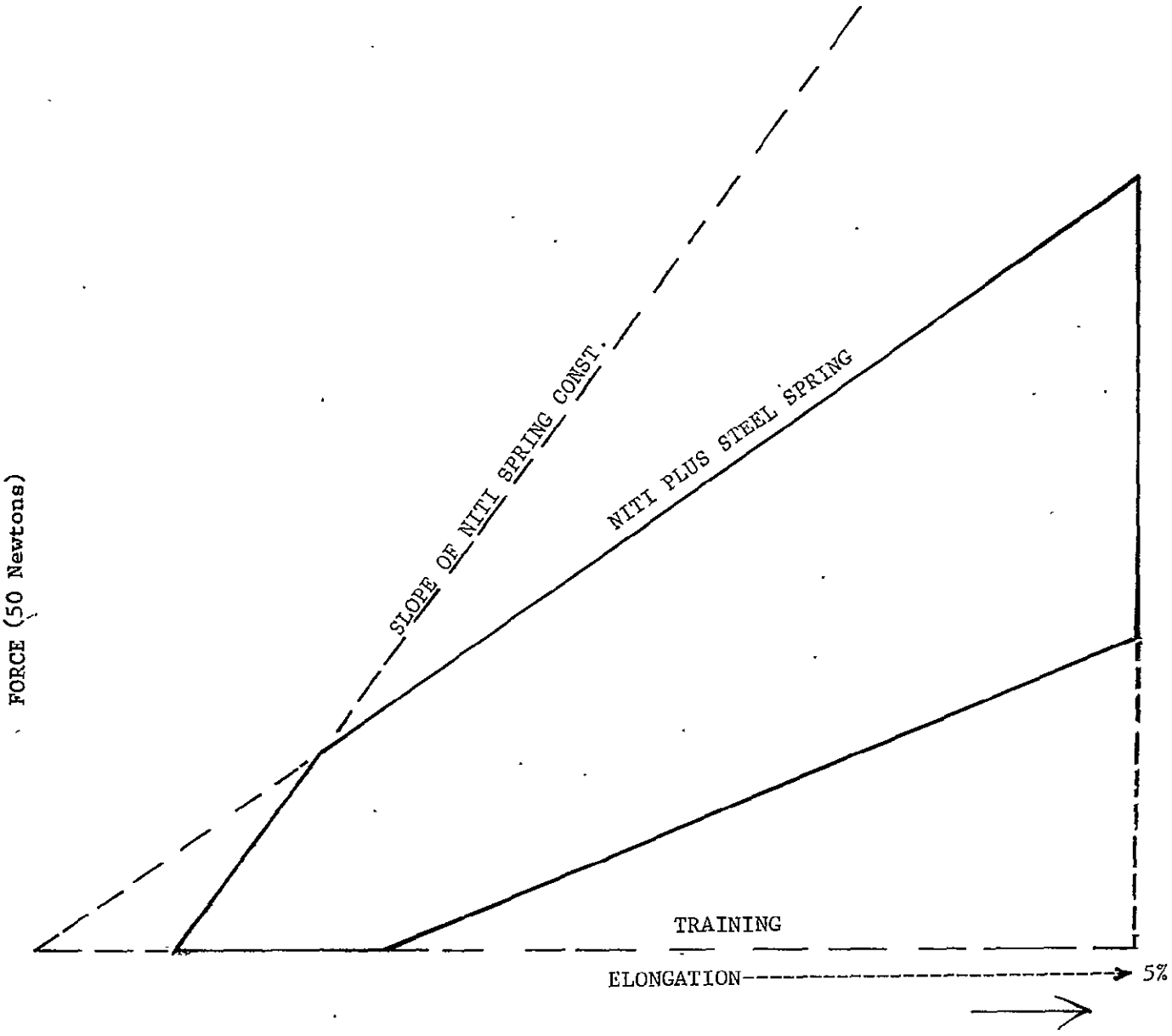

FIGURE C: TYPICAL NITINOL IN LINEAR TENSION ACTING AGAINST A STEEL SPRING

the inlet and outlet pipes forming the axis of rotation which lies north/south and is inclined to the angle equal to the latitude. Attached to the east and west sides of the collector are Nitinol springs that are also connected to the mounting. In addition, on either side are steel return springs that always tend to pull the collector to a horizontal position. The Nitinol springs have blackened outward surfaces to help collect solar heat and insulation on the inward surfaces; they may also have a transparent insulation on the outward surfaces. The collector is elevated sufficiently to allow it to pivot and is provided with rotary seals on the inlet and outlet pipes. During the night, the Nitinol springs are cool, in a related state, and the collector is brought to a horizontal position by the steel springs. As the sun rises in the East, the eastern-most Nitinol spring is exposed fully to the morning sun causing it to contract and tilting the collector to face the sun. As the day progresses the shadow begins to fall on the eastern-most spring, allowing parts of it to cool and relax, returning the collector ot its horizontal position when both springs are in shadow. As the afternoon progresses the sunlight begins to fall on the western-most spring, causing this to contract and the collector to tilt toward the sun, etc.

The research and development involved in this project consisted of (1) the annealing of Nitnol to an appropriate spring configuration; (2) the cycling of the material to reach stability; (3) the incorporation of the Nitinol material into solar collecting systems; (4) the actual testing of the working systems. These steps are described in greater detail below.

2.0 Annealing and Cycling of Nitinol

Nitinol material was made available for this project by Lawrence Berkeley Laboratory. The Nitinol wire and plate were annealed as wire, wire cable, wire wave springs, wire leaf springs, plate leaf springs and plate wave springs and various tests were performed to determine the suitability of each for solar applications. In addition to these tests, the samples were, in general, cycled under the conditions of the work cycle to accomplish shape-memory training and to achieve stable and reproducible data.

Probably the most efficient use of nitinol wire is in linear tension since the whole element is cycled rather than the surface as in bending mode devices. Hence, the initial tests were made on nitinol wire in linear tension. The nitinol was coupled to a steel spring so they could work in conjuction and avoid overstressing the wire at any point in the work cycle. A stress-strain diagram was made using an 0.020 in. diameter wire, 20 in. in length, coupled to a steel spring with a 9 lb./in.^{2} constant. A typical cycle is shown in Figure C; the spring constant of the steel spring as well as the nitinol are presented. As indicated, this cycle produced a decent area within the curve and hence a large amount of net work. The force was up to 50 newtons and the elongation was 5%. The data indicated that a 5% elongation is reproducible.

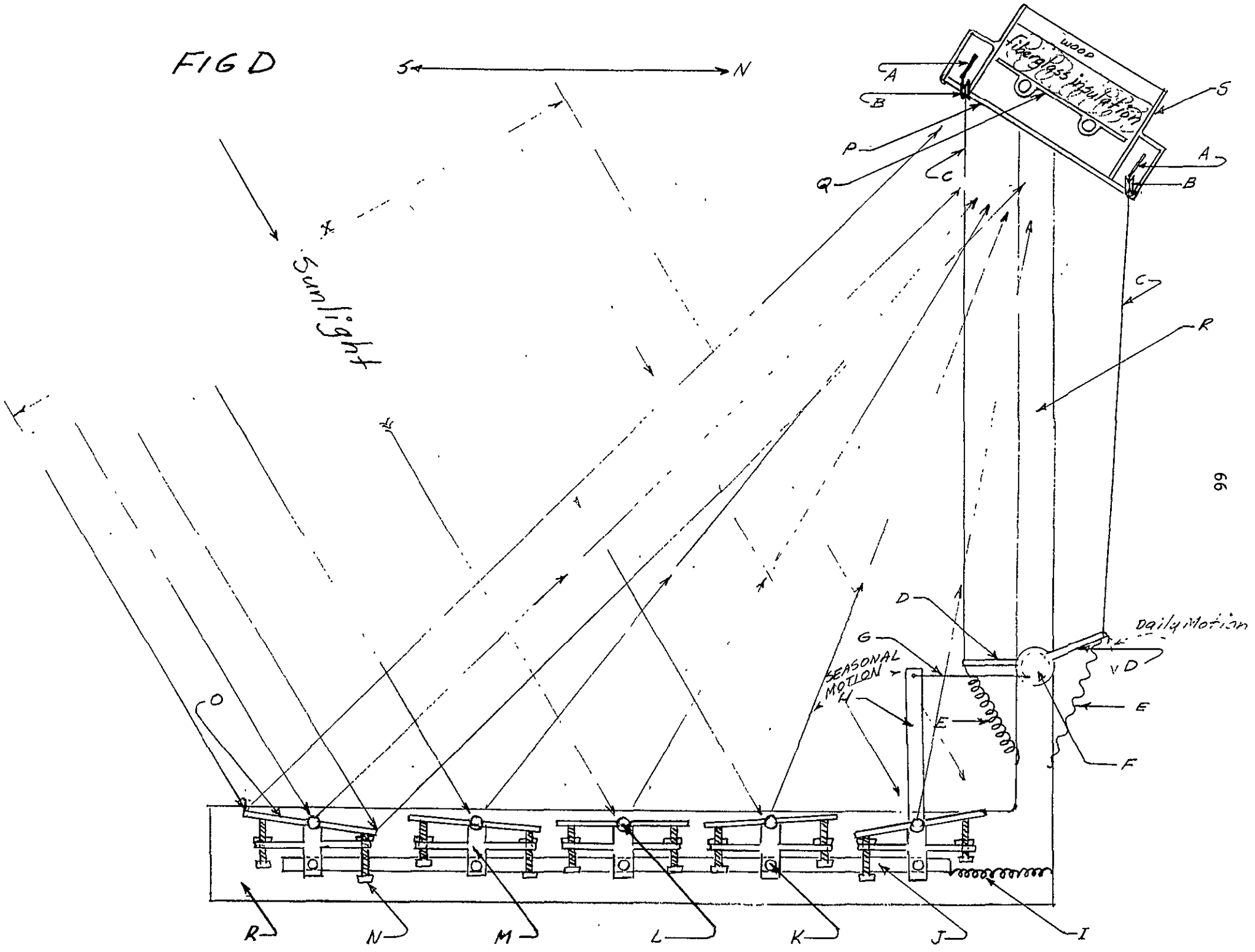
FIG D
S
N
Sunlight
wood
fiberglass insulation
A
B
P
Q
C
S
A
B
C
R
D
G
SEASONAL MOTION
H
E
E
F
Daily Motion
VD
O
R
N
M
L
K
J
I
99

Next, several cables were constructed, annealed and subjected to similar tests using heavier springs. Leaf springs and sinosoidal wave springs from both plate and wire were then constructed and annealed (1000°F) and tested. Although the wires in tension produced high forces per mass compared tothe springs, the springs produced much larger elongation rations (as expected). The cables appeared to have better characteristics than the single wires in tension having slightly higher elongation ratios. The various springs had elongations of from 25% to 150%, depending on geometry.

3.0 Incorporation of Nitinol Into Solar System

Different configurations of nitinol cables and springs were constructed and tested for North-South (concentrating) and East-West (Flat Plate) tracking. These applications are described below.

3.1 North-South Tracking For Concentrating Collectors

A focusing reflecting solar collector was constructed of the type having a number of slat mirrors linked together and focused on a single plane (Figure D). Five mirrors are focused upon a plane of approximately the area of a single mirror so that the concentration is approximately four to one (allowing for geometrical losses). The mirrors are pivoted on parallel East-West axes and focus on an absorber whose axis lies above and parallel to the mirrors. Each mirror is initially rotated to reflect onto the absorber, and is fixed to a linkage control rod so that the mirrors all move in unison. The frame and mirror mounts are made of aluminum and the mirrors are 1/4" x 5" x 48" glass mirrors. The absorber is a 6" x 48" x 1/16" copper plate with two 3/4" diameter copper tubes passing through it. The absorber is blackened and glazed, and has fiberglass insulation on the back (upper) side.

Parallel to and on either side of the focus, blackened nitinol springs are provided and are linked to the slat mirrors by means of cables, pulleys and ratchets. The nitinol springs are made as a sine wave so that one view shows them as a sine wave and another view, as a line. The object of having a line parallel to the focus is to provide a sharp boundary to the focus. As the seasonal change in sun angle moves the reflected light out of focus, it begins to strike the nitinol spring. When heated by the direct sunlight, the nitinol spring contracts approximately two inches, pulling a cable with a force of 30 pounds and turning the ratchet mechanism that moves the slat mirrors back into focus. The response time is approximately one minute in the focused sunlight. (This time depends upon the air temperature within the collector, the nitinol surface to volume ratio, etc.) As long as the sunlight remains on the nitinol, the wire remains contracted and cannot move the collector further. As sunlight is taken from the nitinol element, it cools and return springs bring it back to its original extended length. If for some reason the collector is still out of focus and the nitinol is not allowed to cool, it will not complete the cycle until night. Thus, if one had several cloudy days in which the sun did not come out with sufficient strength to cause the nitinol to focus the collector and this was followed by a series of clear days, it might take the mechanism several days to catch up. The amount of motion per contraction, then, should be more than one day's motion. Intermittent clouds could help by allowing more than one cycle per day. The sharper the focus and the stronger the concentration, the more pronounced the nitinol response. The use of multiple elements would also solve this problem.

FIG E

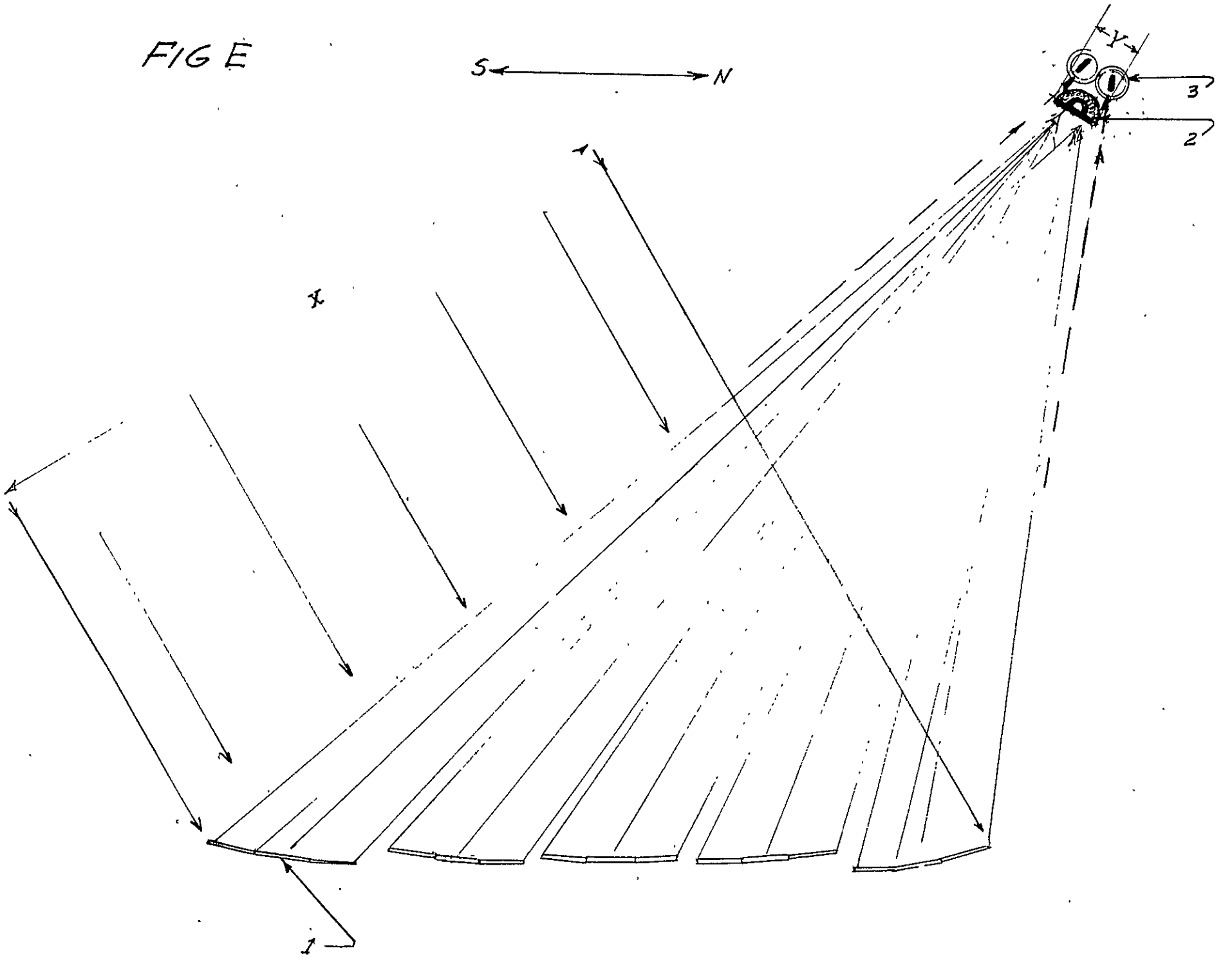

FIG F.

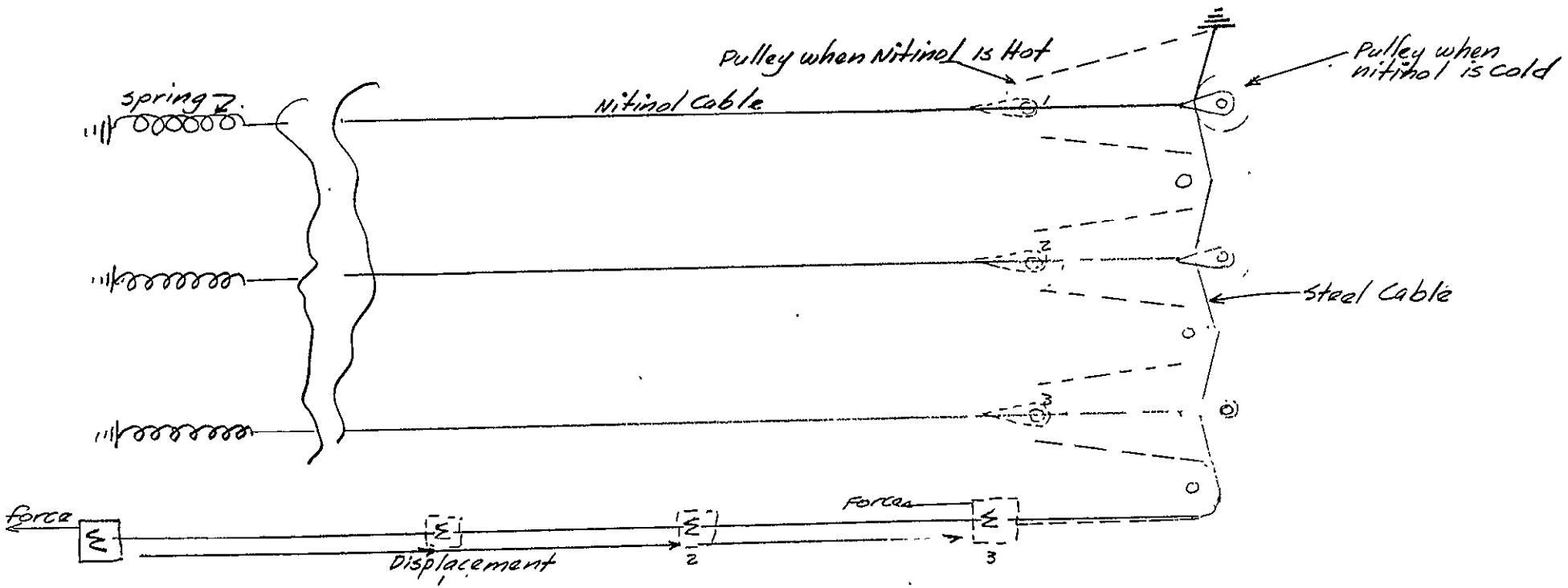

A Device Was Built with the idea That Individual Nitinol Elements Could Be Successively Transformed To Allow A Force To Be Applied Incrementally

The Pulley Friction was Great. The cable Had Too Little Surface Area Exposed to Sunlight to Fully Transform.

The nitinol used in this model is .090 inch diameter wire. The springs are approximately 12 inches long and produce two inches of motion each. The forces involved are on the order of 25 to 35 lbs. The restoring force from spring E was set at 8 lbs. maximum; thus the net force is about 30-8=22lbs. pulling on the ratchet. The ratchet has a 4 1/4" moment arm, turning a spool with 1/4" radius for a mechanical advantage of 17:1. This may be easily varied for either more or less stroke, by changing either the length of the moment arm or the diameter of the pulley. Spring I is set at about 50 lbs. In place of the pulley, cable and return spring moving the control rod which inclines the mirror slats, one could use a small rack and pinion of a variety of other linkages. Two small automotive inside ratchets were used in this model for the ratchet mechanism. They are reversible ratchets and one will have to push both buttons to reverse the direction twice a year at solstice. This could be done automatically by hooking a linkage to the ratchet control; however, this seems a minor improvement and not worth developing at this stage.

Referring to Figure D, a cross sectional view of the collector facing E-W, we see the nitinol springs at A. They are connected to a steel cable C passing through pulleys B and connected to ratchet arms D. The ratchets turn spool F, winding cable G connected to lever H. Lever H is connected to each mirror through pivots K and is held in the other direction by spring I to frame R. The mirrors are initially focused with set screws N. Thus, an area normal to the incident light equal to x times the length is caused to reflect and impinge on an area y times the length for an amplification of x/y, in this case only about 4:1.

Photographs I and II show the collector under construction. Photo III shows a view looking into the mirrors at the absorber housing with the absorber missing. Photo IV shows the completed unit with one end mirror in place. Photo V and VI show the tracking system operating. Photo V shows the ratchets in the nitinol springs' cold position on a cool dewy morning. As the sun came up, the focus moved enough to strike the nitinol and cause the ratchet arm on the right to rotate through about 30° upward which corresponds to a two inch contraction of the nitinol spring. It is quite difficult to get a photograph of this as the focus only changes every couple of days and one never knows when the sun will first strike the nitinol although changes are greatest first thing in the morning. Due to unexpected delays and interruptions on this project, extended tests on this model were not made. However, the observations made indicate that the device was tracking well and staying in focus. Temperatures as high as 220°F were obtained. Data were not gathered on the collector itself as it was constructed more as an experiment for the nitinol than as a working collector.

Figure E shows a proposed refinement of this design. The slat mirrors are each segmented into three (or more) slats to provide a further amplification factor or three. That is, they are installed in the mirror holders as a parabolic sector with a focus at about the average distance from mirror to absorber (1). The result would be an amplification of 12 rather than 4, resulting in higher temperatures, less materials, sharper focus and quicker response in the nitinol controls. The absorber would be smaller (2) and probably would not require glazing. The absorber would be a single fluid

pipe insulated on the back side. The nitinol springs (3) are shown in glass tubing. The dotted line shows the line of focus corresponding to activation of the nitinol springs.

3.2 East-West Tracking For Flat-Plate Collectors

The East-West tracking has proved a more difficult matter due to having unfocused sunlight with correspondingly less heat available for transformation. A number of configurations were tried, some of which worked and others that didn't. Initially, several long nitinol wires were connected in parallel, fixed at one end and attached to a series of pulleys on the other end. (See Figure F.) The pulleys were attached to a common cable that was to move the collector or reflector as the elements were progressively heated by sunlight. There were two problems with this approach: (A) that there was a lot of friction in the pulley system [although the pulleys used were inexpensive and of poor quality and the use of better materials might help alleviate friction] and (B) that unfocused sunlight falling on the relatively small surface area of the wire was not enough to affect transformation [the convection losses were great].

Wave and Leaf springs were then used both in water baths and later in direct sunlight. One sinusoidal wave spring was about 11 inches long and when heated would contract 2.5" at a 30 lb. load. It took five to eight pounds to elongate the nitinol after cooling to ambient air temperature (65° - 75°F). This spring was made of .090" diameter wire with a transition temperature range (TTR) of 120° - 150°F. With a glazing and moderate insulation, this spring would react to unfocused sunlight. The spring was then enclosed in a box with a glass cover and arranged a shadow line to progressively heat it along its length. A pair of weights were attached to the nitinol spring. A three pound weight stayed on all the time and was used to provide the cold elongation. An additional five pound weight simulated the collector friction. As the sun began to strike the nitinol not much happened until the ambient air inside the box rose somewhat. That is, the cold air inside the box provided convection losses. As a further complication, as the nitinol began to transform on the end exposed to the sunlight, rather than lift the weight, it further elongated the cold nitinol. Thus the result was that during the morning nothing happened, then toward noon the weight was rapidly lifted. In order to counter the latter problem, a set of nitinol leaf springs were constructed that were connected by a cable and in which the cable itself limited the stress and prevented any further elongation over the desired amount. (See Figure G.) Numerous tests were run using hot and cold water on this configuration, with satisfactory results. The cold nitinol was uneffected by additional load due to the stress relieving cable. However, there were still convection losses in direct sunlight with that morning lag in transformation.

Next, a piece of flat nitinol ribbon was annealled into a sinusoidal wave spring. The material was .025" x 3/4" x 12". This was blackened on one side and installed in a collector box with glass over the top and some insulation. This configuration seemed to work fairly well except in the very early morning when the fill factor was poor and when there was a lot of reflection on the glass. A weight was used to return the spring at night. The

system uses a five pound pull as return and will lift more than ten pounds a distance of two inches. The thinness of the material was a disadvantage as the spring was not as strong as one would like; however, with a longer and thicker element the E-W tracking would probably work out. Unfortunately, nitinol plate of a larger thickness was unavailable at the time of this testing. As a further experiment thin clear plastic was attached to a nitinol plate in lieu of the box with glass covering. (See Figure H.) This was found to work very well, especially with two layers of plastic. This system has a number of advantages, the foremost being cost. If plastic can be used, then the whole apparatus for moving E-W could conceivably cost less than ten dollars per collector. The sine wave plastic coated and plastic insulated plate nitinol also has the advantage of less reflection in the morning and afternoon as some of the surfaces will be near to normal to the sun's rays (rather than parallel, resulting in reflection off the glass). By using a shadow line the material actually did contract roughly proportionally to the area exposed to the sunlight. One problem was that the hot nitinol tended to further elongate the cold nitinol due to increased force (additonal weights were added). This can be overcome by adding a stress limiting element as was done with the wire springs. A three foot by 1" wide by .125" spring should be adequate to provide E-W collector or reflector tracking and would be able to withstand wind loading (assuming a 3' x 10' collector).

These experiments indicated that a nitinol element of this type will perform such tasks as opening windows, shutters, louvres and the like, and would be benefical to passive solar systems such as homes or greenhouses. The plastic coating concept makes it ideal for a self-opening hinge. This would be a simple piece of plate, blackened and with plastic covering that is used in place of a conventional hinge so that as the sun strikes the hinge, it opens (or closes) the window, door, etc. It looks as if this would be inexpensive to manufacture.

4.0 Other Developments

A rotating nitinol engine was built, using nitinol in linear tension. The nitinol elements are arranged axially forming a cylinder (of varying length) much as the toggle plate engine that was built by the Lawrence Berkeley Lab. This engine overcomes some of the problems encountered by Hernandez and that caused the LBL engine to be unsucessful. Briefly, the improvements are as follows: (1) The elements are doing work on springs and the springs in turn do the mechanical work. This has the advantage of divorcing the nitinol cycle so that the machine does not destroy itself. (2) The nitinol, arranged axially, is linked to a pulley that converts axial motion to radial motion. Thus the machine has a relatively large eccentric resulting in high torque. The problem of the LBL engine was one of large forces over small distances and this is overcome here. The eccentric has a two inch throw. (3) Friction is greatly reduced. The LBL engine required very large bearings (railroad type tapered roller bearings) to handle the large axial loads produced by the wire in tension. In this engine, the nitinol is fixed at the ends so that the only bearing loads are radial (torque loading) except for the pulleys that convert the axial forces to radial forces. Although these bearing loads are high, the motion is very small so that PV is very small and there is little friction. In any individual element, a 2 pound force causes the machine to rotate and overcome friction. This design had eight elements, each capable of about 45 lbs.

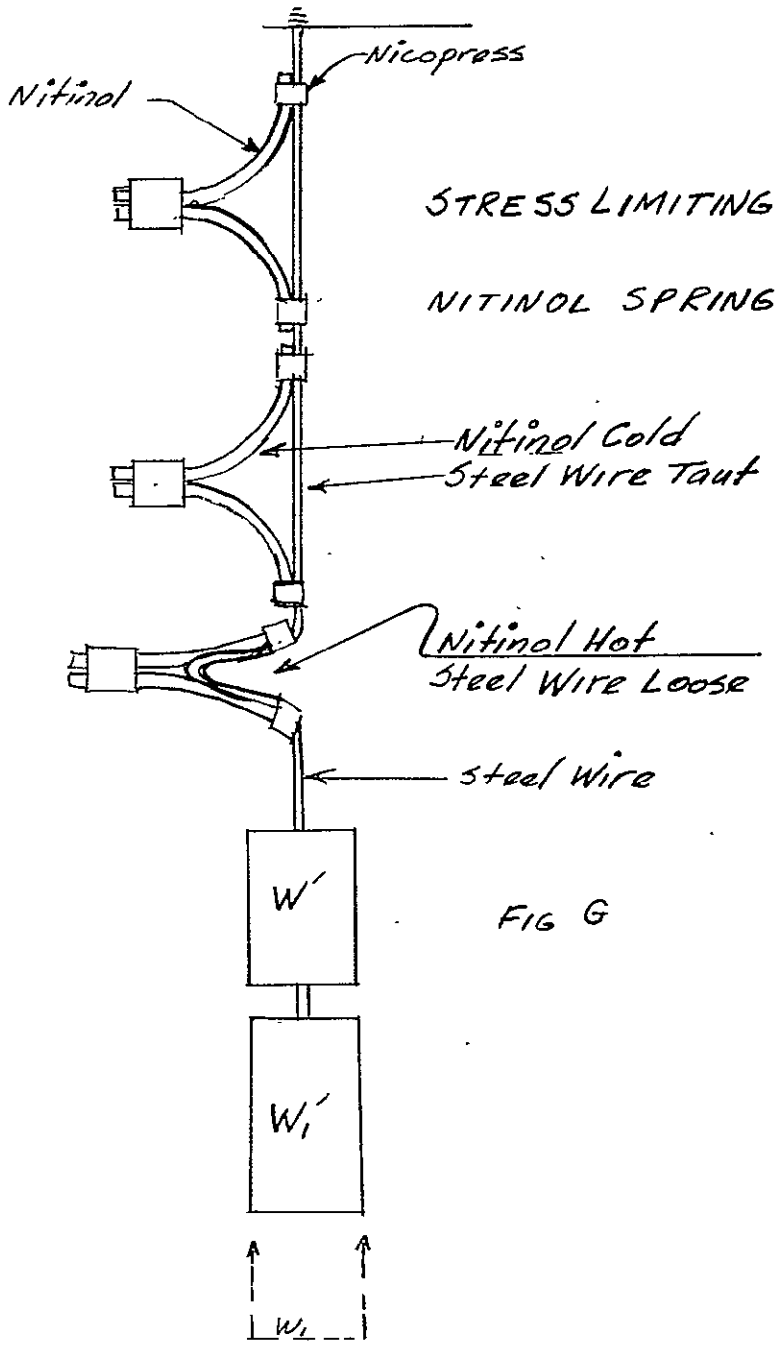
Nitinol
Nicopress
STRESS LIMITING
NITINOL SPRINGS
Nitinol Cold
Steel Wire Taut
Nitinol Hot
Steel Wire Loose
Steel Wire
W'
W1'
W1

FIG G

FIG H

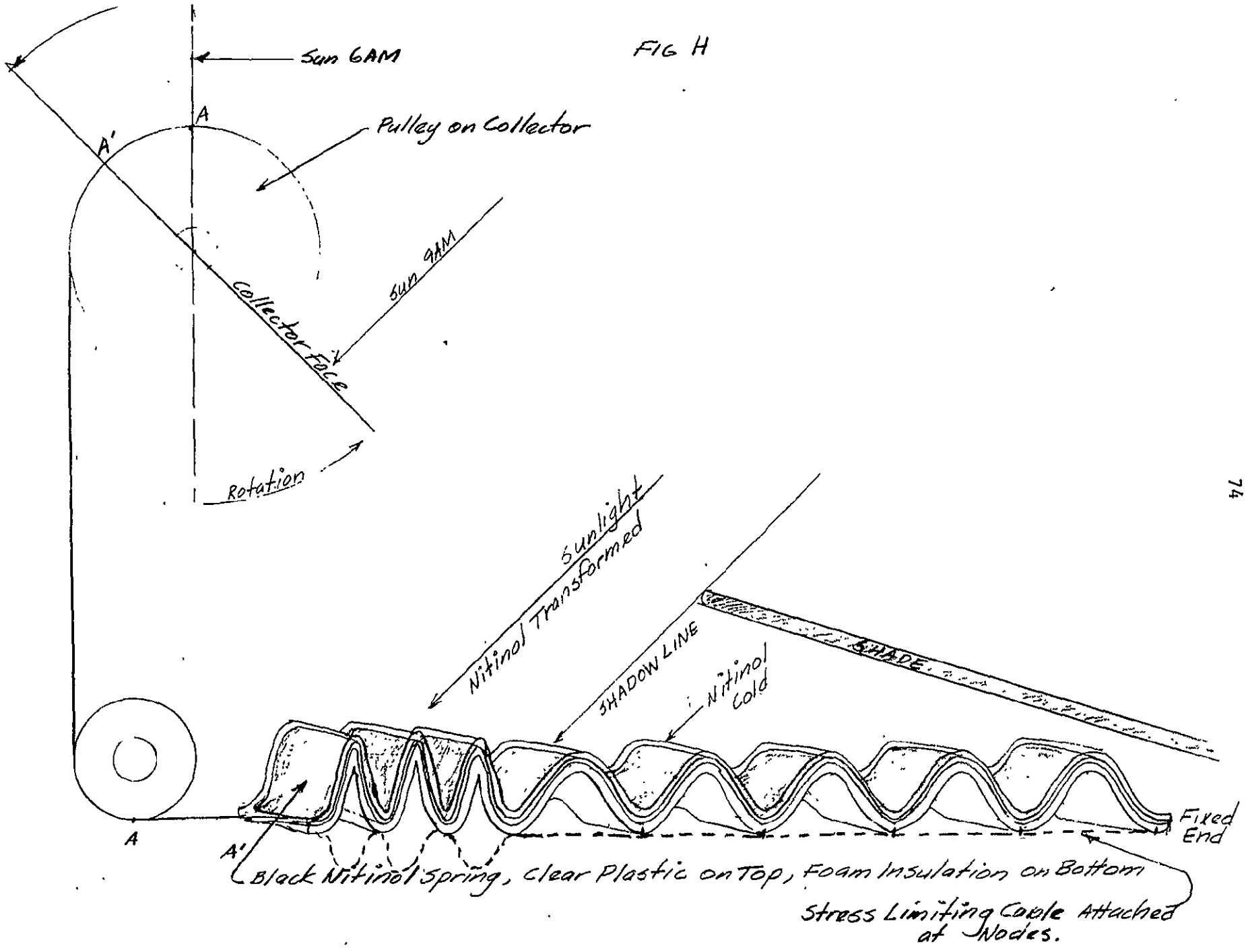
Sun 6AM
A
A'
Pulley on Collector
Sun 9AM
Collector Face
Rotation
Sunlight
Nitinol Transformed
SHADOW LINE
Nitinol Cold
SHADE
A
A'
Fixed End
Black Nitinol Spring, Clear Plastic on Top, Foam Insulation on Bottom
Stress Limiting Cable Attached at Nodes.

A crude nitinol pump was also built, using hot water as the source and evaporation and ambient air as the sink. (See Pictures IX and X) The cycling was gravity assisted (the pump incorporated a gravity engine). The nitinol element, being very large in diameter, made the pump slow; however, it did cycle.

5.0 Conclusions

In conclusion, several potentially valuable products are indicated by this research. The technical feasibility of both E-W and N-S tracking has been established. Possibilities have been identified for passive systems and for solar water pumping. Research should be continued to refine the designs developed under this grand, and to develop cost-effective prototypes for nitinol tracking systems.

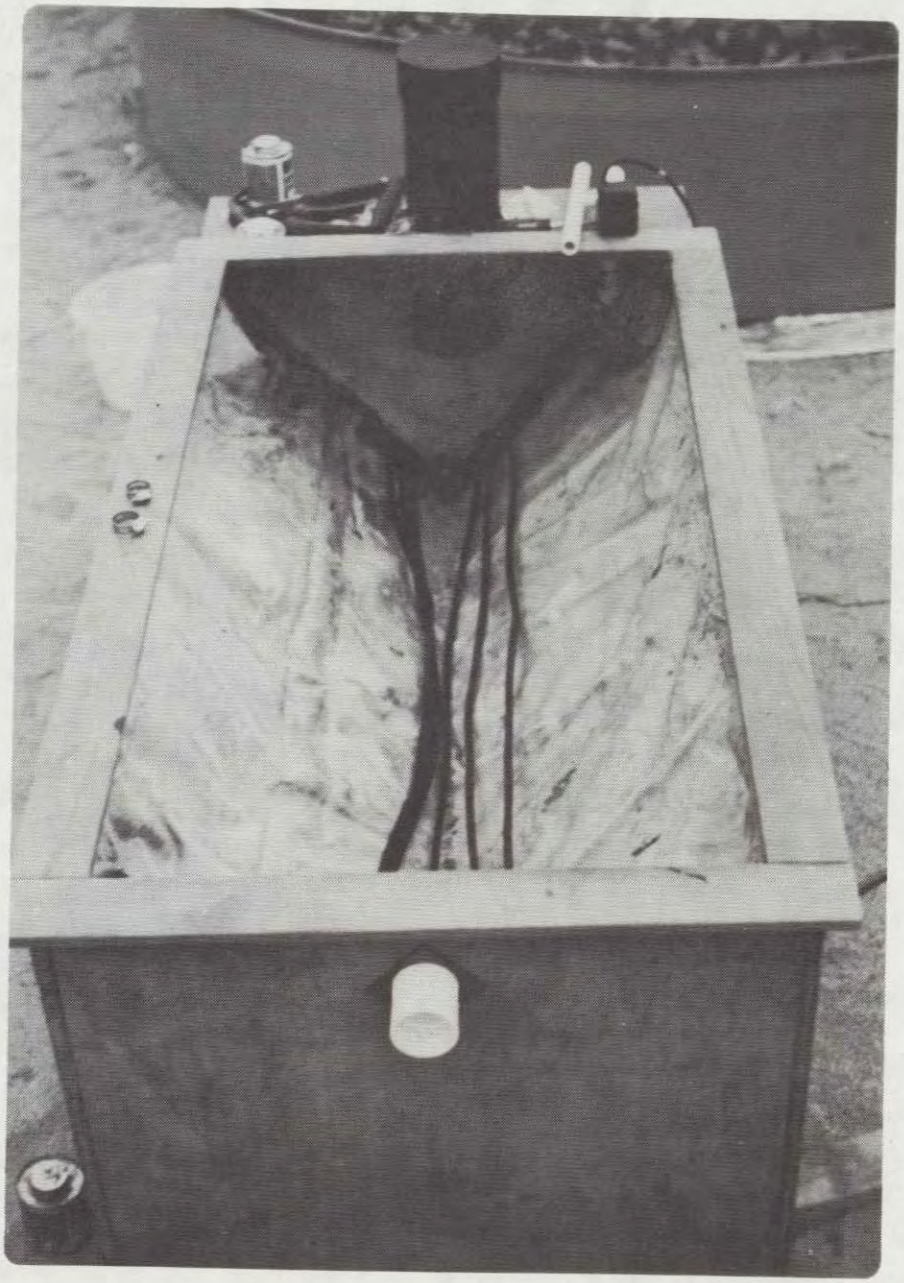

FIGURE 4: Digester showing internal heat exchanger.

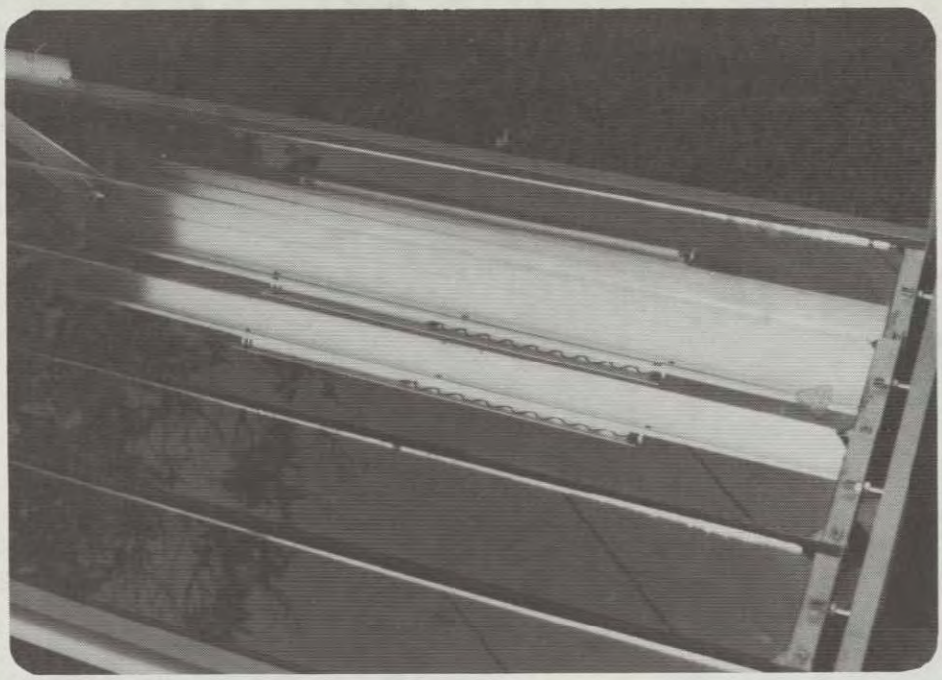

PICTURE III

VIEW LOOKING INTO MIRRORS AT ABSORBOR HOUSING (ABSORBER MISSING)

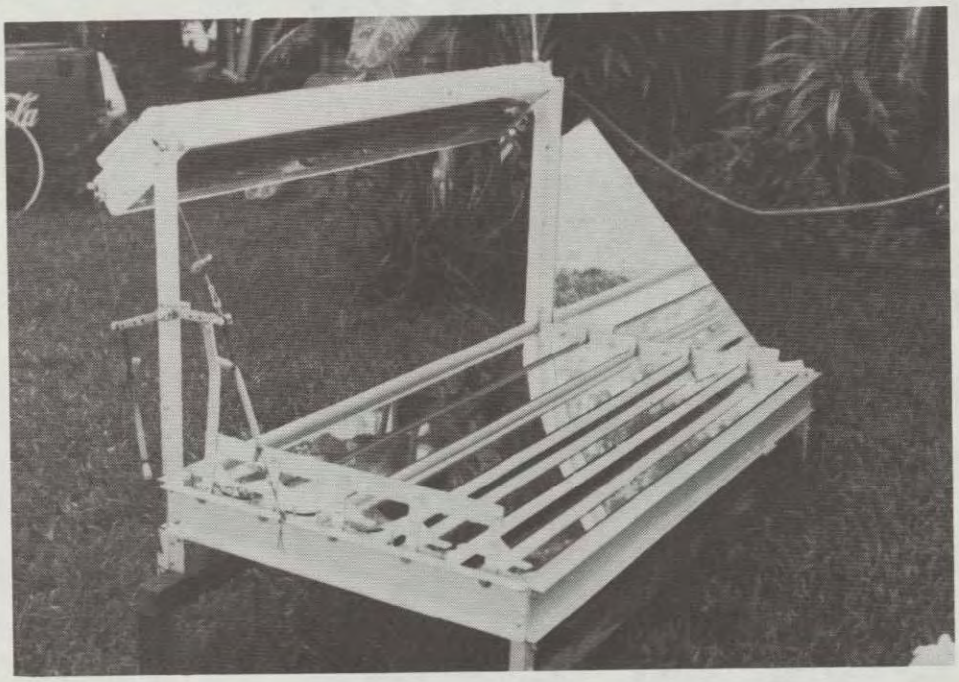

PICTURE IV

COMPLETED UNIT WITH ONE END MIRROR IN PLACE

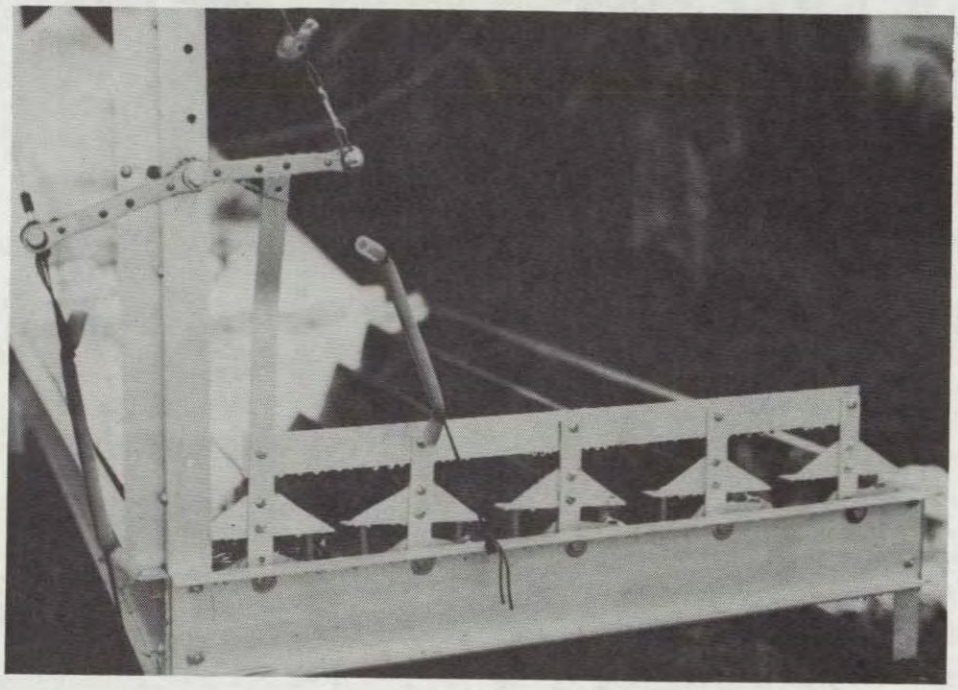

PICTURE V: RACHETS IN NITINOL SPRINGS (COLD POSITION)

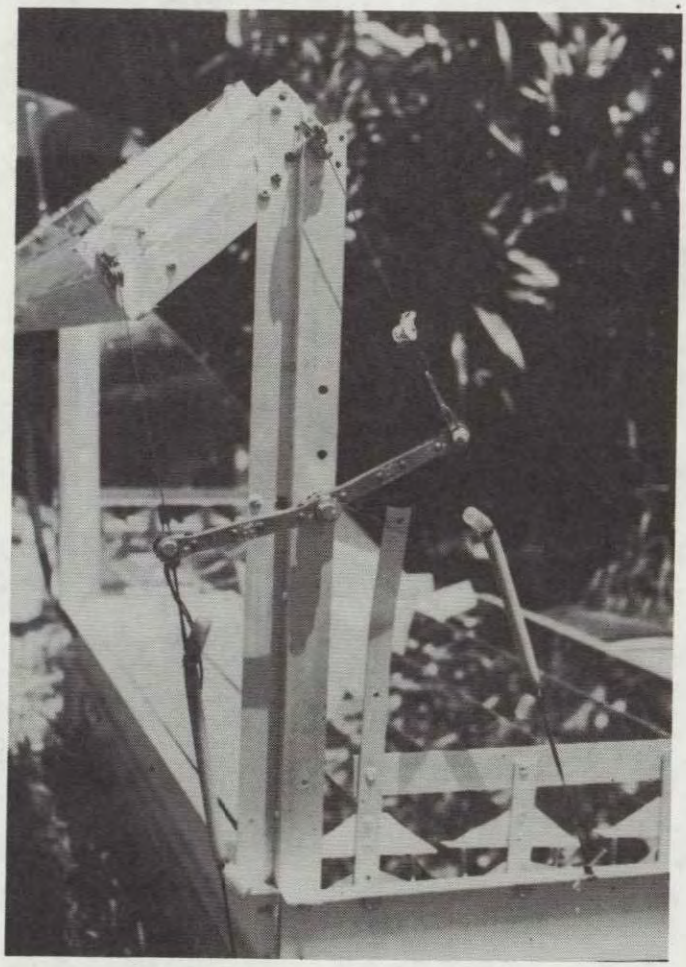

PICTURE VI: COLLECTOR SYSTEM IN COLD POSITION

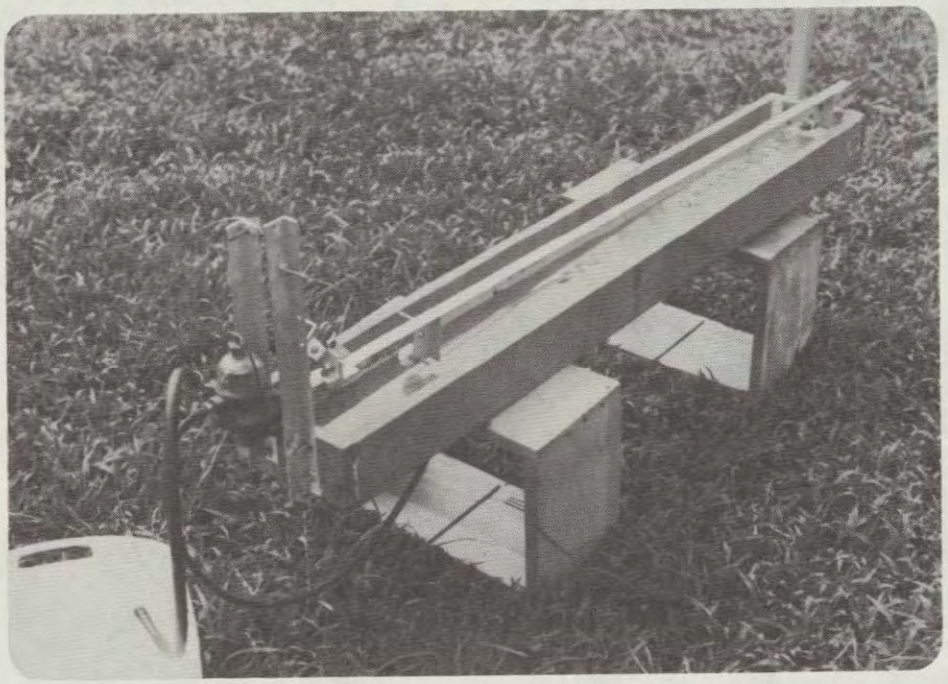

PICTURE IX: NITINOL PUMP

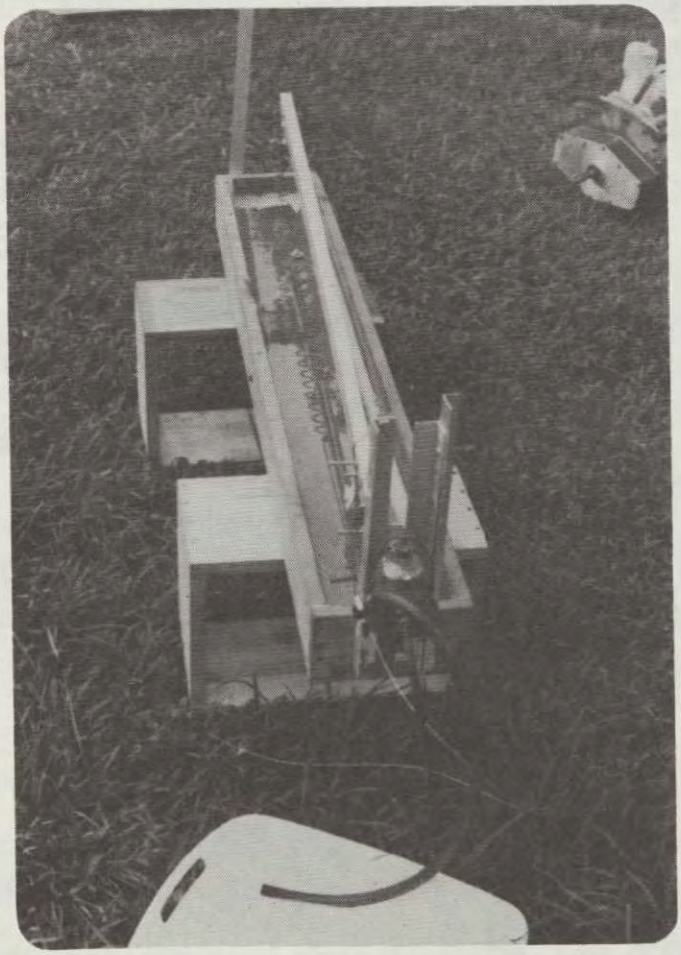

PICTURE X: NITINOL PUMP

V. Free-Formed Insulated Concentrating Solar Collector

Final Report: Grant No. DE-FG0379SF10552
Principal Investigator: Glen Goodwin

1.0 Summary

A free-formed, insulated solar concentrating-collector has been designed, built, and tested. The design utilizes new concepts to achieve simplicity, low cost, high efficiency, and long service life. Tests and demonstrations carried out under this program indicate that the majority of these design goals have been realized. Only the long life reliability requires additional work and evaluation.

Three concepts were utilized to meet these goals: First, the concentrating reflector is free-formed by hand from a thin steel sheet which requires no special skills or equipment. Only a light-weight frame is required to support the concentrating reflector. Second, a transparent cover is placed over the concentrator and insulation is placed on the back and ends. This combination places the collector tube in a hot still-air environment which reduces heat losses and protects the reflecting surface from attack by rain and dust. In effect, the collector tube is placed in a "Solar Greenhouse". Third, a highly-reflective aluminum film, protected by bonding between two thin sheets of UV stabilized polyester, is fastened to the steel substrate by peelable adhesive. This film is inexpensive and can easily be replaced in the event of damage or degradation through longtime use without altering other elements of the collector.

The concentrating collector can be easily built by the average person using only normal hand tools. No special equipment is needed. The material cost of the unit without sun seeking electronics and drive motor is about $6.75 per square foot of sun capturing area. Sun following equipment adds to the cost, however, in units of about 100 square feet sun following equipment contributes about $2.00 per square foot. Labor costs are estimated to be approximately $3.00 per square foot for a $5.00 per hour labor rate for a trained crew. On a do-it-yourself basis a 100 square foot unit would cost about $875. This is a very low cost for an efficient concentrating solar collector.

Tests of the prototype collector performed by a certified solar test laboratory have been made and the results compared with similar tests of a commercial unit. These tests indicate that the efficiency of the prototype is higher than the commercial unit at outlet temperatures below 160°F and comparable with the commercial unit at the boiling point of water.

2.0 Introduction

Efficient production of mechanical power, refrigeration, and most industrial heat applications require temperatures at or above the boiling point of water. Temperatures of this magnitude are beyond the capability of simple flat-plate solar collectors, but are easily within the capability of concentrating collectors. Large-scale utilization of solar energy can be accelerated by the availability of simple, low-cost reliable concentrating

collectors with high efficiency and the ability to maintain this high efficiency over a long working lifetime.

Indeed, many of these applications are presently being demonstrated using concentrating solar collector systems. However, operation of these first-generation systems has uncovered problem areas which must be addressed and solved if solar energy use is to expand into the high-temperature application field. Some of these problems are: high-system cost, questionable reliability of reflecting surfaces directly exposed to the elements, and, in some cases, low thermal efficiency in cold windy weather.

This report describes a simple low-cost, efficient concentrating solar collector utilizing new concepts in the basic design which are aimed at correcting many of the present problems. Simplicity, low cost, long life, and high efficiency are basic design goals of this project.

The report presents concepts, design details, cost and construction information along with performance and efficiency test results of a prototype concentrator utilizing these concepts.

3.0 Concepts

The concentrating solar collector described herein utilizes three new concepts to achieve low-system costs, produce high thermal efficiency, and lead to long life reliability. First, the reflector shape is produced from low-cost steel sheet free formed by a simple hand operation and requiring no special equipment. Light weight frames can be used since the forces required to maintain the reflector shape are very low. Second, the hot collector tube is placed within a "solar greenhouse" which utilizes the heat losses from the reflecting surface and from the collector tube in addition to the greenhouse effect to both produce a warm still environment around the collector tube and to shield the collector tube from wind and cold weather. Third, a highly-reflective aluminum film is used to produce the reflecting surface. The film is bonded to the steel substrate with peelable adhesive which allows, easy simple replacement of the reflecting surface in the event of damage or degradation after many years of use.

3.1 Free-Formed Solar Concentrator

The reflecting solar concentrator used in this design is a free-formed shape achieved by bending a simple flat steel sheet by applying a small force along its edges as shown in the sketch below:

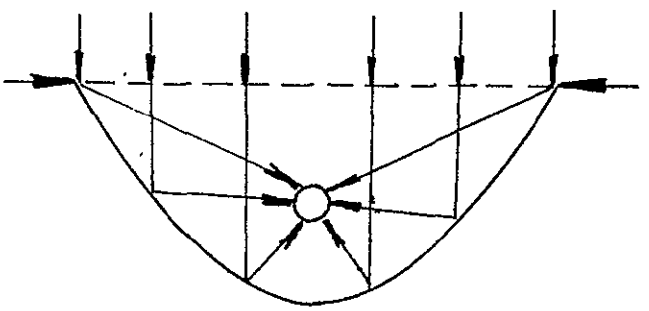

Sketch (a) The Elastica Reflector

The free-formed shape shown in Sketch (a) is known as a ELASTICA and since it follows the well known laws for bent beams, its shape and the position of the focus can be calculated exactly. It is easily formed by hand without the need for any special equipment other than a simple rectangular frame. The force required to hold the shape is low, there are no edge moments (twisting of the edges), thus only light weight frames and supports are required. Moreover, the shape is stable and any incidental loadings, wind loads for example, which might distort the shape momentarily present no problem since the original shape is assumed when these forces are removed.

The plate can be relatively thin, 18 gauge steel plates four feet wide and eight feet long form this shape easily and were used in the present design. Only one person is needed to bend the shape within a simple rectangular frame. Thus the cost is low, approximately $0.80 per square foot of sun capturing area for the present design.

3.2 Heat-Shield Principles

The thermal efficiency of any solar collector depends directly upon the ratio of the heat losses compared to the incident sunlight gathered by the concentrator. High heat losses mean low efficiency. Concentrating collectors have two main sources of heat loss. (Assuming the reflector directs all of the incident sunlight onto the collector tube). If high temperatures are needed in the working fluid the main loss is from the hot collector tube to the atmosphere and surroundings. Winds and cold weather increase these losses greatly for unprotected collector tubes.

The heat losses from a collector tube can be very high. Hot surfaces lose heat to their surroundings unless protected in some way. Under cold windy conditions a concentrating collector with unprotected tubes can not produce much hot water. High efficiency can only be gained if the collector tube is protected.

Poor reflectivity of the reflecting surface is another major source of heat loss. Even the best reflectors used in telescopes will lose about 10% of the radiant energy striking their reflective surfaces simply because no surface is a perfect reflector. Polished aluminum will reflect from 80 to 85% of the energy striking the surface, but oxidized or dirty aluminum may only reflect 50% on less. The sunlight not reflected from the surface appears as heat and causes the bright surface to become very warm. We all know how hot bright automotive trim becomes on a warm sunny day.

In the heat shield concept this heat is trapped and used to protect the collector tube. This is accomplished by placing a transparent cover over the assembly and by using a small amount of insulation around the back of the concentrator as shown in Sketch (b).

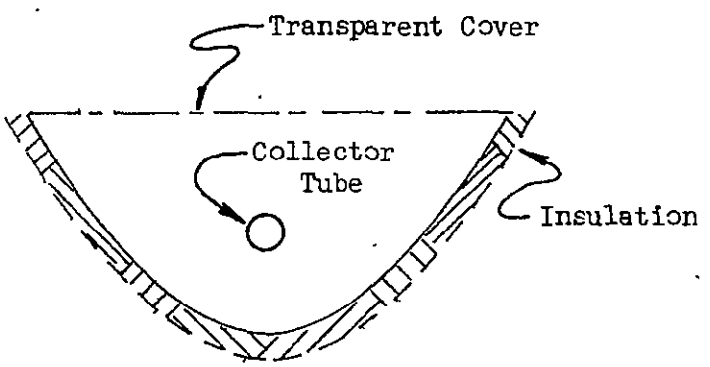

Sketch (b) The Heat Shield Concept

In the present design, the loss caused by imperfect reflection is captured and used to reduce overall heat losses instead of simply being thrown away which is the case of most designs.

Clearly, placing a transparent cover over the collector assembly has other beneficial effects. It protects the collector tube from winds and it protects the reflective surface from the damaging rain and dust. Experience within the Southwest has shown that unprotected aluminum reflector materials lose 50% or more of their reflectivity if exposed to rain and dust for periods of a few years.

The use of a transparent cover and insulation as shown in Sketch (b) places the collector tube in a solar "greenhouse." It is well known that a solar greenhouse will stay warm even in the coldest weather. Thus, in the present design, the collector tube is placed in a warm, still air environment instead of being exposed to winds and cold weather.

Tests on the present design made during the winter of 1980 show that this concept produces air temperature around the collector tube of 120°F even with a 10 to 14 mile per hour wind with an outside temperature of 50°F. Losses of heat from the collector tube are therefore greatly reduced; for a tube temperature of 212°F (boiling point of water) the losses are less than 1/2 that for an unprotected tube under no wind conditions and less than 1/4 of that for windy condtions. For tube temperatures of less than 120°F, the collector tube clearly loses no heat.

We all know that you can't get something for nothing. The transparent cover does reduce the sunlight striking the reflective concentrator by some 10 to 12%. Even so all of this heat is not lost. Ten to fifteen percent of it is trapped within the cavity.

3.3 Replaceable Reflecting Surface

The concept of replaceable reflecting surface is incorporated in the basic design of the solar collector. The reflecting surface is fastened to the steel ELASTICA reflector with a peelable pressure sensitive silicone adhesive. This design concept takes advantage of low-cost reflective materials, foils or vacuum deposited aluminum-plastic sandwich sheets, which are currently available from many commercial sources.

This concept allows for easy replacement of the reflecting surface in the event of accidental damage or loss of reflectivity from longtime use without affecting any of the other elements of the collector.

The useful energy collected by any concentrating system is directly proportional to the surface reflectivity. Sunlight not reflected upon the collector tube is simply lost. Thus it is critical for high efficiency to have as high a reflectivity as possible. Gold, silver, and aluminum are among the best reflector materials. Gold reflects about 75% of the incident sunlight, but is expensive. Silver, vacuum deposited on polished glass, gives values of about 95%. Aluminum, vacuum deposited upon glass and protected by a coating of silica monoxide typically reflects over 90% of the incident

sunlight. Polished aluminum sheet has a reflectivity of about 80% when new but can quickly change to less than 50% if pitted or oxidized. Thus, aluminum has a high value of reflectivity if vacuum deposited or newly polished and is inexpensive, but it must be protected if the high reflectivity is to be retained.

The reflectiviety material chosen for this design is vacuum deposited aluminum laminated between two 0.002 inch polyester plastic sheets with high temperature adhesive. This arrangement provides protection from atmospheric contamination of the reflective film, is strong and not easily damaged by handling. It can be attached to the steel ELASTICA reflector with cross-linked silicone pressure sensitive adhesive. The cost is reasonable for high reflectivity surfaces (70¢ per square foot), and the polyester sandwich sheets are UV stablized and only lose 5% of their transmissivity after 15 years exposure to the elements.

Moreover, the replaceablity feature of this design allows easy substitution of any new superior reflective material which may become available from the current research programs directed toward this end.

It is worth pointing out that there has been some reluctance to use plastic film for transparent covers of solar collectors due to the well-known failure of some of these materials when exposed to sunlight. Within recent years, stable, long life polymer films have been developed which can withstand exposure to strong sunlight. The film chosen for use in this design is UV stabilized polyester which has been tested in direct sunlight for 15 years with only a small (5%) loss in transmissivity and with little change in mechanical strength.

At the present time, many commercially available solar collectors are making use of these new materials with good success.

4.0 Description of System

4.1 Concentrator Reflector

The shape of the concentrator used in the present design is the shape formed by bending a 4 foot by 8 foot sheet of steel (18 gauge) by pressure applied along its edges. The shape is the free form assumed by elastic material of constant cross section loaded in this way. The name assigned this shape by the scientific literature is the ELASTICA. Since the shape follows the laws governing the bending of simple beams, its properties can be calculated and are presented in detail in Appendix A.

The specific ELASTICA used in the present design together with the location and extent of the focal volume produced is shown in Sketch (c).

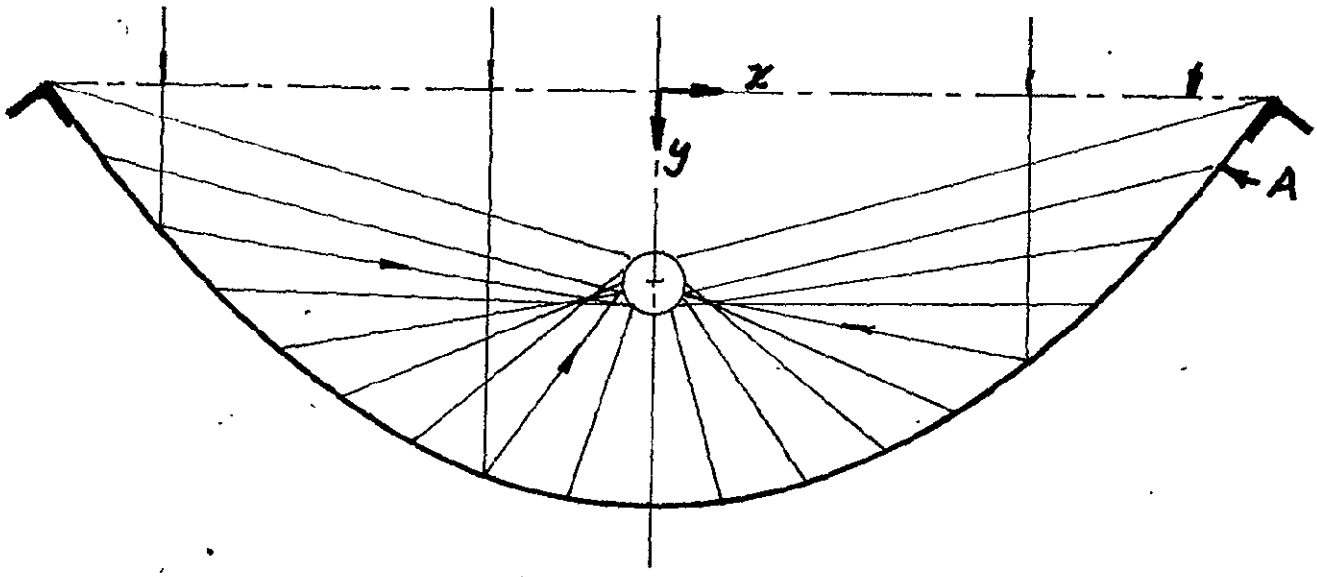

Sketch (c) Concentrator Shape

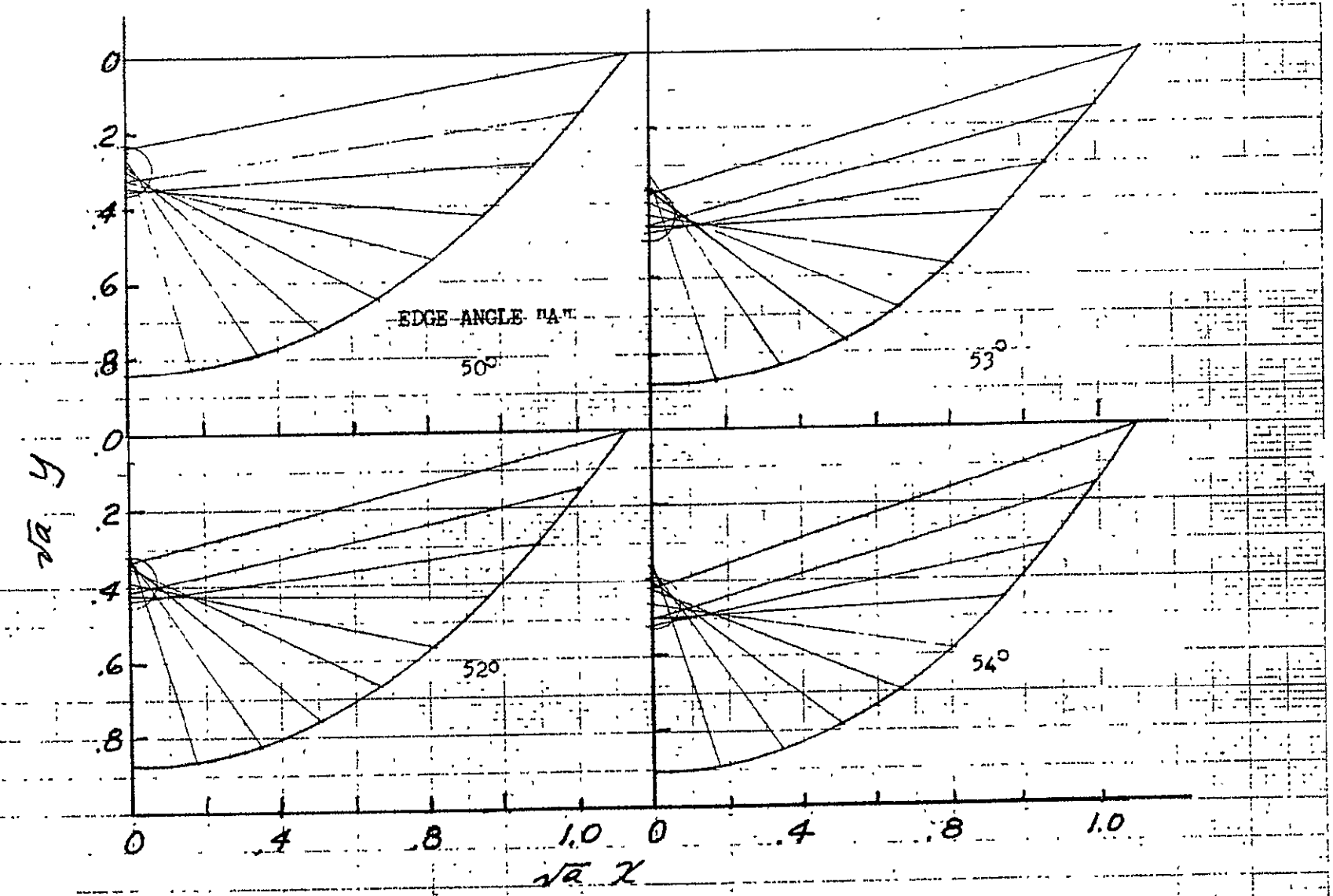

FIGURE 1.- ELASTICA SHAPE FOR VARIOUS EDGE ANGLES

(Parameter a defined by Eq. 7 Appendix A)

The shape shown in Sketch (c) is an ELASTICA with an edge angle "A" equal to 53°. The width is 3 times the depth (approx.). A 48 inch wide plate produces a 38.12 inch wide concentrator. The depth is 12.90 inches.

The location of the focus is 6.21 inch below the top surface. Coordinates for the Elastica together with the equations for calculating other shapes produced by different edge angles "A" are given in Appendix A, therefore no other dimensional information will be presented here.

It can be seen that the focus is rather intense and all of the sunlight striking the concentrator are concentrated is a circle of slightly less than two inches in diameter. The present design used a standard two inch pipe for the collector tube (1.9 inch diameter) and all of the rays were intercepted by the tube.

The non-dimensional shape of the Elastica is a function of the edge angle "A" only. Thus each edge angle produces a slightly different shape (see Appendix A). Each edge angle also produces a different focus and focus location. Figure 1 shows the shape and focus by four different edge angles: 50, 52, 53, and 54 degrees. Of the four, an edge angle of 50° produces the sharpest focus with the important exception of the rays coming from the extreme edge of the concentrator. In the present design 53° was chosen as a reasonable compromise among the group since all of the rays were intercepted by a two inch circle and it was felt that small dimensional errors of construction would be best tolerated by this shape.

Note that the position of the focus changes with edge angle. In an actual case when constructing a concentator the edge angle must be held within rather close limits (1/2°) or the focus line will not be straight along the collector tube. Also the "X" dimension must be held within ± 1/16 inch long the length. This not difficult to accomplish.

4.2 Focus Definition Tests

The location and size of the focus region is critical to the design of a solar concentrator, therefore, a series of focus definition tests was performed in a focus definition test fixture shown in the photograph below:

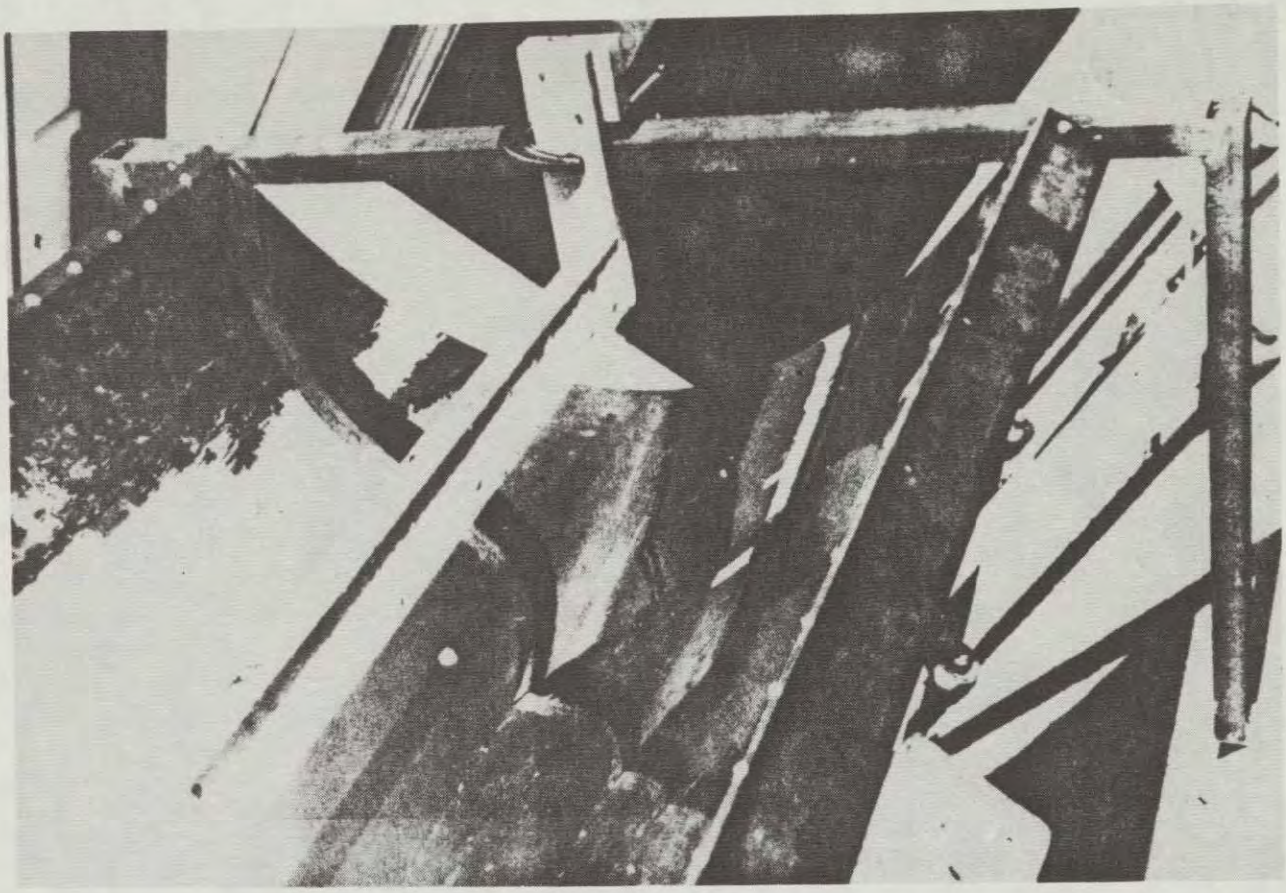

FOCUS DEFINITION TEXT FIXTURE

The test fixture was constructed from 3 inch steel channel to minimize distortion and variation of the X dimension (see Sketch c). It allowed variation of the edge angle "A", the dimension X, and was equipped to measure end torques. A standard fir two by four was clamped along the position of the focus region as shown. The bright area on the fir, shown in the photograph, is the focal region. The focus was intense enough to char the fir and the char lines were used to define the focus. The focus was found to be located 6.30 inches from the top plane of the concentrator.

Focal volume definition parallel to the solar rays were next made by placing the fixture 2^{o} out of alignment with the solar axis. This caused a shadow of the rays to be seen on a plane for measurement of the reflected ray paths. The results of these tests are shown below for edge angles of 50 to 53^{o}.

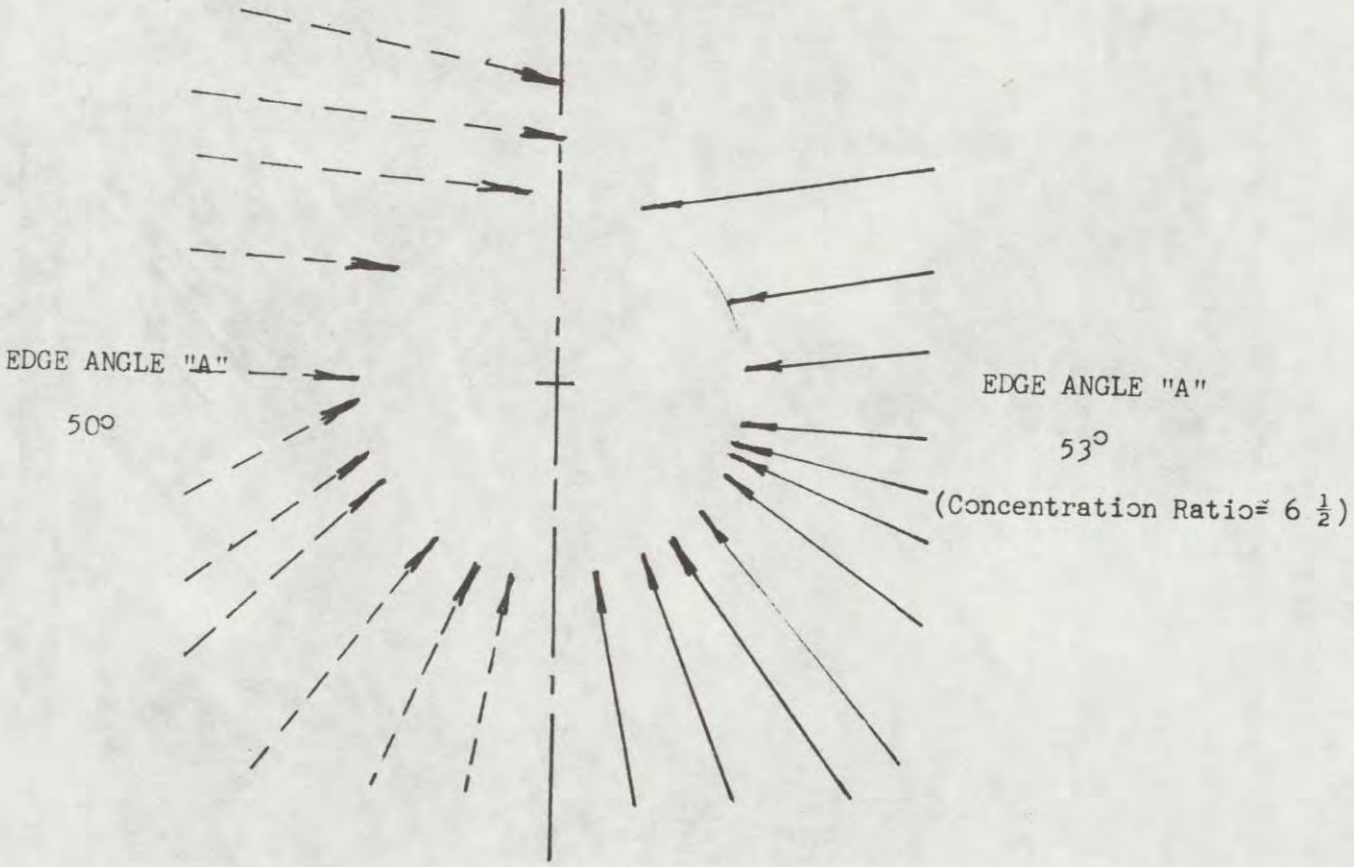

FIGURE 2 - REFLECTED RAYS FOR TWO EDGE ANGLES

It can be seen from the figure that the 53° edge angle produces a superior focus. These measurements confirm the calculated results shown on figure 1, qualitatively. It is difficult to obtain these measurements due to the intense nature of these rays, therefore the rays do not originate from the same position on the concentrator as the calculated ones. They do, however, show the same general trend. A Note of Caution: Anyone attempting to make measurements of this kind should proceed with extreme care. The concentrated rays are hot enough to easily ignite paper or wood and can cause painful burns. Moreover, eye damage can result if the concentrated beam strikes the unprotected eye.

The focus definition test fixture was also used to measure edge moments. According to the calculations presented in Appendix A no edge mements should be present. Edge moments, if present for some reason, will influence the design of the suppporting framework.

The supporting horizontal frames of the focus definition fixture were free to rotate which allowed measurement of these moments. The measurement indicated that these moments, if present, were below 5 inch-pounds, the lower limit of the measuring equipment. Thus, edge moments could be neglected in the design of the support frame.

4.3 Support Frame Loadings

The load imposed in the horizontal direction by a 53° Elastica shown in sketch (c) is 3.52 pounds per foot of length or 28.1 pounds for the eight foot sheet used in the prototype.* The measured force was 30 pounds for the eight foot plate. Thus the forces exerted upon the frame by the bending of the plate were small.

The 4 by 8 foot plate weighed 64 pounds. Thus each horizontal frame member had to carry a vertical load of 4 pounds per foot of length. Thus the combined load (adding the loads vectorially) resulted in a principle load of 5.32 pounds per foot. This is a very small load.

Winds can exert a force on the side frames since they have to resist the forces produced. For a wind normal to the collector top surface the forces are as follows:

Wind Speed mph	Force #
10	2.6
20	10.5
40	42.6
60	94.8
80	168.6

If the wind is blowing across the collector as shown in sketch (d) the loading will be as follows:

Wind Speed mph	Force #
10	0.89
20	3.57
40	14.3
60	32.2
80	57.2

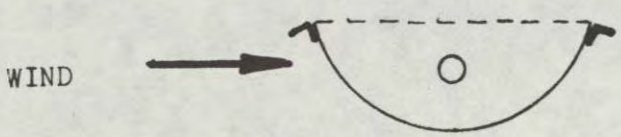

Sketch (d)

*Eq. 7 App. A.

4.4 Frame Design

Any elastic frame material, steel or aluminum, will deflect under load. Large deflections will cause the focus to depart to some degree from the collector tube. In the present design the frame of the reflecting collector was sized to allow no loss of reflected rays for wind speeds up to 40 mph, but to accept some loss at wind speeds above a wind speed of 40 mph. Within the southwest winds above 40 mph are generally rare and in any event are of short duration. A design that could withstand a continuous wind of 80 mph would be very heavy indeed. The frames were designed to withstand winds of this magnitude without undergoing damage, plastic bending, and would return to their normal shape after the extremely high wind gusts had abated.

The frame sizes were 1 1/2 inch aluminum angle having a thickness of 1/4 inch. This size limited the deflection at the center of the span to 0.0635 inches for static loads and to below 0.120 inches if exposed to a continuous 40 mph wind as shown on the sketch above. Deflections of this magnitude have little effect upon the sunlight capturing efficiency as can be seen from Figure 1.

The diagonal frame members shown in the top photograph were 1 inch x 1 inch x 1/8 inch aluminum angles and the cross braces shown in the lower photograph were 3/4 inch x 1/8 inch angles, also of aluminum.

The lower cross braces were added to give torsional stiffness to resist torsional loads imposed by handling and by the sun seeking drive system.

The end and center frames are shown in detail in the photograph below:

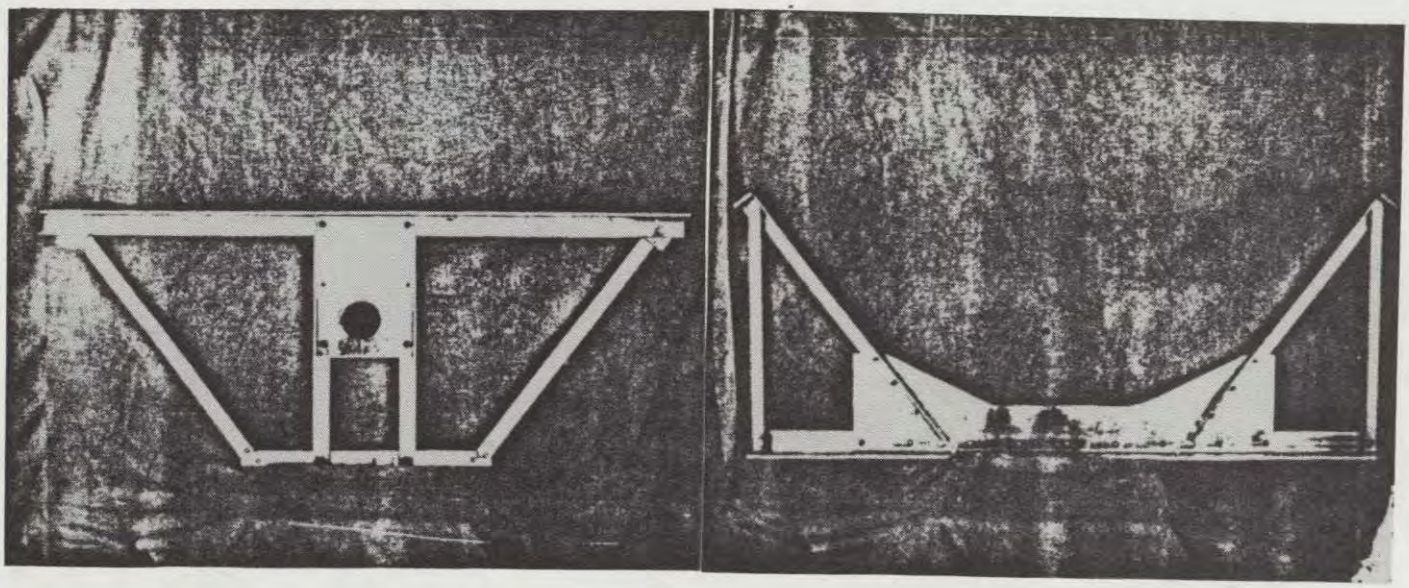

END FRAME

CENTER FRAME

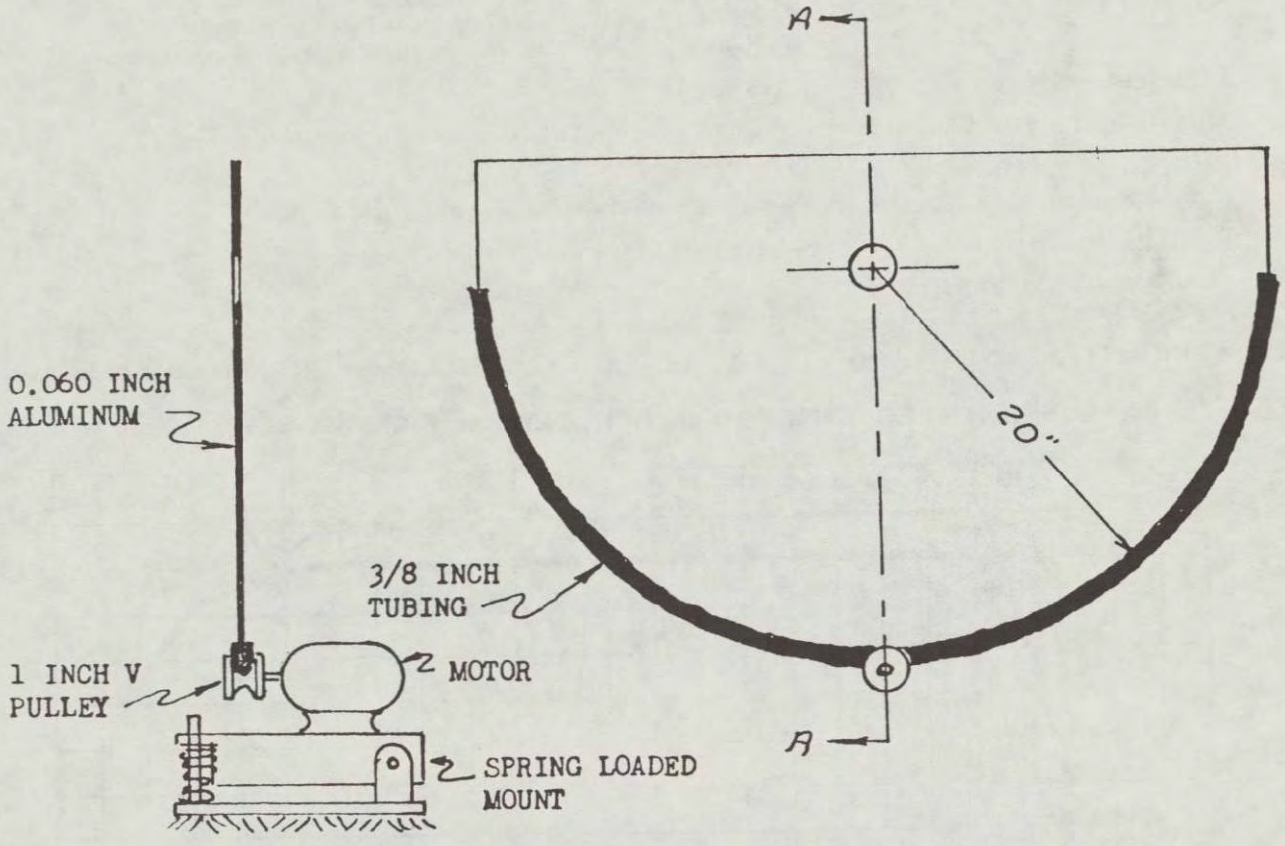

SECTION A--A

FIGURE 4.- DISC DRIVE FOR SUN SEEKING SYSTEM.

PROPERTIES OF UV STABILIZED POLYESTER

FILM USED

UV RESISTANCE:	Excellent. Polyester film normally has limited resistance to weathering due to ultra-violet degradation. However, MARTIN LLumar™ film is impregnated with ultra-violet absorbers that yield a film with excellent weathering resistance.
LIFE EXPECTANCY:	10-15 years
SERVICE TEMPERATURE:	–75 F to 350 F withstands stagnation temperatures of more than 400 F.
LIGHT TRANSMISSION	
Visible spectrum:	88-90% – virtually same as window glass
UV spectrum:	Sharp cut-off at 0.4 microns
FUNGI AND BACTERIA RESISTANCE:	Resists mildew and rot indefinitely

AGING DATA: UNEXPOSED VS. 15-YEAR-OLD EXPOSED LLumar™ FILM (outdoor exposure)

TRANSMISSION SPECTRUM FOR MARTIN LLumar™ FILM (low range)

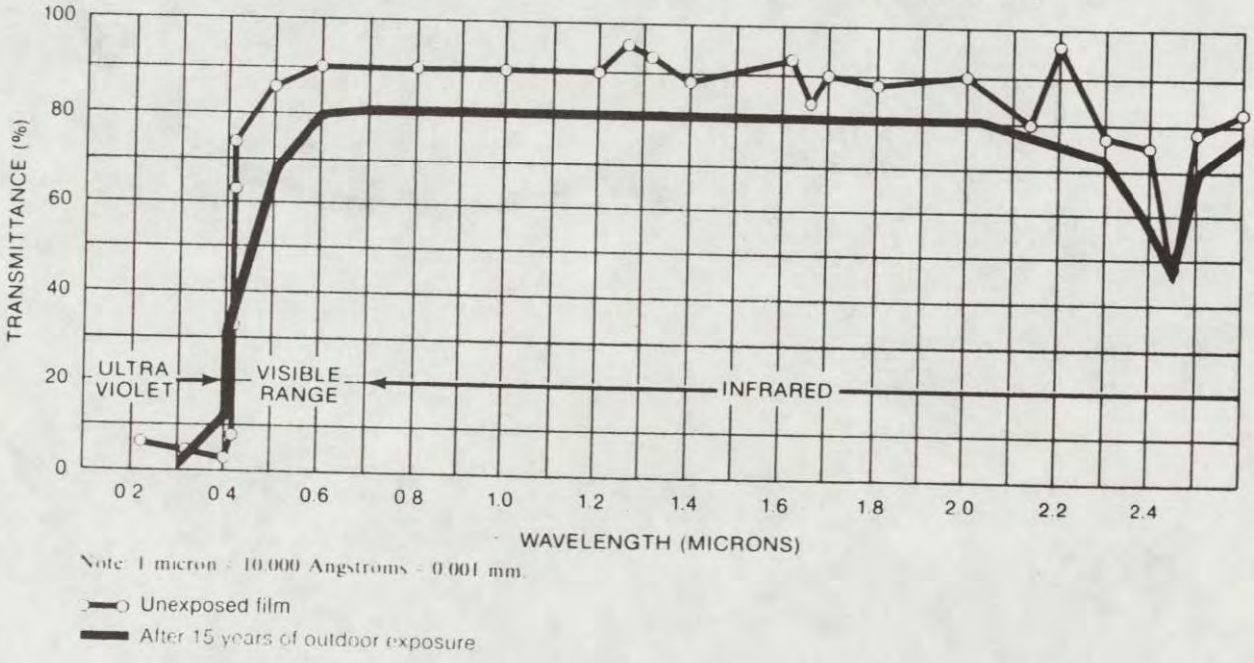

After 15 years of outdoor exposure, the UV absorbers are still operating at 100% efficiency and the entire UV portion of the spectrum is being filtered.

In actual field use on a greenhouse in southern Illinois, Llumar™ film has withstood temperature extremes of 0°F to 96°F, 70 mph winds and hail storms. The film is still in service on the greenhouse and laboratory tests have shown that Llumar™ still retains 80% (20,000 psi) of its original tensile strength and light transmission of approximately 80% after sixteen years of continuous outdoor exposure.

It can be seen that the frames were bolt-up construction which are simple for the average person to build and assemble, since all that is needed is a hack saw, a drill, and an adjustment wrench to tighten the bolts. A weld would be somewhat simpler and less costly, but most people do not own welding equipment.

4.5 Main Support Frame and Collector Tube

The function of the main support frame is to support the collector tube. The collector tube must be supported in some sort of a frame which will allow the collector to rotate freely about the collector tube and to provide support in the longitudinal direction to take the end loads when the frame is tipped upward to achieve a normal solar line direction. Almost any material can be used, in the present case the frame was a simple weldment using 2 inch steel angel as shown in the photo below:

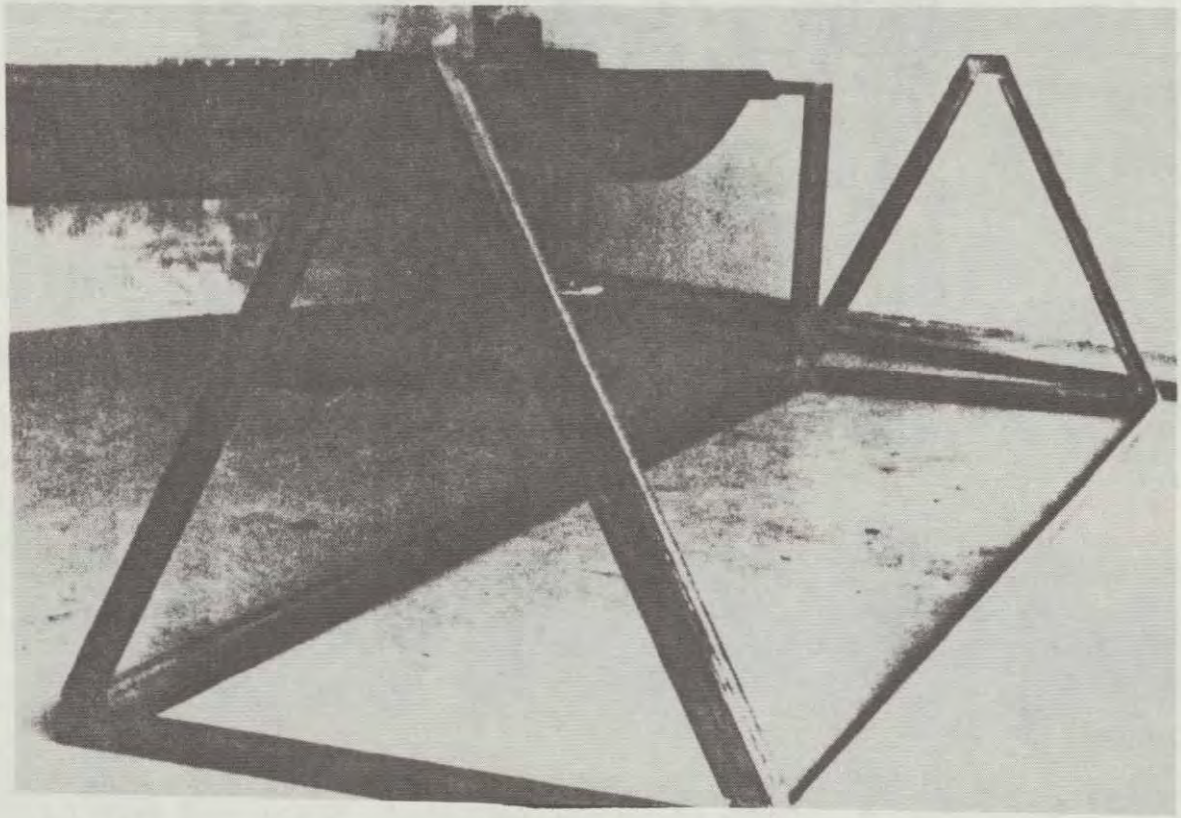

MAIN SUPPORT FRAME

The collector tube is a 9 foot long piece of 1 1/2 inch standard pipe. The absorption surface is obtained by coating the outside of the pipe with 3M NEXTEL 101-C10 "Black Vlevet" coating applied from a spray can. The resulting surface has a solar absorptance of 0.97. The surface is dead black in appearance and is not easily damaged. The surface should be applied after the collector tube is installed in the support frame to avoid scratching the black surface.

The collector is slipped on to the collector tube as shown in the photograph below using standard pipe flanges as bearings. Two of the flanges are fastened to the main frame and the other two are pinned to the collector tube. In this way the collector can rotate freely about the collector tube, but cannot move in the horizontal direction. The partly assembled collector, showing the support frame, the collector tube, and the collector reflector, is shown in the photograph below:

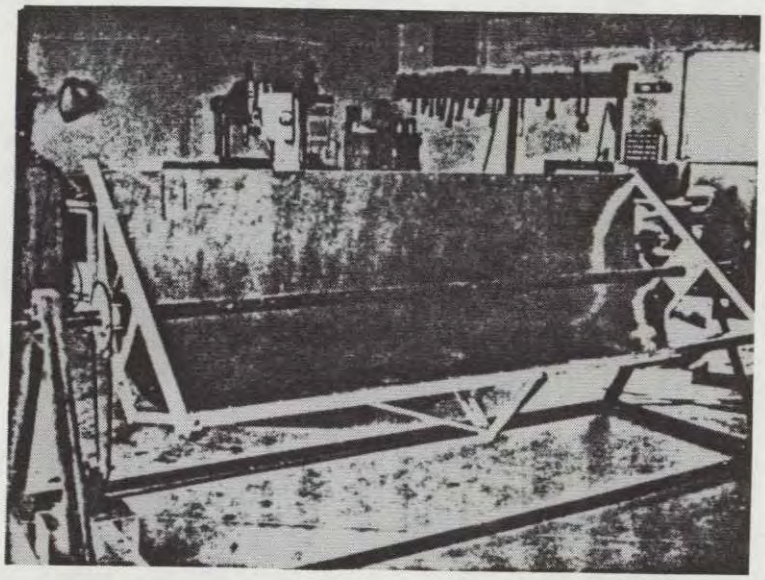

COLLECTOR ASSEMBLY

When assembled as shown the collector reflector rotates easily about the collector tube. Since the focus is located very near the center of gravity there is very little torque required to rotate the unit. This is important since it allows a small motor to be used to drive the collector and keep it aligned with the sun.

4.6 Sun Sensing System

The sensing system consists of a pair of phototransistors mounted in a control box as shown in the photograph below; a simple bridge circuit, a pair of summing amplifiers, and a set of relays. The semi-circular shade above the phototransistors produces a sharply defined sunlight-shaded region over the detectors. As the sun moves across the sky one detector is shaded while the other is sunlit. Since the output of the phototransistors varies with the amount of sunlight impinging on them, an unbalance is produced in the bridge circuit. This unbalanced voltage is amplified by the summing amplifiers and closes one of the relays which drives the control motor. The control motor rotates the collector until both sensors are evenly illuminated by the sun. A simplified circuit diagram of the system is shown on Figure 3.

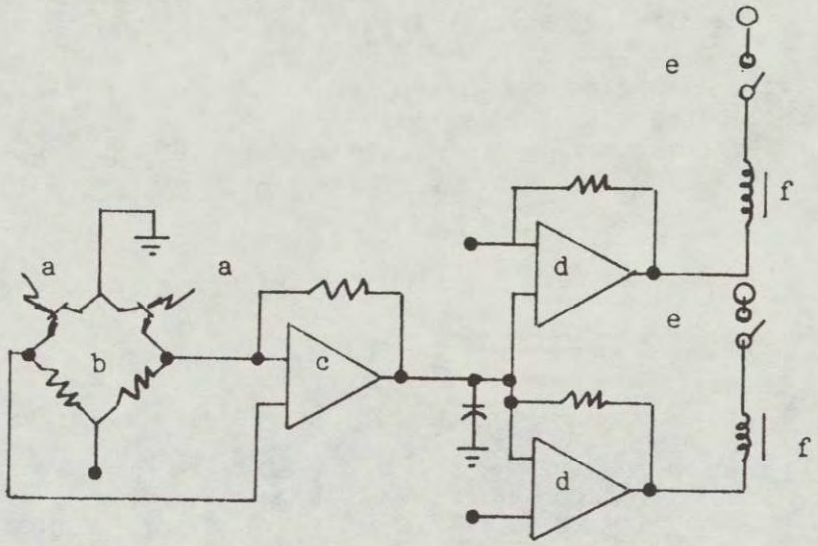

a) PHOTOTRANSISTORS
b) BRIDGE CIRCUIT
c) SUMMING AMPLIFIER
d) RELAY AMPLIFIERS
e) MERCURY LEVEL SWITCHES
f) RELAYS

FIGURE 3. SIMPLIFIED CIRCUIT DIAGRAM OF CONTROL SYSTEM

4.7 Motor Drive System

The output of the relays of the sun seeking system were connected to a simple AC/DC 1/15 hp gear motor with a gear reduction ratio of 1787:1. This motor can be driven either from a 110 volt AC power source or from a DC source of the same voltage. The rated speed of the motor is 2.8 rpm, but the actual speed varies somewhat with load. The measured speed of the motor in this application is 2.5 rpm.

The motor drives the collector-reflector through a disc drive constructed from 0.60 inch aluminum sheet which also serves as the end plate for the concentrator. A 3/8 inch tube (automotive windshield wiper tubing) was split and cemented to the disc as shown on Figure 4.

The disc drive arrangement produced a reduction of 40:1 between the gear motor and the collector-reflector system. With this gear reduction (70,000:1) the collector reflector moved very slowly and was able during tests to hold the sun line within $\pm$ 1/2° which is a very acceptable value for this collector.

The disc drive system installed upon the collector is shown in the photograph below:

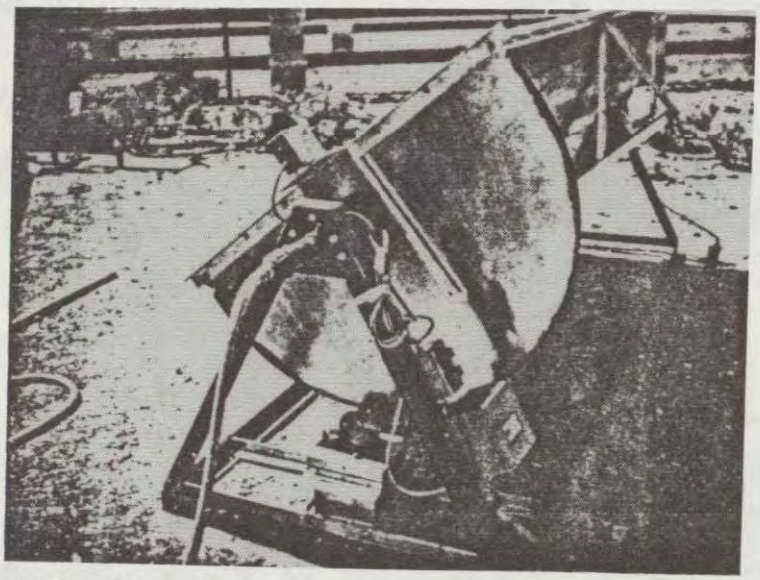

4.8 Reflecting Surface

The reflecting surface of the concentrator is vacuum deposited aluminum bonded between two polyester UV stablized clear polyester sheets. The total thickness of the film is 0.003 inch. The material is fully reflective, with a reflectance between .80 and .86 of the solar spectrum. The material is easily handled and the polyester surface film protects the aluminum from oxidation and damage from handling.

The material was bonded to the steel substrate using General Electric Company's Siligrip cross-linked silicone pressure sensitive adhesive. The actual material used was SR 6574 and was applied with a paint roller to both the steel substrate and the reflective material.

As originally applied, the reflective film assumed the shape of the steel substrate, was smooth and even and produced an excellent focus with a sharp definition. This focus is shown in Figure 2.

After two months exposure to the sun during tests some film separation was observed. The film appeared to develop small bubbles between the substrate and the polyester reflective film. At the present time these bubbles do not destroy the focus, but do spread it out somewhat. Additional testing is needed to define the problem and use of Siligrip with higher cross-links density needs to be investigated to solve this potential problem. Tests are planned for the summer of 1981 and the results will form an addendum to this report.

4.9 Transparent Cover Material

The film chosen for the transparent cover for the collector was 0.007 inch thick UV stabilized polyester film. The film has a tensile strength of 25,000 psi (1/3 the strength of steel), resists mildew and rot indefinitely, has a service life of at least 15 years and has somewhat better transmissivity than glass. This film has been exposed to sunlight in field service for 15 years and the results of tests before and after exposure are given in the following summary presented on page 103.

4.9.1 Greenhouse Protection for the Collector Tube

One of the concepts used in this design is to place the collector tube in a "solar greenhouse" to protect the tube from cold winds and to produce a hot still-air environment around the tube to reduce its heat loss. This concept tends to combine the principles of a flat plate solar collector with the advantages of a concentrator.

Placing a transparent cover over the concentrator-reflector, as discussed earlier, provides part of the greenhouse effect as it traps the radiant energy within the cavity. To make the greenhouse effective and to produce high temperatures this energy must not be allowd to escape by convection through the back and ends of the concentrator-reflector. To prevent this escape, insulation is installed on the back and ends of the concentrator-reflector. This is illustrated in Sketch (b) page 84.

The final temperature and thus the protection afforded by this concept depends upon several factors. The heat loss caused by imperfect reflection at the reflector surface, the heat not transfered to the working fluid within the collector tube caused by imperfect absorption of the black surface, ambient temperature and wind speed, solar intensity, and the heat losses through the transparent cover and through the concentrator-reflector back and ends.

Tests test on the operating collector and analysis were used to determine a reasonable thickness of insulation. For example, with an ambient temperature of 50°F and no insulation, the temperature within the cavity was 80°F. With 3/4 inches of insulation the cavity temperature was 120°F for the above ambient temperature even with a 10 mph wind. Increasing the insulation thickness above this value did not result in much increase in cavity temperature (approx. 10°F) and was simply not cost effective. This loss in effectiveness with increasing insulation thickness is due to the convective heat losses through the transparent cover which constitutes 40% of the surface area of the concentrator. Double glazing of the transparent cover could reduce the cover conventive loss, but it also reduces the level of the solar radiation striking the reflective surface and is not cost effective except under very extreme climatic conditions.

The insulation used on the prototype collector was a closed cell elastomeric flexible material having a thermal conductivity of 0.27 Btu/ft^2-hr (°F/inch). Three quarters inch thickness was used. The material is available commercially as Armstrong "Armaflex", is waterproof (water absorption less than 8%) and was fastened to the collector surface with Armstrong 520 adhesive. The material is easy to apply as shown on the photograph below.

Use of this insulation produced an R value of 4.78 for still air conditions and a value of 4.0 for windy conditions.

When Armaflex Sheet is used with full adhesive coverage, adhesive is easily applied with brush or roller.

5.0 Construction Costs

The cost of the materials used in the construction of the collector are presented in Table 1 on page 100. These material costs are divided into two sections; those showing the costs of the concentrating reflectors, cover and collector tube which scale directly with the area of the system being considered, and those costs particular to this size prototype which do not scale directly with area. For example, the sun sensing system used in the prototype could serve a much larger system.

It can be seen that the base cost of the system, concentrating reflector and collector tube is $6.00 per square foot of sun capturing area. Waterproof insulation would add another $0.85 per square foot to the cost if one of the low cost systems (to be discussed later) is used instead of the experimental material that was used on the prototype to test the effectiveness of insulation. Thus the base cost of the solar collector main components adds up to $6.85 per square foot. This is a very low material cost.

Labor costs are difficult to estimate from limited production items. Labor costs vary with labor rate and the scale (size) of the operation. In the prototype system it was possible to build the reflector frame in 16 hours and the assembly of the rest of the system in 8 hours. At a labor rate of $5.00 per hour this amounts to $80.00 or $3.16 per square foot of sun capturing area. It is to be pointed out that these figures bear little resemblence to the actual time spent in building the first unit, but are the estimated times that would be required by an experienced work force building these units in quantity.

The lower portion of Table 1 gives the construction cost of items peculiar to the experimental nature of the unit constructed and are not representative of an actual commercial or field application of this collector. The collector built was smaller than those that would be used in most applications, thus some of the items were oversize. For example, the sun seeking and pointing system represents almost 50% of the cost of the entire system, but it is capable of performing this function for a system many times its size. There is little one can do about this; the basic sun sensor and electronics for a large system and a small system must perform the same function and do not scale with size.

The steel frame used to support the reflecting concentrator and the collector tube was built to allow the collector to be moved easily from one test area to another and was therefore stronger and more rigid than would be needed in a field application where the collector would not need to be moved.

The insulation used in the experimental unit cost $2.66 per square foot of sun capturing area. This represents 44% of the base cost of the major components, the concentrating reflector and the collector tube. The material, a flexable waterproof elastomer closed-cell foam, was used to allow different thickness systems to be tested to determine an optimum thickness. It is almost impossible to make these kinds of tests using a steel jacketed fiber insulation commonly used for outside installations. In an actual field installation the use of steel jacketed fiber insulation would reduce this cost to $.75 per square foot of sun capturing area.

If this collector were built in 100 square foot modules the material costs would be about $8.00 per square foot. This is a very low cost for a concentrating collector of this performance.

TABLE 1.
SOLAR CONCENTRATOR MATERIAL COSTS

ITEM	UNIT COST ($/Unit)	TOTAL COST ($)	COST PER FT.2 (APERTURE) ($)
CONCENTRATING REFLECTOR	1.62/ft.^{2}	41.09	2.04/ft2
Steel Sheet	0.62 "	19.90	0.78
Reflective Material	1.00 "	32.00	1.26
REFLECTOR FRAME		38.47	1.52
Main Frame	1.03/ft.	24.03	0.95
End Frames	0.58/ft.	14.44	0.57
TRANSPARENT COVER		31.43	1.24
Transparent Material	0.85/ft.^{2}	21.53	0.85
Cover Frame	0.45/ft	9.90	0.39
COLLECTOR TUBE		31.10	1.23
10 ft. 1 1/2 Std. Pipe	2.61/ft.	26.10	1.03
Black Surface		5.00	0.20
MISC. (Bolts, washers, Glue, etc.)		10.00	0.39
TOTAL COSTS FOR CONCENTRATING REFLECTOR AND COLLECTOR TUBE			$152.09
COST PER SQUARE FOOT	"	" "	$6.00
SUPPORT FRAME USED IN PROTOTYPE		25.00	
SUN SENSING SYSTEM		281.26	
Sun Sensor and Electronics		211.26	
Drive Motor and Mount		57.50	
Disc Drive System		12.50	
INSULATION USED IN EXPERIMENTAL UNIT		67.50	2.66
TOTAL MATRERIAL COST OF EXPERIMENTAL UNIT			$525.85

6.0 Performance Of Solar Collector

The performance of the prototype solar collector was measured by a major Arizona certified test laboratory during January 1981. The tests were conducted in accordance with ASHRAE Standard 93-77 thermal performance test method by the DSET Laboratories located at New River, Arizona. DSET has tested over 1000 solar collectors for certification by the various states across the nation. Their results can be relied upon as being accurate (2% probable error) which is not the case for many tests conducted by inexperienced groups. Very large errors are easily possible if the test variables are not rigidly controlled.

The results of their tests are presented in Figure 5 for four water outlet temperatures. The test were conducted during still-air clear-day conditions.

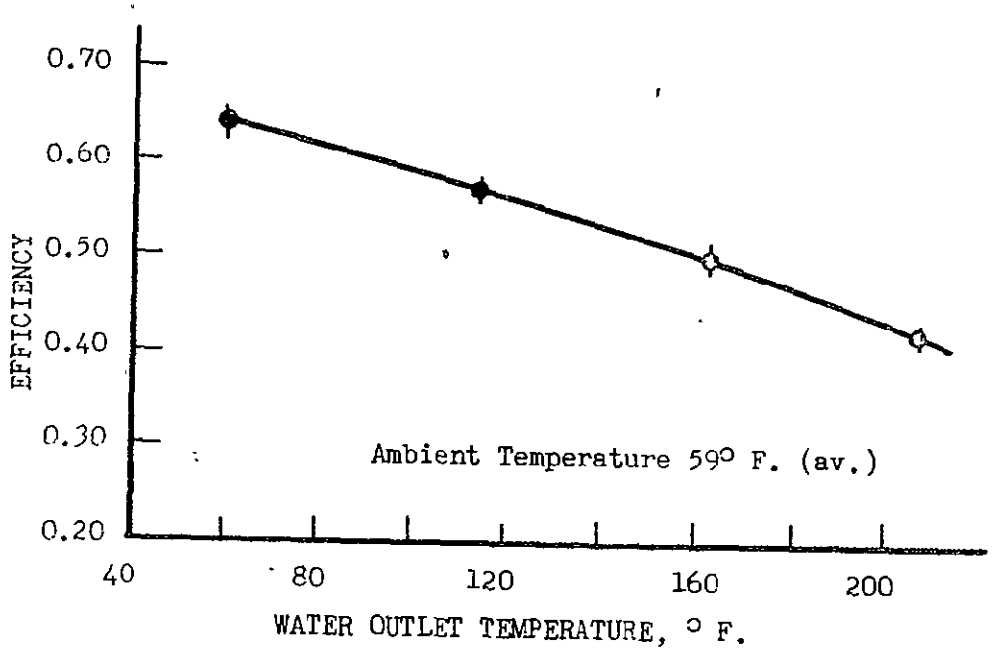

FIGURE 5-COLLECTOR EFFICIENCY AS A FUNCTION OF WATER OUTLET TEMPERATURE (Results based upon direct insolation and aperature area - 24.33 ft^2

Figure 5* shows that the collector had an efficiency of 64 percent at an outlet water temperature very near ambient and an efficiency of 41 percent at the boiling point of water. The decrease in efficiency with increasing water outlet temperature is primarily a result of losses from the collector tube.

These efficiencies are not as high as expected and the reduced efficiency appears to be due to the bubbles which formed under the reflective surface and caused some of the sunlight to miss the collector tube. This problem will be solved and the results reported in an addendum to this report at a later time. In spite of this problem, however, the efficiencies compare well with other concentrating collectors. These comparisons are shown in Figure 6.

---

* Complete details and test results are available in DSET Report 81S0123-32. As report was 52 pages long only the amjor results are reported herein. The complete report is available from Goodwin Consulting upon request.

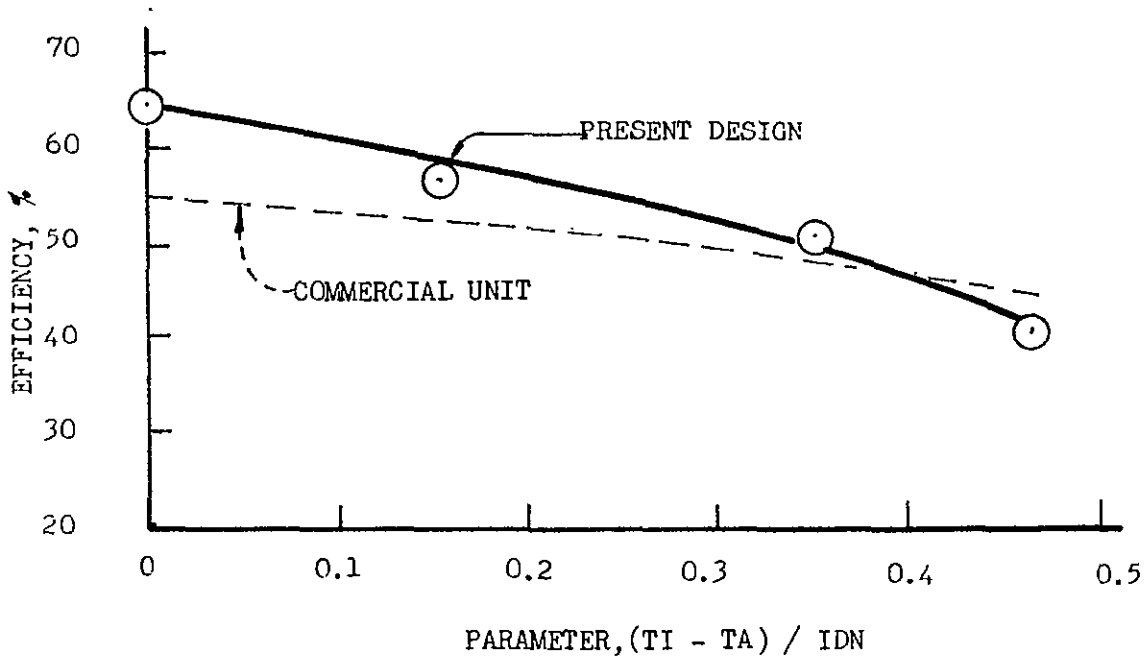

FIGURE 6-COLLECTOR EFFICIENCY COMPARISON

Specifically, Figure 6 shows the instantaneous efficiency as a function of the parameter (TI-TA)/IDN. The instantaneous efficiency is defined as the ratio of the heat added to the working fluid (water flowing through the collector) to the direct solar energy striking the aperture per unit time with the collector aligned with the sun. The parameter (TI-TA)/IND is the difference between the inlet water temperature and the ambient water temperature divided by the direct component of the solar radiation striking the aperture. This parameter is used in ASHRAE methods to allow comparison of different collectors to be made on a reasonable basis.

Figure 6 shows the test results for two concentrating collectors. The solid line with the data points represents the test results of the present prototype collector, the dashed curve is the result of tests by DSET of a commercial concentrating collector. Both curves are based upon net collector area (aperture) and the direct component of solar radiation. The commercial collector is a model 400 Sunpower Systems unit and these data were obtained from the Arizona Solar Energy Commission's public files.

It can be seen that the present prototype collector efficiency compares well with that of a commercial unit. The efficiency of prototype is somewhat higher than the commercial unit at low and medium values of the parameter and about equal at high values. (Values of the parameter near 0.45 represent water outlet temperatures near the boiling point of water.)

Both sets of tests were conducted on still days with little wind, thus only part of the protection provided by the present design was operative. There was no wind to protect against. Some efficiency decrease is expected at high values of the parameter since the temperature of the collector tube is much higher than the cavity temperature for these conditions. The general level of the efficiency for the present design is lower than expected, even for still air conditions, and is believed to be due degraded reflector performance. Examination of the reflector surface after the unit was returned from DSET indicated that the bubbling of the adhesive had progressed to the point where some of the incident sunlight was being deflected and was not impinging upon the collector tube. This, of course, would decrease the efficiency of the unit.

It appears from the comparison of the two collectors that the concept of heat shielding is effective in increasing efficiency even with a degraded reflecting surface. This is shown by the higher efficiency at low and medium values of the parameter (TI-TA)/IDN. Under windy, cold conditions the differences should be even more marked, and more tests are planned to prove this point.

7.0 Conclusions

In general the objectives of this project have been realized. The first objective, producing an effective solar concentrator from a simple flat-steel sheet by free-forming, has been realized and tested successfully. The theoretical analysis which predicted this result has been verified by test.

The objective, to produce a low cost system, has been realized. The main components, the concentrating reflector, collector tube and frames have been produced for a material cost of $6.00 per square foot of sun capturing area. This is a very low cost indeed. It appears that the material costs for an all-up system in modules of 100 square foot size would be about $8.80 per square foot including solar tracking and support. A rough estimate of the labor costs is about $3.00 per square foot for a labor rate of $5.00 per hour for a trained crew.

The third objective, to produce a high quality, efficient solar concentrating collector that can be built by the average person without special equipment has been met.

Tests of the concentrator, conducted by a certified test laboratory, indicate that the efficiency of the unit is higher than comparable commercial concentrating collectors now on the market at outlet water temperatures up to 200°F and comparable to a commercial unit at the boiling point of water. More tests are needed to verify the predicted superior performance of the present unit during cold windy weather. Record high temperatures all over Arizona during the winter of 1980-81 precluded obtaining this data as of this writing.

The reliability of the present design in terms of long life service at high efficiency has not been proven. After two to three months continuous testing during the fall and winter of 1980 some delamination of the

reflecting film from the steel substrate was observed. At first the bubbles formed between the reflecting film were too small to destroy the focus, but as time went on the situation deteriorated and examination of the focus after the unit was returned to Goodwin Consulting from the test laboratory revealed that some of the reflected rays were not striking the collector tube. It is believed that this situation contributed to the poorer than expected efficiency measured during these tests.

The writer has been in consultation with a number of groups in an attempt to solve this problem. The groups consulted were: The Solar Energy Research Institute, the Chemical Research Projects Office of NASA, Chemplast Corporation, 3M Corporation, and the Silicone Products Department of the General Electric Company. Considerable help has been obtained.

Samples of adhesive have been received from these sources and evaluation of these materials will begin shortly. The above experts believe that the difficulty stems from outgassing of the adhesive caused by the relatively high temperatures within the cavity. All are in agreement that the material used in the adhesive must be cured (for the case of silicone cross linked) before the reflective sheet is assembled on the steel substrate. A number of silicone formulations with different cross-link densities in the basic polymer will be evaluated. Clearly, the problem can be solved since the automotive industry have used these adhesives for years in fastening decorative panels to the bodies of their automobiles. The correct formulation simply must be found.

It is worth pointing out that loss of reflectivity is a problem that plagues all unprotected solar concentrator reflectors at the present time. Reflectivity losses of 50% or greater have been reported after several years service within the southwest. The present design might well solve this problem if a satisfactory solution can be found to the adhesive problem. Not only will it solve a problem for this collector, but it would allow a retrofit solution to be obtained for the concentrators presently in the field that are suffering from this problem.

In order to acquire more data on the reliability problem and at the same time to acquire data during windy conditions, Goodwin Consulting has obtained a test site in the White Mountains of Eastern Arizona where these weather conditions exist during the spring and fall. It is planned to move the collector to this site during the spring of 1981 and acquire the necessary data. The results of these tests together with the results of the adhesive tests will be reported to DOE at no additional cost and the results will form an addendum to this report when the data are available.

APPENDIX A

THEORY OF THE SOLAR REFLECTOR SHAPE

SOLAR REFLECTOR

The object of this section is to discover some shape which can be free-formed without special equipment and will focus the incident radiation into a small volume where it can be easily collected. The shape sought must be stable and hold its contour under wind loads. Conic sections have these properties, but require special forming equipment not available to the average householder or small shop. A simple bent beam produces a radius of curvature proportional to the local moment. If the moment variation across the span could be supressed a shape would result that would be a reasonably good concentrator. One shape which might have reasonably good focusing capabilities and still meet the free-form criteria is shown below. Morover, this shape has a variety of forms depending upon the paramaters of the problem and might well contain at least one useful form. The shape is formed by bending a plate with forces applied at the edges as shown in the sketch below.

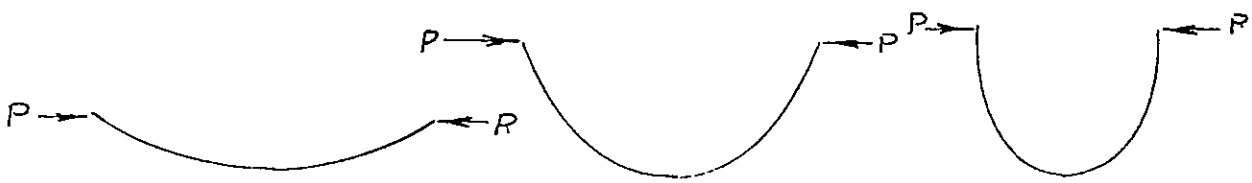

It is clear that the region of the plate near the center will produce a focus along the centerline. The problem at hand is to determine which of these shapes will produce a distributed focus in a volume small enough to te easily collected by a black body absorber.

The relationships which give the shape in terms of physical parameters of the problem will now be derived.

ANALYSIS

The arrangment to be analyzed is sketched below:

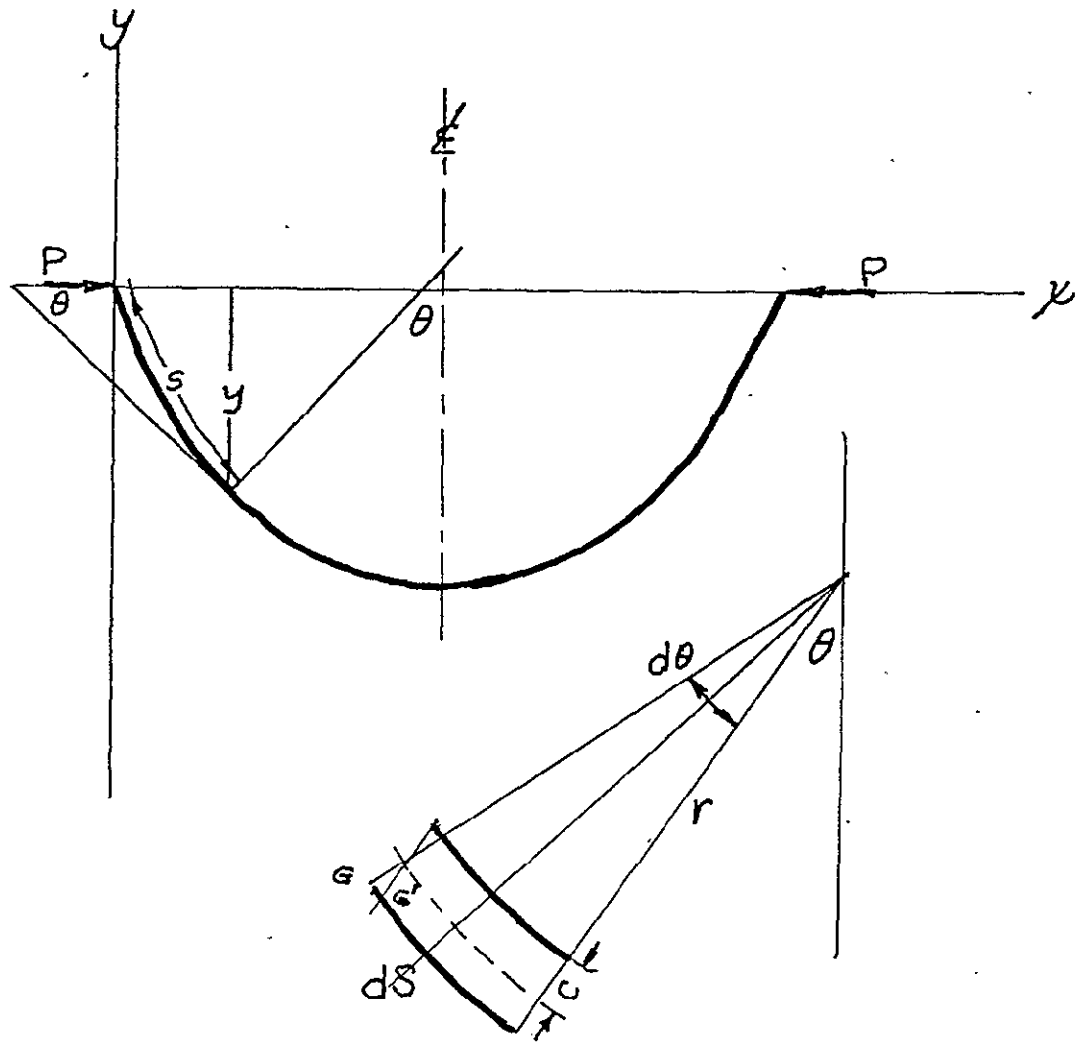

The strain in the outermost fibers of the length dS is the distance G, G', thus the strain per unit length is simply G-G'/dS or cdθ/dS. The stress, is by Hooks law, simply the strain multiplied by the modulus of elasticity, E. Therefore the stress is given by cE dθ/dS. For simple beams the stress is also given in terms of the beam characteristics and the bending monent as Mc/I. Where I is the section modulus of the beam. Equating the two expressions for the stress gives:

$$EI\, d\theta/dS + Py = 0 \qquad \text{----------(1)}$$

Equation (1) can also be written:

$$d^2\theta/dS^2 + a \sin \theta = 0 \quad \text{----------(2)}$$

Where $a = P./EI$

Equation (2) can be integrated once to yield:

$$d\theta/dS = 2\sqrt{a}\left[\sin^2(1/2\theta) - \sin^2(1/2\,\psi)\right]^{1/2} \quad \text{----------(3)}$$

It is possible to integrate equation (3) directly, however it is convienent to introduce a new variable in order that intergals appearing in the solution be of well known form with their values tabulated in the literature.

Let $\text{Sin}(1/2\,\theta) = k \text{ Sin } \phi$ and $k = \text{Sin}(1/2\,\psi)$

where ψ is the maximum value of θ.

This change in variables gives simple limits to θ. At $\theta = 0$ $\phi = 0$, and at $\theta = \theta_{max}$ $\phi = \pi/2$

Making the change of variables indicated equation (3) becomes:

$$S = 1/\sqrt{a} \int_{\phi_1}^{\phi_2} \frac{d\phi}{\left[1 - k^2 \sin^2 \phi\right]^{1/2}} \quad \text{----------(4)}$$

which is the general form of an elliptical integral of the first kind and tabulated values are given in the literature in terms of the limits ϕ_1 and ϕ_2.

Inserting the limits equation (4) becomes

$$S = \sqrt{a}\left[F(k, \pi/2) - F(k, \phi)\right] \quad \text{----------(5)}$$

where F is the elliptic intergal of the first kind.

The deflection, y, is given by:

$$y = 2\,k\,a^{-1/2} \cos(\phi) \quad \text{----------(6)}$$

And the distance x, is given by:

$$x = 1/\sqrt{a}\left[2\,E(k, \phi) - F(k, \phi)\right] \quad \text{----------(7)}$$

where E is an elliptical intergal of the second kind with argument k, & ϕ.

It is interesting to note that the non-dimensional shape of the curve, $y\sqrt{a}$ and $x\sqrt{a}$, is a function of just the maximum value of θ for a given plate thickness and material. The constant, a, contains the physical characteristics of the plate dimensions, material, and magnitude of the force P.

$$a = P/EI$$

Where P is the restraining force along the plate edge, lbs.

E is the modulus of elasticity of the material, lbs./ $in.^2$

I is the section modulus of the plate, $\frac{(\text{width} \times \text{thickness}^3)}{12}$

The shape of the curve given by equations (6), and (7) is known in the mathematical literature as an elastica and was solved about a century ago as an academic problem . It found some use in industry before the development of accurate testing machines in the measurment of modulus of elasticity and to determine the characteristics of heavy cloth and leathers. More recently, light weight space structures have considered its use. So far as the author is aware, its use as a reflector or concentrator of solar radiation does not appear in the literature. Some typical shapes are shown below.

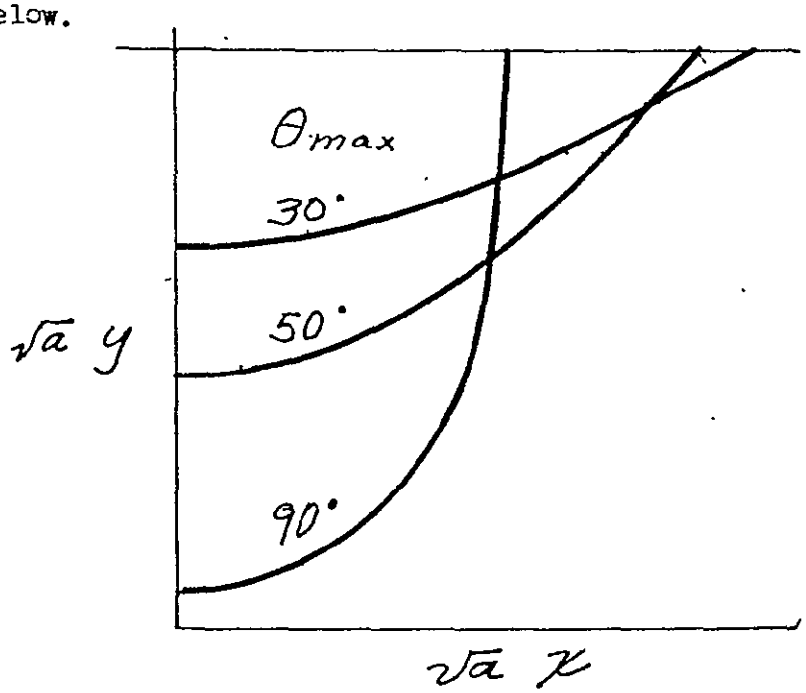

The characteristics of the focal region produced by the elastica can easily be calculated from the simple geometry of the reflected rays. The intercept of these rays on the y axis (x=0) is given by:

$$(y/a)_{x=0} = y/a + x/\sqrt{a}\cot(2\theta) \quad \text{for } 2\theta < 90^\circ \quad \ldots\ldots\ldots(8)$$

$$(y/a)_{x=0} = y/a + x/\sqrt{a}\tan(2\theta - 90) \quad \text{for } 2\theta > 90 \quad \ldots\ldots\ldots(9)$$

Figure 1a shows that the result of this calculation for θ_{max} of 30°. It can be seen that a poor focus is obtained. The rays reflected from the central region of the elastica are reasonably well focused, but those near the edges are not. Increasing θ_{max} should cause these edge rays to be turned inward thus producing a better focus.

The result for θ_{max} of 50° is shown on Figure 1b. For this case all of the rays are confined to a region of about 4% of the width, thus it seems that a useful focus can be obtained. Moreover, the focus is located within the envelope of the elastica. The focal region is small enough to allow a small collector tube to collect all of the sullight striking the elastica.

The calculated results for θ_{max} of 70° is shown in Figure 1c. Note that the focus is destroyed and this shape is not useful for this purpose.

The assumptions used in the analysis produce some restrictions when this analysis is used to produce concentrating shapes. One is that Hook's law holds thus the elastic limit of the material used must not be exceeded. This limit can be easily calculated by noting that the stress is given by Mc/I (see page A-2) and is not a serious limit for thin plates. The other restriction arrises from the neglect of the unit plate weight in the calculation of the bending moment. This can be calculated for any specific case by simply including the weight term in equation 1. There are no known analytic solutions to the resulting equation, thus the solution

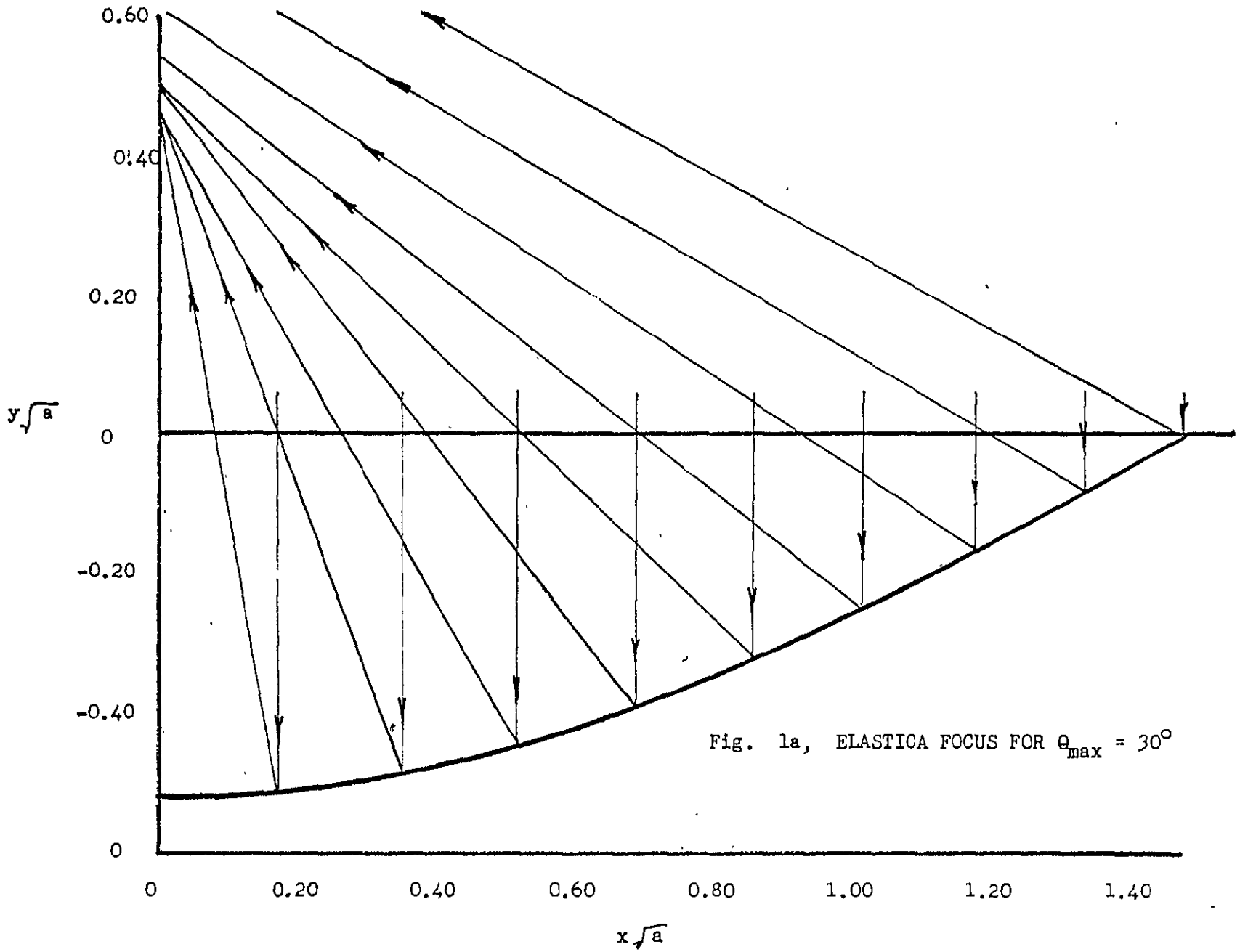

Fig. 1a, ELASTICA FOCUS FOR $\theta_{max} = 30^{\circ}$

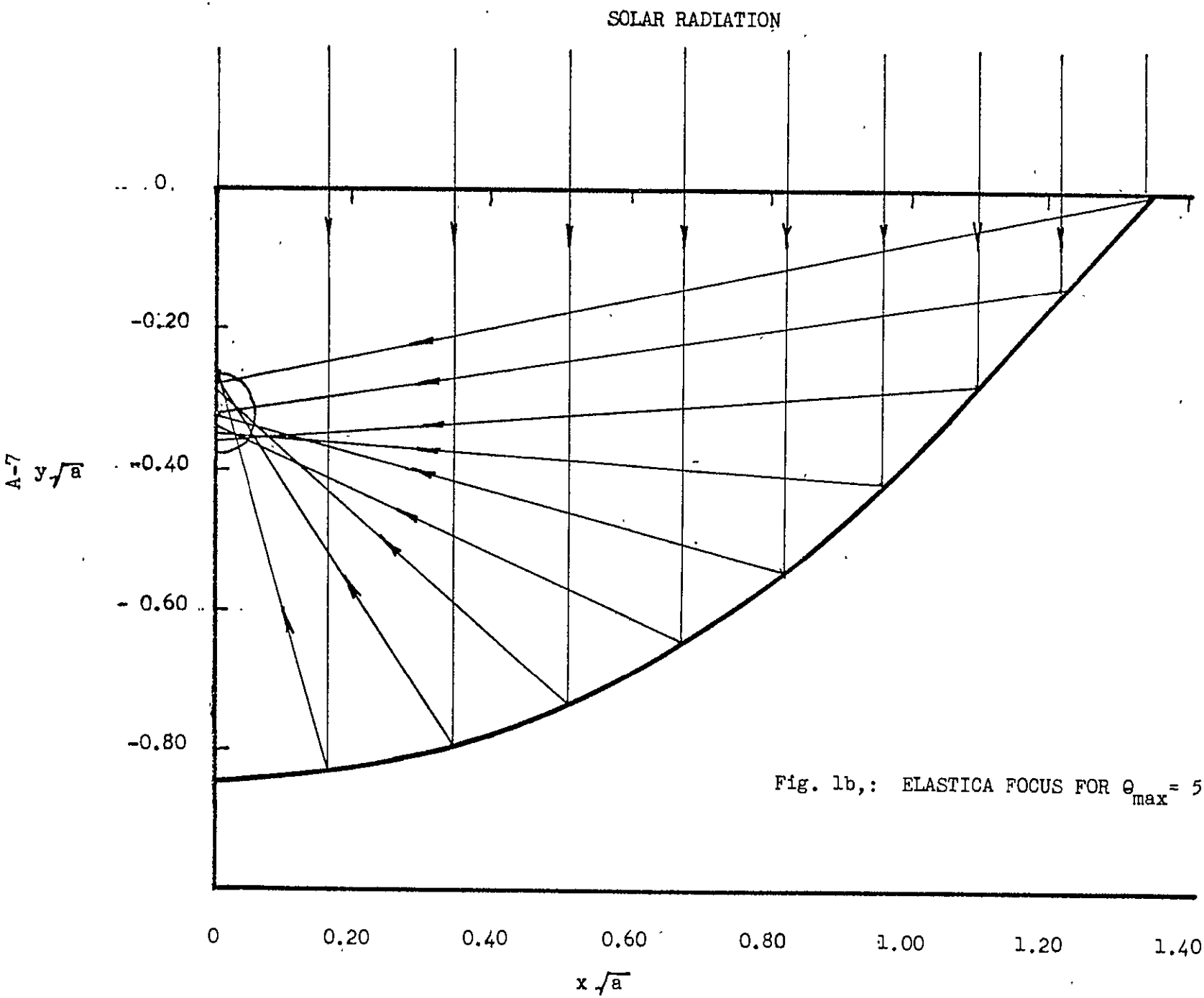

Fig. 1b,: ELASTICA FOCUS FOR $\theta_{max} = 50^{\circ}$

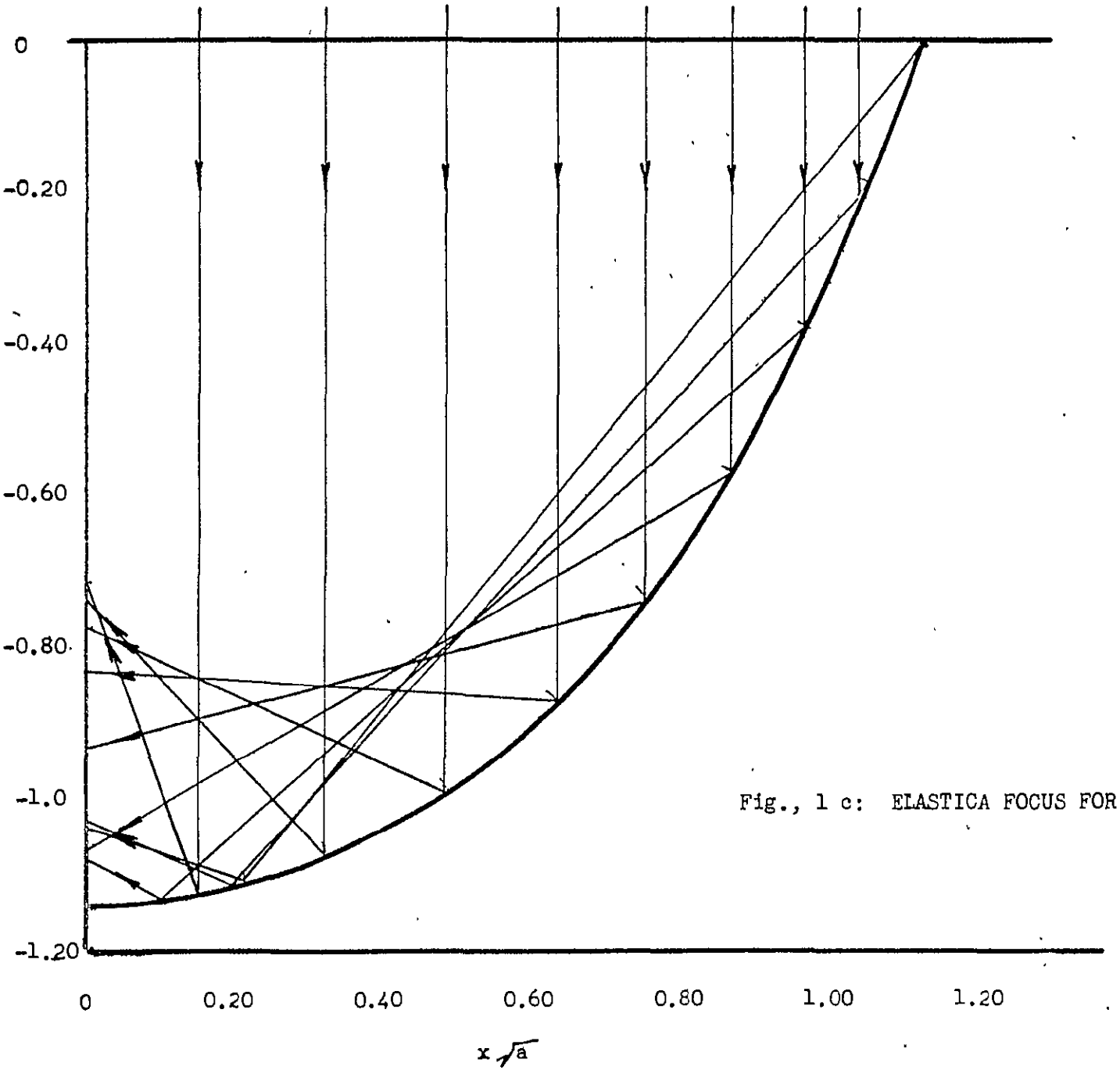

Fig., 1 c: ELASTICA FOCUS FOR $\theta_{max} = 70^{\circ}$

must be obtained on a computer or by experiment. Experiments by the author on a number of plates indicate that this is not a serious restriction for thin plates.

The coordinates and intercepts are given in non-dimensional form in the following table for θ_{max} of 50,52,53 and 54 and these results are plotted on Figure 1 of the main report.

θ_{max}	$y/\bar{a}$	$x/\bar{a}$	$(y/\bar{a})_{int.}$
50	0.84524	0.0000	~
	0.8324	0.1740	0.257
	0.7923	0.3453	0.265
	0.7320	0.5113	0.284
	0.6475	0.6700	0.306
	0.5433	0.8201	0.332
	0.4226	0.9617	0.353
	0.2891	1.0951	0.358
	0.1468	1.222	0.326
	0.0000	1.3472	0.237
52	0.8767	0000	~
	0.8634	0.1740	0.3098
	0.8239	0.34505	0.322
	0.7593	0.51037	0.340
	0.6716	0.66735	0.367
	0.5636	0.81614	0.397
	0.4384	0.9552	0.426
	0.2999	1.0852	0.439
	0.1522	1.2089	0.414
	000000	1.3291	0.331

θ_{max}	$y/\bar{a}$	$x/\bar{a}$	$(y/\bar{a})_{int.}$
53	0.8924	0.000	~
	0.8788	0.1740	0.336
	0.8385	0.3549	0.334
	0.7728	0.50956	0.340
	0.6836	0.6672	0.368
	0.5736	0.8140	0.400
	0.4462	0.9514	0.429
	0.3052	1.0799	0.441
	0.1550	1.2016	0.414
	0.0000	1.3196	0.379
54	0.9098	0.000	~
	0.8918	0.1739	0.361
	0.8532	0.3447	0.373
	0.7863	0.5094	0.395
	0.6955	0.6656	0.425
	0.5836	0.8118	0.461
	0.4539	0.9479	0.498
	0.3105	1.0747	0.520
	0.1576	1.1943	0.505
	0.0000	1.3101	0.425

APPROPRIATE ENERGY TECHNOLOGY
U.S. Department of Energy
333 Market Street
San Francisco, Ca. 94105